Diploma Thesis

Sedimentology, paleoecology and petrographic characterization of microbial mounds in a Middle Jurassic ramp (Central High Atlas, Morocco)

for the attainment of the academic degree
Diploma Geologist

by

Martin Homann

submitted at the
University of Potsdam
Department of Earth and Environmental Sciences

under the supervision of

Prof. Dr. Maria Mutti and Dr. Sara Tomás

Potsdam, September 23, 2010

Erklärung

Hiermit versichere ich, dass ich die vorliegende Arbeit selbstständig verfasst und keine anderen als die angegebenen Quellen und Hilfsmittel benutzt habe, dass alle Stellen der Arbeit, die wörtlich oder sinngemäß aus anderen Quellen übernommen wurden, als solche kenntlich gemacht sind, und dass die Arbeit in gleicher oder ähnlicher Form noch keiner Prüfungsbehörde vorgelegt wurde.

.....

Martin Homann (721780)

Potsdam, September 23, 2010

Abstract

In the Bajocian (Middle Jurassic) microbial mounds developed on a low-angle carbonate ramp on the southern flank of the Central High Atlas (Morocco). The mounds are well-exposed along the Amellago canyon, situated 50 km NW of the city of Rich in central Morocco. They belong to the Assoul Formation, which consists of a approx. 300 m thick alternation of shallow-water carbonates and terrigenous sediments. The mounds appear embedded within ooidal shoal deposits forming a continuous layer, which can be followed laterally for 80 m. The microbial mounds exhibit domical growth morphologies and are on average 1.3 m high and 2.5 m wide (n = 28). The mean distance between individual mounds is usually 2.7 m, but occasionally the mounds are connected laterally, bridgelike and pendant hemispheroids grow downward in their interspace.

The microbialites are characterized by a peloidal clotted fabric with no internal lamination and are therefore classified as thrombolites. Specific analysis of 37 polished slabs and 38 thin sections show, that the thrombolites are composed of polymorphic mesoclots (2 - 4 mm wide), which define the clotted fabric and form branches of 1 - 2 mm width. The mesoclots are composed of dark, micritic peloids (30 - 60 μm). In the interspace between individual mesoclots, growth framework cavities with a silty, geopetal infill occur. A detailed study of the microfabric, obtained from scanning electron microscopy (SEM) coupled with energy-dispersive X-ray spectroscopy analysis (EDX), revealed the presence of organic matter in form of bacterial coccoids (1 - 3 μm) and filamentous-like structures (5 - 15 μm), which occur both inside the fossilized EPS (extracellular polymeric substances) matrix. The EPS shows a characteristic honeycomb-like structure which is either mineralized by calcite with different amounts of Al - Fe silicates and some Mg, K ions or is completely composed of high-Mg calcite. The peloidal clotted fabric of the thrombolites has been interpreted to be the result of *in situ* calcification of coccoid-dominated microbial communities and the degradation and calcification of organic EPS, driven by sulfate reducing bacteria. The presence of sulfate-reducing bacteria is also evidenced by the occurrence of framboidal pyrite (5 - 15 μm). In contrast to their modern counterparts in the Bahamas, the studied microbialites were not growing simultaneously with the surrounding shoal deposits and almost did not trap or bind allochthonous sediment.

Their distinct domical shapes with a preferential horizontal growth direction, suggest that the available accommodation space was probably limited. The shallow, low-energetic environment is also reflected by the mound inhabiting biota, mainly consisting

of *in situ* branching corals, erected-growing bryozoans and boring lithophagid bivalves. These bivalves are particularly abundant during periods of growth interruption of the microbialite and may record variations in the trophic conditions. The microbial mounds were growing in a subtidal shallow-water environment under low to zero sedimentation rates. Sea level fluctuations are thought to be a key controlling factor responsible for their development and demise.

Contents

Chapter 1

Introduction

1.1 Motivation

Microbial carbonates provide the earliest macro-fossil evidence for life on earth and still exist today. The metabolic activities of microbes, which induce the precipitation of these carbonates, are thought to be largely responsible for the increasing amount of free oxygen in the primeval atmosphere of the earth and consequently for the evolution of life on our planet. During the last decades numerous studies on fossil and modern microbialites have been carried out and contributed to a basic knowledge about the processes involved in the formation of these deposits. However, most of these studies were either focused on the mega- and macrostructural scale, dealing with the depositional environment, ecological requirements and growth morphologies of microbialites (e.g. Leinfelder et al., 1993; Schmid et al., 2001; Andres & Reid, 2001) or focused on the meso- and microstructural scale in order to identify the involved bacterial communities and discuss the processes of carbonate precipitation and biomineralization (e.g. Kennard & James, 1986; Dupraz et al., 2004, 2009; Kazmierczak et al., 2009; Myshrall et al., 2010). Examining microbialites only at the mega- and macrostructural scale does not give insight into biological processes present or their geochemistry and mineralogy. On the other hand, only examining thrombolites at the meso- and micro- structural level does not allow the interpretation of the depositional environment and the associated faunas. Nevertheless, comprehensive studies, trying to combine all scales of observation are rare (e.g. Feldmann & McKenzie, 1998). Microbialites were important reef builders in Precambrian and Paleozoic (Riding, 2000). During the Mesozoic microbialites were particularly abundant in the Early Triassic and Late Jurassic (Flügel, 2004). Many studies focussed on coral-microbialite reefs and microbial mounds of Upper Jurassic

age. Less attention has been paid to the Middle Jurassic period so far, where reefs and microbial carbonates are scarce and only few reported occurrences exist. Microbialites have been identified in coral-microbialite reefs of the Paris basin (Olivier et al., 2006) and in reef horizons from the Central High Atlas (Ait Addi, 2006). To my knowledge, the microbial (thrombolite) mounds reported from the Bighorn Basin in Wyoming (Parcell et al., 2003), represent the only example for almost pure thrombolite mounds of Middle Jurassic age described in the literature.

This study will show another example of Middle Jurassic microbial (thrombolite) mounds, which have been found in the Central High Atlas of Morocco. These mounds represent the first reported occurrence of pure microbial mounds in that region and eventually also in the southern Tethyan domain. The purpose of the present study is to examine the microbial mounds at all levels of scale in order to identify the involved microbes, responsible for their formation and infer the environment of deposition. The studied outcrops are of outstanding quality and the rocks show a remarkable preservation, which allows a very detailed analyses.

Modern microbialites are not as abundant and widespread as in the past and often occur in restricted or stressed environments. They occur in hypersaline lakes in the Bahamas (Dupraz et al., 2004) or restricted to hypersaline embayments of the Indian Ocean (Logan, 1961) and also in open marine environments of subtidal channels in the Bahamas (Dill et al., 1986). In these channels the microbialites grow in shallow water under high energetic conditions (strong currents) within migrating ooid shoals. This is an interesting aspect, because the studied examples from Morocco also occur embedded in ooidal grainstones. In the fossil record the co-occurrence of microbialites and (ooidal) grainstones is not exceptional and has also been observed in other works (e.g. Pratt & James, 1982; Riding et al., 1991; Shapiro & Awramik, 2006). Hence, the close relationship between both carbonate deposits might indicate a similar environment of deposition like in the modern examples from the Bahamas.

1.2 Classification and terminology

1.2.1 Mounds

The first formal definition of the term "mound" was proposed by Toomey and Finks (1969), who described them as "an organic carbonate buildup, commonly of relatively small size, devoid of obvious bedding features, and containing a biota different from the usually bedded surrounding sediments". Mounds form flat lenses to steep conical to domical piles with slopes of up to 40° and commonly begin to grow below the wave base (James, 1978). They form a wave-resistant structure and consist of poorly sorted bioclastic lime mud with minor amounts of organic boundstone (James, 1978; 1983). According to Schmid et al. (2001) mounds are defined as structures, which contain more than 25 % of detrital or microbially generated structureless micrite. These structures can develop in deep and shallow waters, but are generally associated with low-energy environments such as deep basins, lower slopes, slope/shelf breaks, intra-shelf areas and lagoons (Schmid et al., 2001 and references therein).

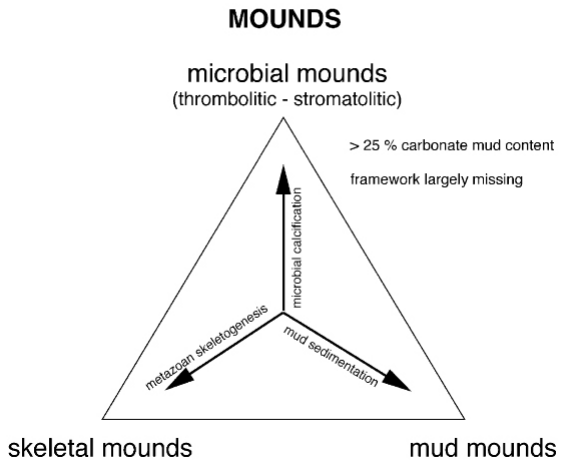

Figure 1.1: *Process related compositional classification of different mound types (taken from Schmid et al., 2001).*

Several authors have proposed a terminology for fossil carbonate buildups dominated by mud and micrite (James & Bourque 1992; Riding 1990, 2002). Following James and Bourque (1992), mounds can be subdivided into three categories: (1) microbial mounds, dominated by peloidal or dense micrite produced by calcifying benthic microbial associations (thrombolites, stromatolites, leiolites); (2) skeletal mounds, in which skeletal metazoans (e.g., corals, sponges) are the dominant framework builders; and

(3) mud mounds, mainly composed of detrital mud (Fig. 1.1). In the present work the term mound refers to microbial (thrombolite) mound and is used in a descriptive way, referring to their domical morphology.

1.2.2 Microbial carbonates

Microbial carbonates have the longest geological history of all biogenic carbonates extending back for almost 3.5 Ga and they are still forming today (Lowe, 1980; Hofmann et al., 1999). The term **microbialites** refers to mineral deposits resulting from organomineralization *sensu lato*, which encompasses microbially-induced and microbially-influenced mineralization (Burne & Moore, 1987; Dupraz et al. 2009). Biologically-induced mineralization is the result from the interaction between biological activity and the environment, whereas biologically-influenced mineralization is defined as passive mineralization of organic matter, which can be biogenic or abiogenic in origin (Dupraz et al. 2009). The formation of microbial carbonates is associated with the presence of **microbes** (microscopic organisms) such as bacteria, fungi, small algae and protozoans, but also requires a favorable saturation of calcium carbonate (Riding, 2000). The key organisms involved in the formation are bacteria, especially cyanobacteria, which thrive in shallow-water and oxygenated environments (Riding, 2000). Several metabolic processes, such as cyanobacterial photosynthesis and sulfate reduction by other heterotrophic bacteria can increase alkalinity and stimulate carbonate precipitation (Knorre & Krumbein, 2000; Riding, 2000). The communities which create microbial carbonates are termed **microbial mats**, reflecting the densely interlayered and intertwined orientations of coccoid and filamentous cells and the resulting sedimentary structures (Flügel, 2004). Stolz (2000) considered the microbial mats as complex **biofilms** and described them as masses of microcolonies in a honeycombed matrix composed of **extracellular polymeric substances (EPS)**. EPS represent a protective and adhesive matrix that attaches microbes to substrates and contain internal water channels, which facilitate nutrient and oxygen delivery, as well as waste removal (Riding, 2000). Many microorganisms can produce EPS but in microbial mats, cyanobacteria are generally recognized as the most important EPS producers (Richert et al., 2005; Dupraz et al., 2009). From a organomineralization point of view, the EPS matrix represents the location where the carbonate minerals nucleate and grow (Dupraz et al., 2009).

Microbial carbonates are very heterogeneous and are formed by two contrasting processes: (1) microbially mediated precipitation on or within EPS; and/or by (2) microbial trapping and binding of sediment (Riding, 2002). These processes lead to the formation of early lithified structures, wich can be subdivided into three main categories of microbialites: **stromatolites** (Kalkowski 1908), **thrombolites** (Aitken, 1967) and **leiolites** (Braga, 1995). Most microbialites can be classified into one of these categories, based on their macro- and microscopic features. Stromatolites are characterized by a laminated macrofabric, formed by episodic accretion via trapping, binding and cementation of grains by biofilms. Thrombolites display a non-laminated clotted fabric and the dominant sediment-forming process is *in situ* calcification, not sediment trapping. Leiolites have a structureless macrofabric, without clots or laminations. These three end members of microbialites display a wide range of microstructures including micropeloidal, densely micritic, or agglutinated microfabrics and can appear in diverse transitional phases (Fig. 1.2, Schmid, 1996; Riding, 2000).

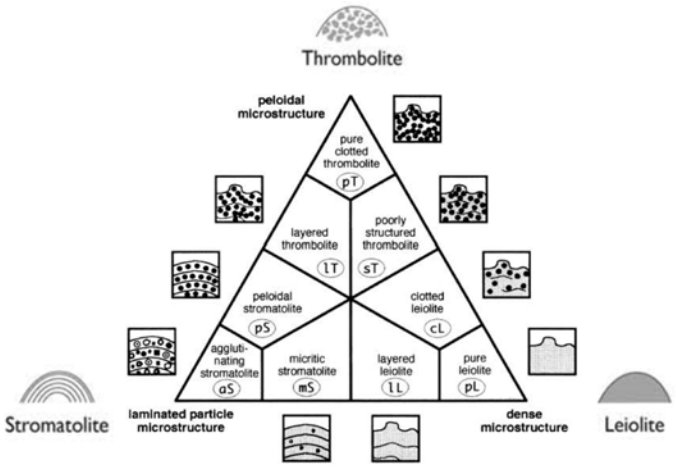

Figure 1.2: *Classification of Mesozoic microbialites. According to their fabric three main types with several transitional phases can be distinguished: thrombolite, stromatolite and leiolite (mod. after Schmid, 1996).*

The individual laminae within stromatotlites are generated by a dynamic balance between periods of frequent sediment accretion (mainly performed by vertical oriented filamentous cyanobacteria, which trap and bind sediment) and intermittent lithification of the cyanobacterial mats, characterized by the formation of laterally continuous sheets of micrite in surface biofilms (Reid et al., 2000). In contrast, the clotted fabric within thrombolites is interpreted to represent discrete colonies or growth forms of coccoid-dominated cyanobacterial communities (Kennard & James, 1986).

1.2.3 Thrombolites

Aitken (1967) proposed the term thrombolite (from the Greek *thrombos*, clot and *lithos*, stone) to describe "cryptalgal structures related to stromatolites but lacking lamination and characterized by a macroscopic clotted fabric". Thrombolites have been reported from strata as old as 1.9 Ga, but are not as well known and studied as stromatolites (Kah & Grotzinger, 1992). Some authors have speculated that the clotted, non-laminated fabric of thrombolites may result from the disruption and modification of a primary laminated stromatolite by bioturbation and diagenesis (e.g. Walter & Heys, 1985). But in general most thrombolites represent unique sedimentary structures, which are composed of dark, micritic clots. These so called "mesoclots" are the typical mesostructural components of thrombolites and make up at least 40% of the volume of a thrombolite rock (Kennard & James, 1986). The mesoclots display a variety of different shapes and are composed of dense micrite, peloids and cement. The origin of the mesoclots has been attributed to *in situ* calcification of coccoid or coccoid-dominated microbial communities (mainly cyanobacteria), but also calcified filaments may play a significant role in the formation (Kennard & James, 1986; Burne & Moore 1987). Furthermore their peloidal clotted fabric has been interpreted to be the result of incomplete EPS calcification, but the specific processes involved are not completely understood so far (Riding, 2000; Dupraz et al., 2004).

Another mesostructural component of the thrombolites are internal, sediment-filled cavities. Aitken and Narbonne (1989) stated that at one point in their formation, the thrombolites have formed an open, three-dimensional framework, with 25 to 40% cavities. Many thrombolites are inhabited by a diverse skeletal and soft-bodied fauna, which makes them to a "complex, fossilized microbial-metazoan ecosystem" (Kennard & James, 1986). They can occur in a variety of macrostructural forms, such as columns, domes, ridges and thick crusts, but typically develop meter-scale domical growth morphologies (Shapiro & Awramik, 2000). Aitken (1967) inferred that thrombolite mounds developed in conditions ranging from the lower intertidal zone to depths greater than 12 m. Other authors concluded that thrombolites, in contrast to stromatolites, form essentially under subtidal conditions (Fig. 1.3, Pratt & James, 1982; Flügel, 2004). It is likely that thrombolites can develop in settings of varying bathymetry, water-energy, salinity and oxygen/nutrient concentrations, but they require a very low to zero sedimentation rate which allows them to grow on top of sediments (Leinfelder et al. 1993).

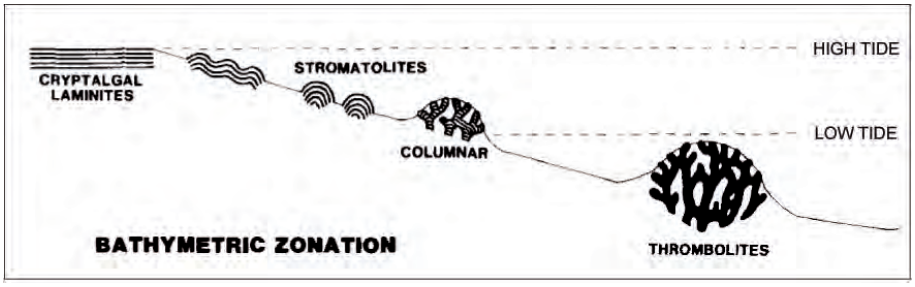

Figure 1.3: *Proposed bathymetric zonation of microbialites, showing that stromatolites develop preferentially in intertidal to subtidal settings, whereas thrombolites occur restricted to subtidal environments. Note that the growth morphology of microbialites (stromatolites and thrombolites) is controlled by the available accommodation space and changes from planar crusts, to small close lateral and spaced lateral domes, to columnar growth forms and finally to domical mounds (mod. after Pratt and James, 1982).*

1.2.4 Peloids

The descriptive term "peloid" refers to micritic aggregates of polygenetic origin (McKee & Gutschick, 1969, Macintyre, 1985). The peloids forming in modern and ancient microbialites are regarded to be autochthonous in origin, due to the fact that they constitute the most common microfabric of microbialites (Kennard & James, 1986; Dupraz & Strasser, 1999; Riding, 2000). However, it has also been described that similar micromorphologies can be created by purely abiotic mechanisms (Macintyre, 1985; Bosak et al., 2004). Chafetz (1986) and Riding (2002) proposed that peloids can be calcified bacterial aggregates resembling bacterial microcolonies in Phanerozoic fossil biofilms. It has been reported that CaCO3 precipitation as result of degradation of organic matter by heterotrophic bacteria, plays a significant role in the lithification process of microbial mats (Riding & Tomás, 2006). This observation is supported by studies on modern microbial mat lithification, in which the formation of peloidal carbonate precipitates is associated with the metabolic activities of bacteria (Paerl et al., 2001; Dupraz et al., 2004; Spadafora et al., 2010). Therefore the peloidal microfabrics are formed *in situ* during very early diagenesis, closely linked with the degradation and calcification of organic matter (EPS) driven by heterotrophic bacteria; mainly sulfate-reducing bacteria (Krumbein et al., 1977; Visscher et al., 2002; Riding & Tomás, 2006; Dupraz et al., 2009). After the organic matter is removed the interpeloidal spaces are filled successively by abiotic precipitation of microsparite (Spadafora et al., 2010).

1.3 Jurassic

The Jurassic represents the middle of the three geologic periods in the Mesozoic Era and spans the time from roughly 200 to 146 Ma (ICS, 2009). Stratigraphically the Jurassic can be subdivided into three main units: Early, Middle and Late Jurassic; also referred to as Lias, Dogger and Malm. The microbial mounds, which are object of this study, were deposited in the Bajocian (Dogger).

The evolution of reefs is governed by biological and global factors. Furthermore, it is reflected by changes in the composition of reef-building organisms during geological time, changes in mineralogical composition of reef carbonates and changes in the tectonic setting of reefs (Kuznetsov, 1990). The main factors controlling the reef development in the Jurassic are thought to be the rising sea level and the tectonic opening of new seaways, which had a major impact on oceanic circulation and climate (Leinfelder et al., 2002). Therefore it is important to have an idea about these factors.

1.3.1 Paleogeography, paleoceanography and paleoclimate

During the Late Triassic to the Early Jurassic the break-up of Pangaea into Laurasia (in the north) and Gondwana (in the south) disconnected Africa from North America, resulting in the opening of the North Atlantic Ocean and a western extension of the Tethys Ocean (Fig. 1.4). These tectonic events formed a narrow seaway that connected the North Atlantic with the Tethys, and placed the African and South American continents in the tropics. Due to the ongoing rifting/drifting processes during Middle and Late Jurassic another new oceanic gateway was formed with the opening of the so-called "Hispanic Corridor", which connected the eastern Pacific to the western Tethys Ocean. This new seaway had a huge impact on the ocean circulation and initiated a global east-west current system (Leinfelder et al., 2002). The seaway was fully established during the Late Jurassic, allowing a significant exchange of water masses between the two ocean basins (Rais et al, 2007 and references therein).

The global sea level history shows, that the sea level rose throughout the Jurassic. The flooding of large portions of the continents permitted the formation of shallow epicontinental seas in the tropical - subtropical shelf areas of North Africa and large parts of western and central Europe. Particularly during the Late Jurassic the sea level was about 100 to 150 m higher than today (Haq et al., 1988). The low paleolatitudes favored the establishment of carbonate platforms inside epicontinental seas along the

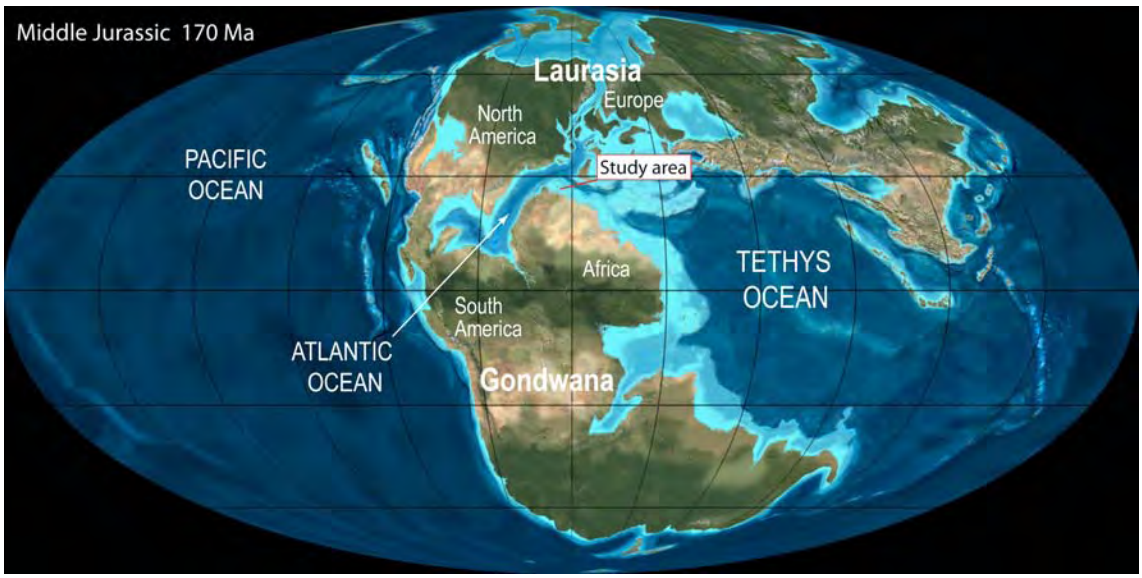

Figure 1.4: *Paleogeographic map for the world, showing the distribution of land masses during the Middle Jurassic with respect to the study area (mod. after Blakey).*

margins of the Tethys. The distribution and thickness of carbonate deposits along the Tethys margins can be used as an indirect evidence for a warm climate (Hallam, 1975). The Jurassic climate was characterized by contrasted seasons with alternating arid and humid conditions related to monsoonal effects (Hallam, 1993). In general, the climate in the Jurassic was hotter and drier than today and moreover it was equable. No significant polar ice-caps existed at this period.

1.3.2 Jurassic reefs

The Jurassic represents an important period of major and widespread reef growth with the development of very different reef types in shallow to moderately deep shelf seas connected to the Tethys (Leinfelder, 2001). It has been observed that the abundance of reefs generally increased during the Jurassic and thar they were more widespread on the northern Tethys shelf, than on the southern (Leinfelder, 1994). After the mass extinction at the end of the Triassic, the reefs slowly recovered during the Early Jurassic and a first major reef domain developed in the southern Tethys realm of Morocco (Leinfelder et al., 2002). During the Middle Jurassic the reefs occurred in scattered domains, which were often distant from each other, but show a wider distribution, expanding from the northern to the southern Tethys realm. The opening of the "Hispanic Corridor" (fully established in the Late Jurassic) and the beginning circumequatorial

ocean circulation facilitated the distribution of coral larvae and initiated a global distribution of (coral) reefs; resulting in mainly interconnected domains in the western and northern Tethyan realm, but also in the Atlantic area (Leinfelder et al., 2002). The Late Jurassic, also known as the "Reef Age" show the peak of reef occurrence and diversity.

According to Leinfelder et al. (1993, 2001) the basic types of Jurassic reefs can be grouped into three main categories: coral reefs, siliceous sponge reefs and pure microbialite reefs. These three end members have different transitional types which can grade into each other (Fig. 1.5, Leinfelder et al., 1993). The occurrence of these types

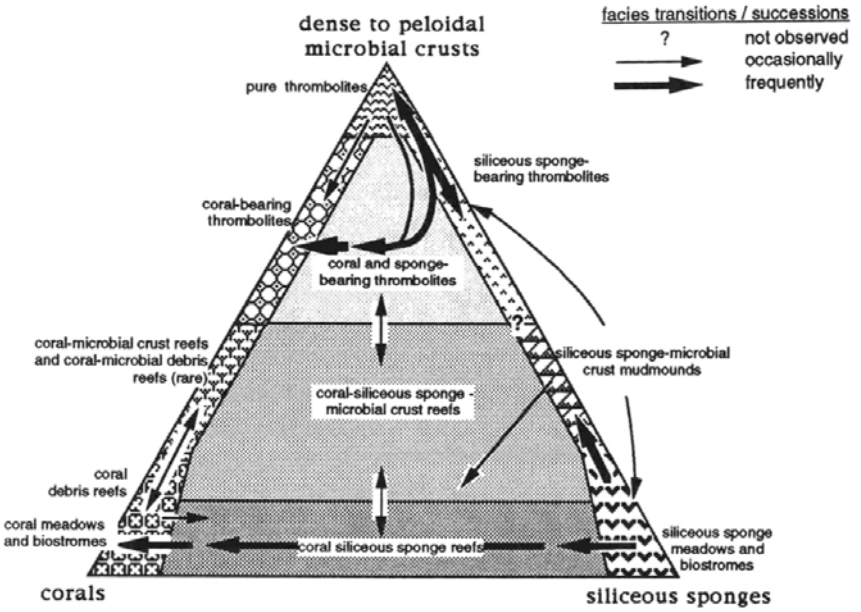

Figure 1.5: *Composition and transitional relationships of Jurassic reefs (taken from Leinfelder et al., 1993).*

is controlled by the ecological requirements of the different organisms and theinterplay between sedimentation rate, bathymetry and fluctuations in oxygen and nutrient content. Coral reefs occur in general in shallow water with high to moderate energy, whereas siliceous sponge reefs are mainly restricted to low-energetic, deep water settings. Microbialites are not restricted by bathymetry, but require a low sedimentation, low-energetic environments and hard substrates for nucleation. They often occur, when other reef building organisms are excluded by some ecological stress (e.g. high nutrient contents, oxygen depletion or increased salinity). The increased tectonic activity in the Jurassic with associated high terrigenous influx (nutrients) may have promoted the

development of microbialites.

During the Mesozoic microbial reefs are clearly dominated by thrombolitic fabrics, which can either occur as pure thrombolites or contain a variable amount of other reefal organisms, such as corals and siliceous sponges (Leinfelder & Schmid, 2000). It has been observed that pure thrombolites often grade into sponge-bearing thrombolites and or into coral-bearing thrombolites, which has been interpreted as shallowing-upward trend (Leinfelder et al. 1993). The general increase in the abundance of thrombolite mounds in the Mesozoic corresponds with rises in global and regional sea level during that time (Fig. 1.6, Leinfelder & Schmid, 2000). In the Upper Jurassic microbialites reached their peak of development within the entire Mesozoic and were particular abundant in the northern Tethyan realm, where they occur in shallow-to deep-water settings (Leinfelder, 2001; Leinfelder et al., 2002). Microbialites were a major constituent of many Upper Jurassic reefs (Parcell, 2002), encrusting surfaces within coral and sponge reefs or forming large thrombolite mounds (Leinfelder, 1993). The abundance and distribution of micro-encrusters has been used as a proxy for the estimation of the bathymetry of mircobialites (Leinfelder et al. 1993).

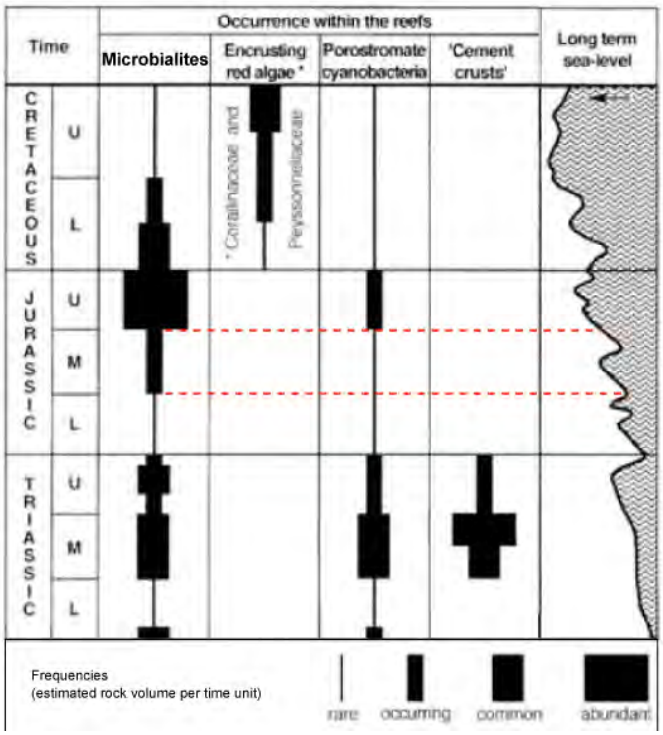

Figure 1.6: *General trends in Mesozoic microbialites. Marked in red is the period of the Middle Jurassic (taken from Leinfelder and Schmid 2000).*

Chapter 2

Geological and stratigraphic setting

Geological setting

The study area is located in the Amellago canyon, approx. 50 km NW of the city of Rich, on the southern flank of the Central High Atlas Mountain range. The Atlas Mountains extend from Morocco towards Algeria and Tunisia along 2000 km and represent the most significant relief in North Africa. In Morocco the Atlas Mountains consist of four main ranges: the Anti Atlas, High Atlas, Middle Atlas and Rif.

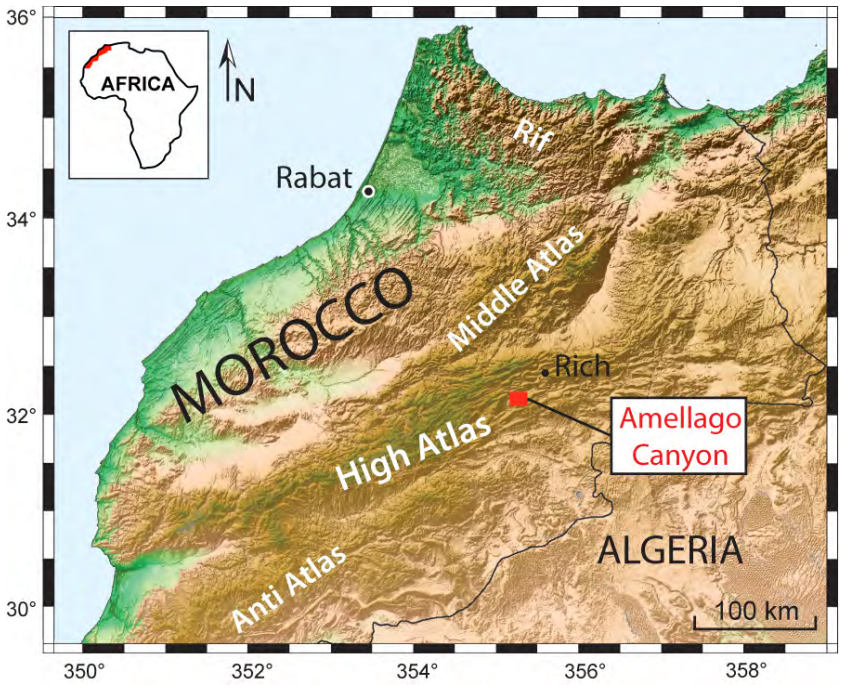

Figure 2.1: *Topographic map of Morocco showing the Atlas Mountain ranges and the location of the study area in the Amellago Canyon, situated in the Central High Atlas.*

The study area is located in the High Atlas, which is approx. 700 km long and 100 km wide and forms a ENE-WSW trending relief, rising in the west at the Atlantic coast and stretching in an eastern direction to the Moroccan-Algerian border. In the north the High Atlas adjoins to the Middle Atlas and in the south to the Anti-Atlas (Fig. 2.1). The High Atlas Mountains are an intracontintental fold-thrust belt, which was formed by the inversion of a preexisting Mesozoic rift system during the Cenozoic collision of the African and European plate (Jacobshagen, 1988; Beauchamp et al., 1996). During the Late Triassic to the Early Jurassic the break-up of Pangea disconnected Africa from America, resulting in the opening of the North Atlantic Ocean. An ongoing extensional regime led to the formation of rift grabens with sedimentary basins throughout northern Africa (Brede et al., 1992).

The basin evolution of the "Atlasic Basin" can be summarized into two main tectonically-induced sedimentary phases, which are both linked to the Western Tethys and Central Atlantic rifting-drifting processes that occurred during the Triassic to Jurassic (Ait Brahim al., 2002; Laville et al., 2004). The first phase took place in the late Triassic to the late Lias when a true rift basin, formed by NE - SW extensional faults, developed at the northern boundary of the Saharan Craton. The rift basin was connected to the Western Tethys and isolated the Sahara Craton from two microplates, the Moroccan and the Oran Mesetas (Fig. 2.2). The created half grabens of the "Atlasic rift" became filled with tholeitic basalts, continental red beds and evaporites (Pique & Michard 1989). During the early and middle Lias, the rifting phase continued, leading to a rapid increase in accommodation space. Block tilting, caused by high strain normal faults, led to a major marine incursion from the (Western) Tethys Ocean and to a well-developed hemipelagic depocentre bordered by carbonate platforms (Wilmsen & Neuweiler 2008). These platforms formed the the so-called "Lower Carbonate Complex", which was established along the borders of the basin or on the tilted blocks (Pierre et al., 2010). At the end of this rifting phase, during the lower and the middle Toarcian, a eustatic rise of sea level caused a major drowning of this Lower Carbonate Complex (Wilmsen & Neuweiler 2008). The second tectonically-induced sedimentary phase, which represents the post-rift evolution of the "Atlasic Basin", began during the late Toarcian, when a sinistral movement of Africa relative to Eurasia created a transtensional regime. This stress regime led to the development of a mosaic of rhomb-shaped sub-basins bounded by syn-sedimentary ridges (Brede et al. 1992; Laville et al. 2004). From the late Toarcian to the late Bajocian these sub-basins became filled with hemipelagic marls, but also carbonate platforms, the so-called "Upper Carbonate

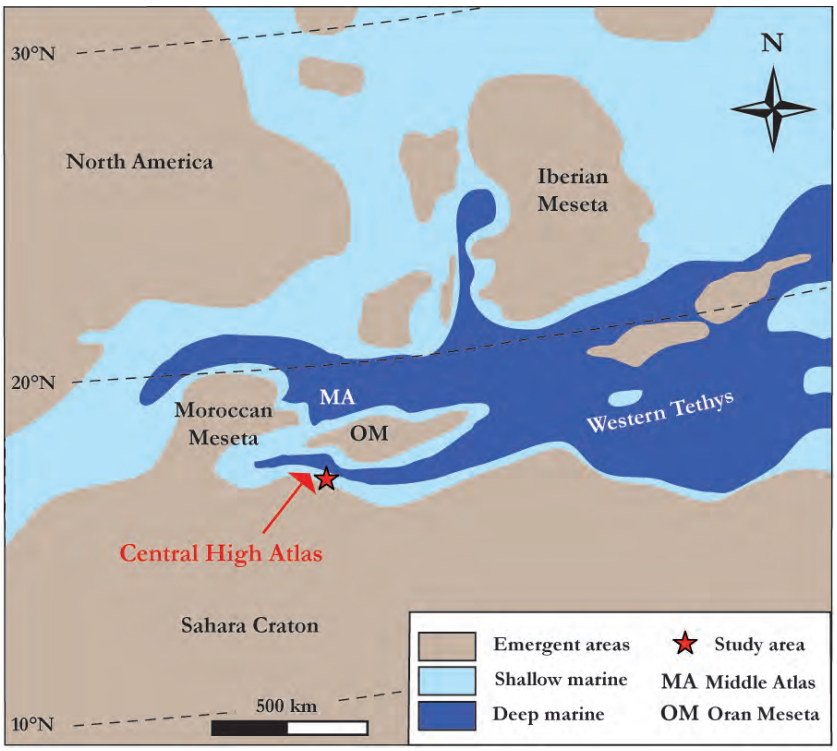

Figure 2.2: *Early Jurassic palaeogeography of the Atlas Rift Basin which was connected to the Western Tethys and isolated the Sahara Craton from the Moroccan Meseta and the Oran Meseta microplates (mod. after Christ et al., accept.).*

Complex", established on the margins of the rhomb-shaped basins. Also the analyzed carbonate succession was deposited in such a sub-basin. It has been proposed by Stanley (1981) that topographic highs, which are characterized by shallow-water deposits, may represent the crests of several tilted blocks. During the Aalenian-Bajocian tectonic instability in association with a relatively high sedimentary supply initiated a change of the platform geometry from a rimmed platform into a ramp platform (Aid Addi, 2006). The last phase in basin evolution is marked by the infilling with terrigenous sediments (the so called "Upper Red Beds"), which have been dated by fossilized terrestrial reptiles as Middle Bathonian (Monbaron, 1979; Jenny et al., 1981).

In the Early Cretaceous the inversion phase of the "Atlasic rift" system began, which formed the High Atlas Mountain range. The major uplift and inversion of the rift system occurred between 30 and 20 Ma (Oligocene-Miocene) and corresponds to the Alpine orogenic event (Beauchamp et al., 1999). According to Teixell et al. (2003) the total shortening during the Cenozoic compression varies between 15% and 24% from west to east along the central High Atlas.

Stratigraphy

The Jurassic carbonate succession outcropping in the High Atlas consists of the Lower Carbonate Complex and Upper Carbonate Complex, which are separated by a 100 m thick succession of deep hemipelagic marls deposited in the Toarcian (Warme, 1988). These two carbonate complexes represent two progradational phases of the carbonate platform in the southern margin of the "Atlasic basin". On top of the Upper Carbonate Complex the Upper Red Beds were deposited, which consist of limestones with terrigenous sediments and indicate the infilling of the basin (Fig. 2.3). Most of the studies carried out in this region focused on the Lower Carbonate Complex, whereas few attention has been paid to the Upper Carbonate Complex.

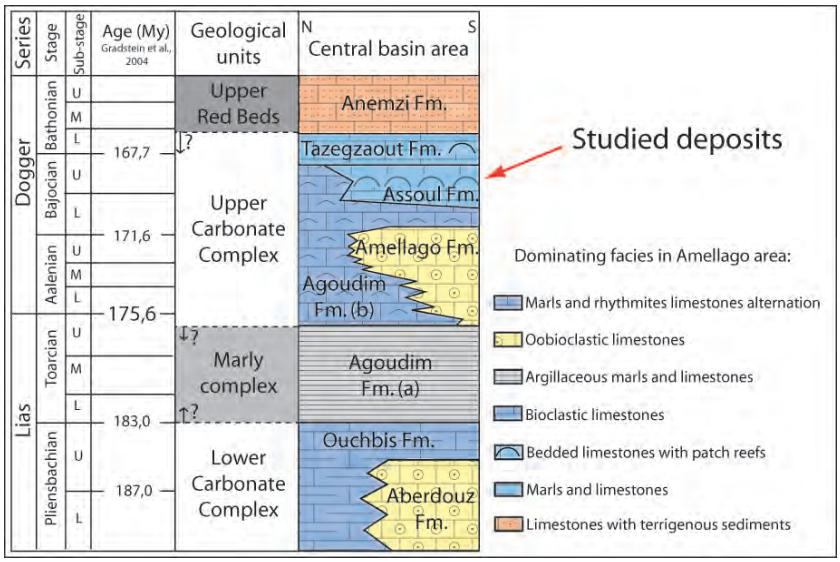

Figure 2.3: *Stratigraphic setting of the study area during the Early and Middle Jurassic (mod. after Amour et al., subm.).*

The studied deposits belong to the Assoul Formation, which belongs to the Upper Carbonate Complex and is approx. 300 m thick (Fig. 2.3, Poisson, 1998). The Assoul Formation mainly consists of an alternation of shallow-water carbonates and terrigenous sediments, which have been deposited in a lagoonal setting with shoals and patch reefs (Poisson, 1998). The age of this stratigraphic unit has been inferred by means of brachiopod biozones as Early - Late Bajocian (Pierre, 2006). The geometry of the Assoul Formation is still under debate, according to Pierre (2006) these deposits build a rimmed platform, whereas recent studies suggest that it forms a low-angle carbonate ramp system; at least in the Amellago canyon (Amour et al., subm.; Christ et al., accept.).

The outcrops in the Amellago Canyon are of outstanding exposure and almost not covered with vegetation, which allows an easy lateral correlation of corresponding sediment packages and deposits in the field. The main focus of this study is to investigate the microbial mounds, occurring in these deposits. For the study of the mounds two locations have been selected, referred as East Island Wall (E-IW) and as North Island Face (N-IF, Fig. 2.4). The E-IW is located at the east side of an isolated relief named the "Island", which is separated by a river incision from a cliff wall in the North, the N-IF. The horizontal distance between both outcrops is approx. 150 m and the deposits have a gentle dip of 5 - 10° NNW. In each location a stratigraphic section (E-IW 1 and N-IF 1) was measured in order to capture texture and compositional variability of the deposits below and on top of the mounds (Fig. 2.5). The results reveal that both outcrops belong to the same stratigraphic interval and that the mounds in both outcrops can be correlated with each other. According to Amour et al. (subm.) all the identified lithofacies in the study area are characteristic for shallow marine environments.

Figure 2.4: *Field panorama view of the two locations for the study of the microbial mounds in the Amellago canyon, the East Island Wall (E-IW) and the North Island Face (N-IF). Highlighted in red is layer of shoal deposits, in which the mounds are embedded.*

The base of the succession in both sections correspond to a thin layer of marls, which have a varying content of bivalves, brachiopods and small echinoids. These marls occur below, laterally and on top of a coral-microbial patch reef, which is 3.5 m high and 8 m wide. Overlying the reefs and the marly deposits a 1.5 m thick package of bioclastic wackstones to floatstones, which is mainly composed of coral fragments, bivalves brachiopods and echinoderms, occurs in the E-IW. On top of this package a differently composed bioclastic wackstone with interbedded marls, bivalves and echinoids appears for 1.3 m. In the N-IF only the bioclastic wackstones with interbedded marls occur for 1.7 m in this interval, whereas the wackstones to floatstones were not

observed. A good correlation of the two sections could be made with a 4 m thick package, mainly composed of ooidal packstones and grainstones, in which the mounds occur (this package will be described in detail in chapter/section 4.1). The lower part of the package is composed of peloidal-ooidal packstones and grainstones (G1) and has a condensed upper surface, that is overlain by a thin layer of echinoid-oyster floatstones. Above the floatstones the microbial mounds occur, which are surrounded by layers of ooidal packstones and grainstones (G2). On top of this interval a 50 cm thick layer of peloidal-oidal grainstones with bivalves and coral fragments appears in both sections. Overlying the peloidal-ooidal grainstones a 1 - 1.5 m thick layer of bioclastic peloidal wackstones with bivalves, coral fragments and oncoids occurs in both outcrops. This layer is interrupted by a 1 m thick interval of marls and bioclastic wackstones with interbedded marls. Followed by, several layers of bioclastic peloidal wackstones with oncoids and thin marly interlayers which allow a good correlation.

Analyzing the vertical stacking patterns of the described lithofacies types two main deepening/shallowing trends can be inferred, possibly corresponding to a 4th order sea level fluctuation. The first deepening trend is reflected by the deposition of predominantly marly deposits on top of the patch reefs, followed by a shallowing trend represented by a more grainy sedimentation (ooidal grainstones). However, this interpretation does not explain the occurrence of the condensed surface below the echinoid-oyster floatstone layer and the microbial mounds, which could be interpreted considering a higher order shallowing/deepening/shallowing trend. This interpretation is consistent with the work of Schmid et al. (2001), who stated that the the growth of significant mound structures might be the result of a 5th order cyclicity. Nevertheless, the interpretation of this part of the succession is difficult and remains controversial. The transition above this part, from peloidal-dominated grainstones to bioclastic peloidal wackstones and to an interval of more marly deposits can be interpreted as the second deepening trend. Followed by a (relative) shallowing trend expressed by the deposition of oncoidal-dominated wackstones.

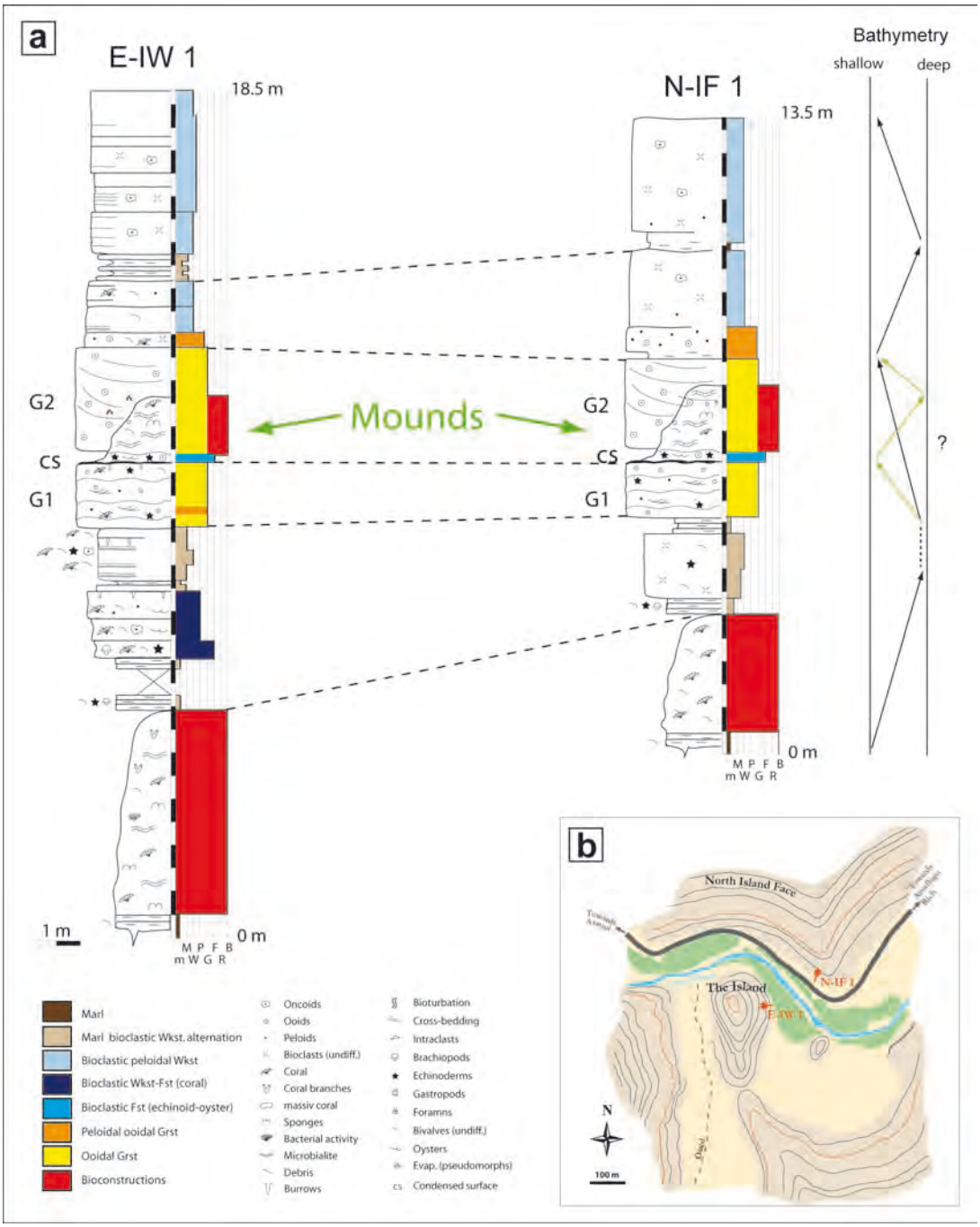

Figure 2.5: *Stratigraphic sections and their location in the study area. a) Correlation of the stratigraphic section in the E-IW and N-IF and interpretation of stacking pattern. b) Simplified map of the Island study area showing the two outcrops and the locations of the measured stratigraphic sections (mod. after Christ et al., accept.).*

Chapter 3

Methodology

The methods used in this work can be summarized in two big categories: 1) field work, comprising traditional data collection in the field, as well as modern d-GPS measurements of the dimensions and distribution of the mounds; and 2) laboratory work, including thin section analysis with the petrographic microscope and analysis of the microstructure and elemental composition with scanning electron microscope (SEM) and energy dispersive X-ray spectroscopy (EDX).

3.1 Data collection

The field work in the Amellago Canyon was carried in the time between the 9th and the 29th of March 2009 and is partly based on previous work of Frederic Amour (University of Bochum) and Nicolas Christ (Ruhr-University Bochum), who both work on their PhD thesis in that area. In the field a total number of 28 individual mounds have been precisely mapped in the two outcrops (E-IW and N-IF). The height, width and space between individual mounds has been measured for all the mounds. In both outcrops a stratigraphic section has been logged to collect informations about the lithological characteristics (texture, fabric and components) of the deposits below and on top of the mounds. Three excellent preserved mounds with a good accessibility were chosen and sampled systematically and described in detail. Two of these mounds are from the E-IW outcrop and one is located in the N-IF. Form these three mounds and the surrounding shoal deposits 52 samples of various sizes were collected. While collecting samples it was taken care that the sample locations are not too close to each other and equally distributed throughout the whole mound, in order to get a representative overview. Due to the presence of a portable printer, the field work could

be optimized a lot. Photographs taken during the day were printed and discussed in the evening and served to record the location of single mounds and the position of samples. Furthermore, large scale photo panoramas helped with the orientation in the field and were also useful for the lateral correlated of the strata in the field. The exact position of every mound was also captured using a Leica d-GPS 1200, coupled with a binocular. For every mound at least two measurements were taken, one at the top and one always left and right at the base of the mound. Later this complete dataset can be digitalized and imported in the 3d modeling software PETREL for further studies. This software can be used to perform an object-based modeling in order to predict the distribution of the mounds in the study area. Furthermore the microbial (thrombolite) mounds can be used in outcrop analogue studies with respect to their significance as potential reservoir for oil and gas or their impact on fluid flow in the carbonate rock.

3.2 Sample analysis

A total of 38 thin sections have been made from the 52 collected rock samples collected in the field. Moreover, 47 polished slabs were produced to study the macroscopic features of the samples. Photographs of these slabs were taken with a Sony DSC-W17 digital camera. The thin sections were studied with the petrographic microscope LEICA DM RXP equipped with a LEICA DFC 420 camera for photomicrographs. For a better identification of dolomite four of the thin section chosen and stained with alizarin-Fe for 1 min and after rinsed in distilled water. After this treatment all present calcite appears in red and the dolomite sticks out and is easy to distinguish.

For SEM and EDX analysis 7 rock chips were chosen and polished. The surfaces were cleaned in distilled water and dried for 10 minutes. Afterwards they were etched in 2% hydrochloric acid for 1 min. Various of acid concentration and etching times were tested, and the 2% hydrochloric acid for 1 min yielded the best results. After etching the samples were rinsed in distilled water and immediately dried and carbon-coated. The samples were kept isolated in a sterile desiccator to avoid contamination. The samples were analyzed on a JEOL JSM - 6510 scanning electron microscope operating at 11 - 15 kV and equipped with an Oxford Instruments Energy Dispersive X-ray Spectrometer system. The elemental composition and mappings obtained with the EDS were analyzed with the Microanalysis Suite INCA 4.15 from Oxford Instruments.

Chapter 4

Results

4.1 Mound / shoal relationship

The microbial mounds appear embedded in a 4 m thick layer mainly composed of ooidal packstones and grainstones, interpreted as shoal deposits. The layer can be followed laterally along 70 m in the East Island Wall (Fig. 4.1) and along 80 m in the

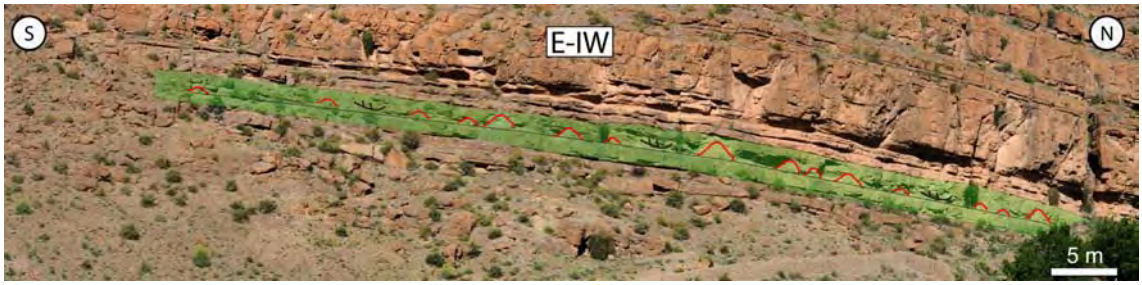

Figure 4.1: *Field outcrop view from the East Island Wall outcrop (E-IW), depicting the mounds (red) embedded within cross-bedded shoal deposits (green).*

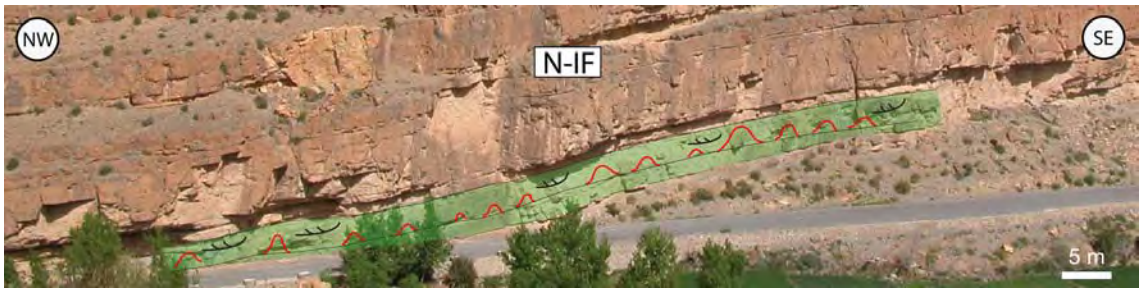

Figure 4.2: *Field outcrop view from the North Island Face outcrop (N-IF), depicting the mounds (red) embedded within cross-bedded shoal deposits (green).*

North Island Face (Fig. 4.2). The shoal deposits can be subdivided into two parts with significant differences; the first one below the mounds (G1) and the second one lateral and above them (G2, Fig. 4.3 a). The first shoal deposit (G1) is a 1.5 m thick layer and show wavy to low angle planar cross-bedding (Fig. 4.4). The ooids have spherical to ellipsoidal shape with a diameter of 400 μm. They are medium sorted and cemented by blocky calcite. The ooids display few thin radial laminated cortices and mainly belong to type 3 ooids sensu Strasser (1986). Superficial ooids occur occasionally, but are generally rare. Furthermore, the ooids are partly micritized and as nuclei often act different bioclasts (shell fragments, forams). G1 has a distinctive upper surface with horizontal burrows and scattered accumulations of brachiopods (Fig. 4.3 b).

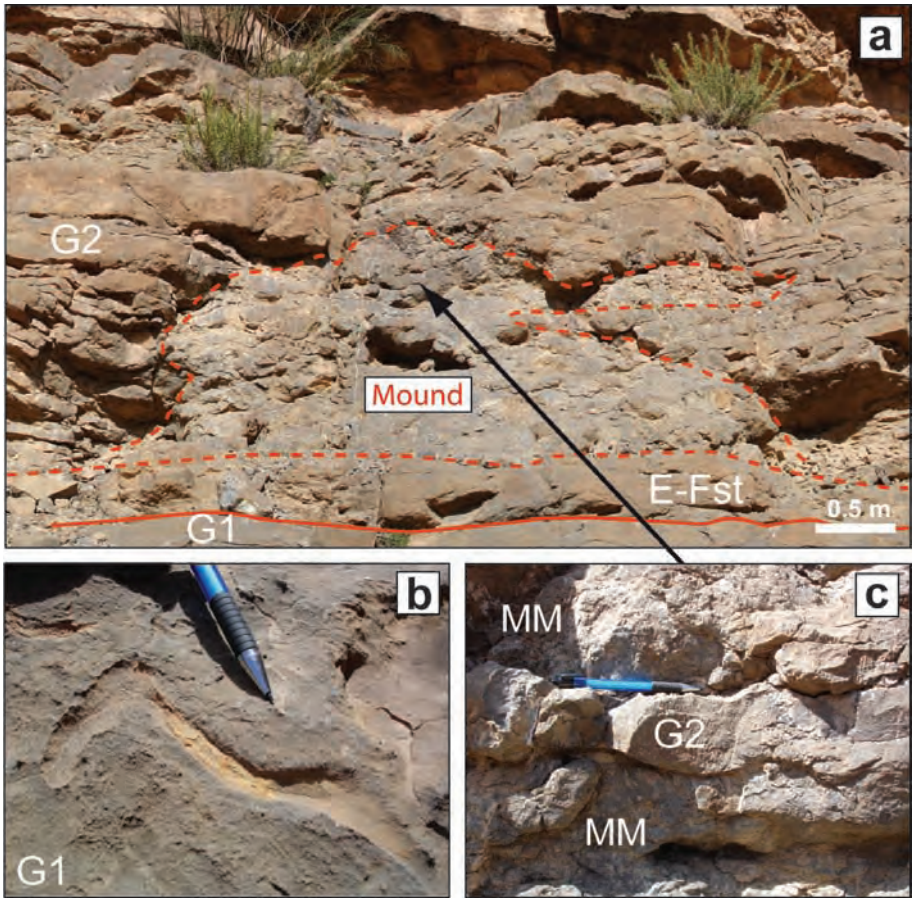

Figure 4.3: *Field photographs showing a) a single mound on top of an echinoid-oyster floatstone layer (E-Fst) and the shoal G1. The mound is embedded in the shoal G2. b) Condensed surface on top of G1 with horizontal burrows. c) Layer of ooidal grainstone (G2) cutting the mound (MM).*

This surface has been interpreted as an interval of condensation and shows a sharp contact with the overlying deposits, which is consist of echinoid-oyster floatstones (Fig. 4.5 a). This contact is not erosional, since no eroded or incorporated components (of

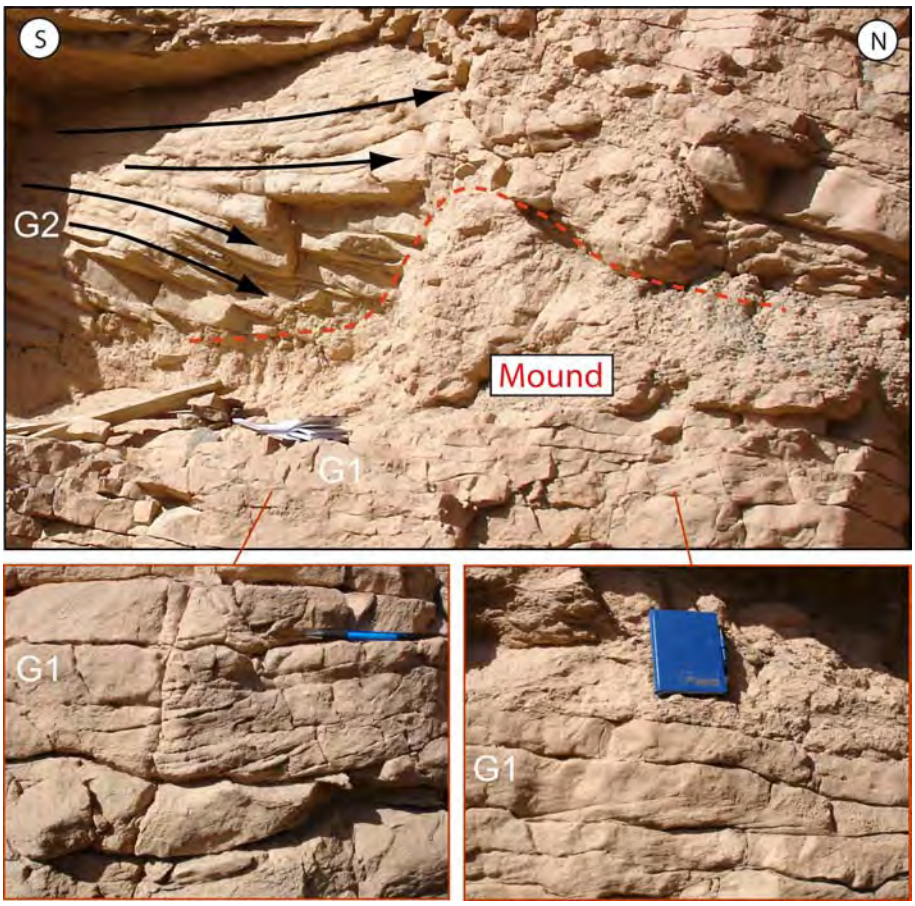

Figure 4.4: *Field photographs highlighting the different bedding structures of the two shoals deposits (G1 and G2): wavy, low angle planar cross-bedding in G1 and high angle trough cross-bedding in G2.*

G1) are found in the floatstone layer. The two main components of the floatstones are echinoid spines and oyster shells, which are well preserved, disarticulated, horizontally arranged and not fragmented (Fig. 4.5 b, c, d). The spines are up to 4 cm long with a diameter of 0.5 cm and show syntaxial calcite overgrowth cements. The oyster shells show a cross-lamellar microstructure and are approx. 2 cm long and 500 μm thick. Furthermore, the oyster shells are partly surrounded by a dark, micritic envelope, in which bryozoans and calcareous sponges occur, encrusting each other. Minor components are radial ooids, *Cayeuxia*, brachiopods, gastropods, as well as bryozoans, calcareous sponges and corals also occur. The corals are surrounded by a similar dark micritic envelope, as that of the oysters (Fig. 4.5 e). The matrix is micritic and with some more marly areas, but this could also be due to exposure and weathering. In the E-IW and the N-IF the echinoid-oyster floatstone occurs as a continuous layer on top of the condensed surface of G1. The floatstone layer passes vertically into the microbial

mounds (Fig. 4.5 a). The contact between both fabrics is transitional.

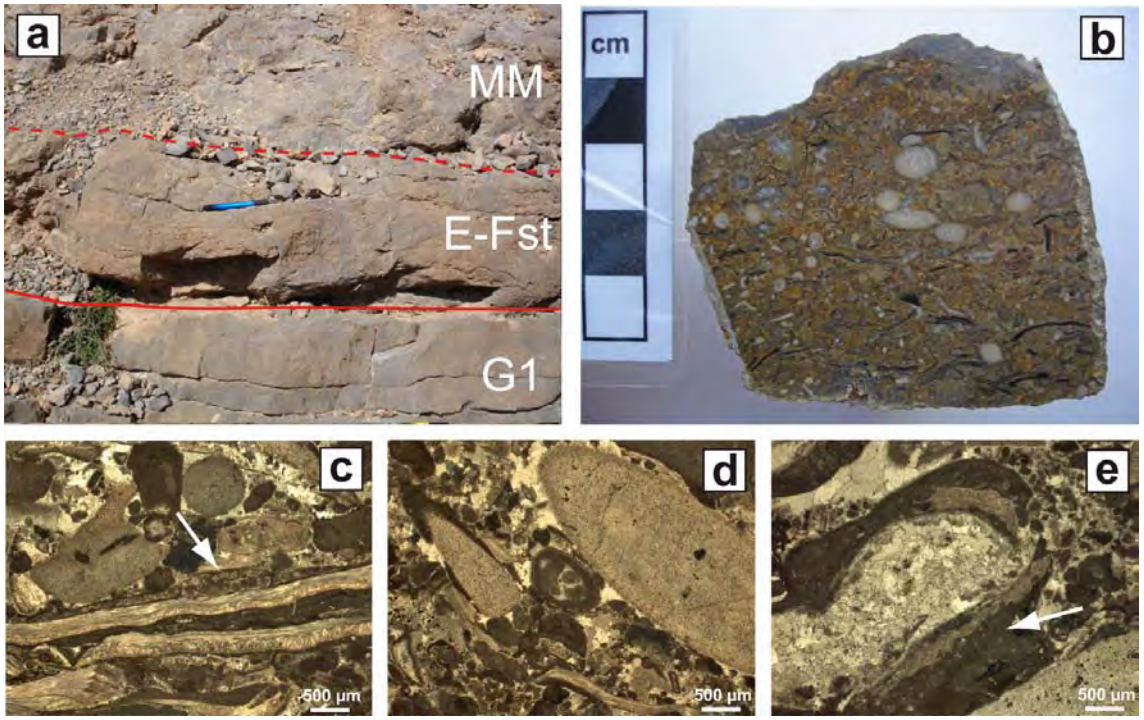

Figure 4.5: *a) Field photograph from the echinoid-oyster floatstone layer (E-Fst) on top of the shoal deposit (G1) overlain by a mound (MM). b) Polished slab photograph from the floatstone, note the preferential horizontal arrangement of the skeletal components. (c - e) Thin section photomicrographs: c) cross-lamellar oyster shell encrusted by bryozoans (white arrow), d) cross sections of echinoid spines and e) recrystallized coral surrounded by dark micritic envelope with encrusting bryozoans (white arrow).*

The second shoal deposit (G2) occurs laterally and above the mounds. It consist also of ooidal packstones and grainstones with high angle trough cross-bedding (Fig. 4.4). Angles of up to 22° occur, where the shoals are in close contact to the mounds, giving the impression that the topography of the mounds is responsible for the inclination of the shoal deposits. The ooids of G2 have a diameter of approx. 750 μm and are mainly spherical with fine radial to radial-fibrous structures and similar nuclei to those of G1. The ooids are well - medium sorted and sometimes micritized; they mainly belong to ooid types 3 and 4 of Strasser (1986). They display several (5 or more) cortices, but also superficial ooids with 1 or 2 cortices occur sometimes. Often the ooids show outer cortices with bands of small grains of iron oxide, most probably hematite. Except of this outer cortex the ooids are composed of calcite (Fig. 4.6).

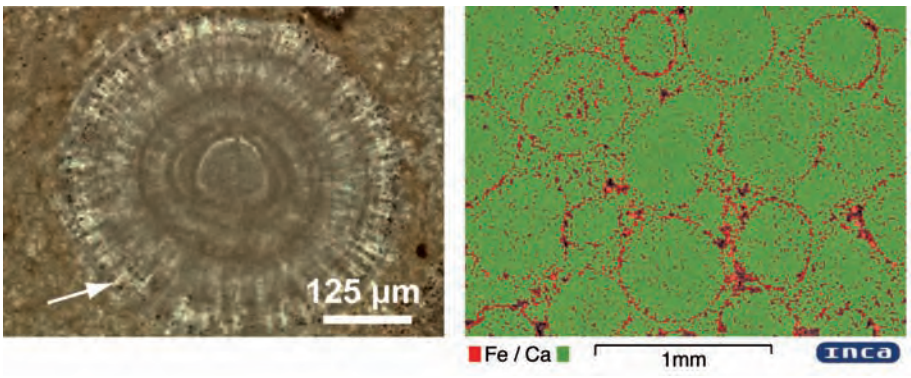

Figure 4.6: *Thin section photomicrograph (left) and EDX mapping (right) from the ooids of the shoal deposit G2. The ooids are mainly composed of calcite (in green); iron oxides (in red) occur concentrated in the outer cortex of the ooids (arrow).*

Although they could be interpreted as ferruginous ooids, it looks unlikely since ferruginous ooids are primary composed of iron oxides and contain calcite only in trace amounts (Collin et al, 2005; Ramajo et al., 2008). Nevertheless, the outer iron-oxide-rich cortex may have formed under similar conditions to those of iron ooids form. The origin of ferruginous ooids is a subject of long-lasting discussion. They can form in a variety of environments under different conditions. Generally, they are thought to form in very weakly agitated, but not stagnant water from remobilization of underlying iron-rich sediments (Gygi, 1981). Some studies also indicate that microbial activity plays a significant role in the genesis of these ferruginous ooids (Burkhalter, 1995; Preat et al., 2000). Nonetheless, which is common in all the aforementioned cases is the fact that ferruginous ooids occur in times of non-deposition, which can be either the result of starvation or a balance between sedimentation and erosion. Locally, G2 contains less ooids and shows dolomitized wackstone to packstone textures (Fig. 4.10) where iron oxides occur, developing dendritic growth forms. Within this dolomitized matrix calcite pseudomorphs after gypsum also occur, which will be described below (chapter/section 4.3). The comparison of the ooids of the two shoals, G1 (below the mounds) and G2 (lateral and above the mounds), reveals that both are well to medium sorted, however G2 contains ooids that are almost two-times bigger than the ooids in G1 and have an iron-oxide-rich outer cortex (Fig. 4.7).

In the field, complex interfingering relationships and incorporations between mound and shoal fabrics have been observed. It looked like that they were growing simultaneously. Occasionally 8 - 10 cm thick layers of ooidal grainstones occur inside the mound and seem to cut them (Fig. 4.3 c). Just in one case it is obvious that this layer is

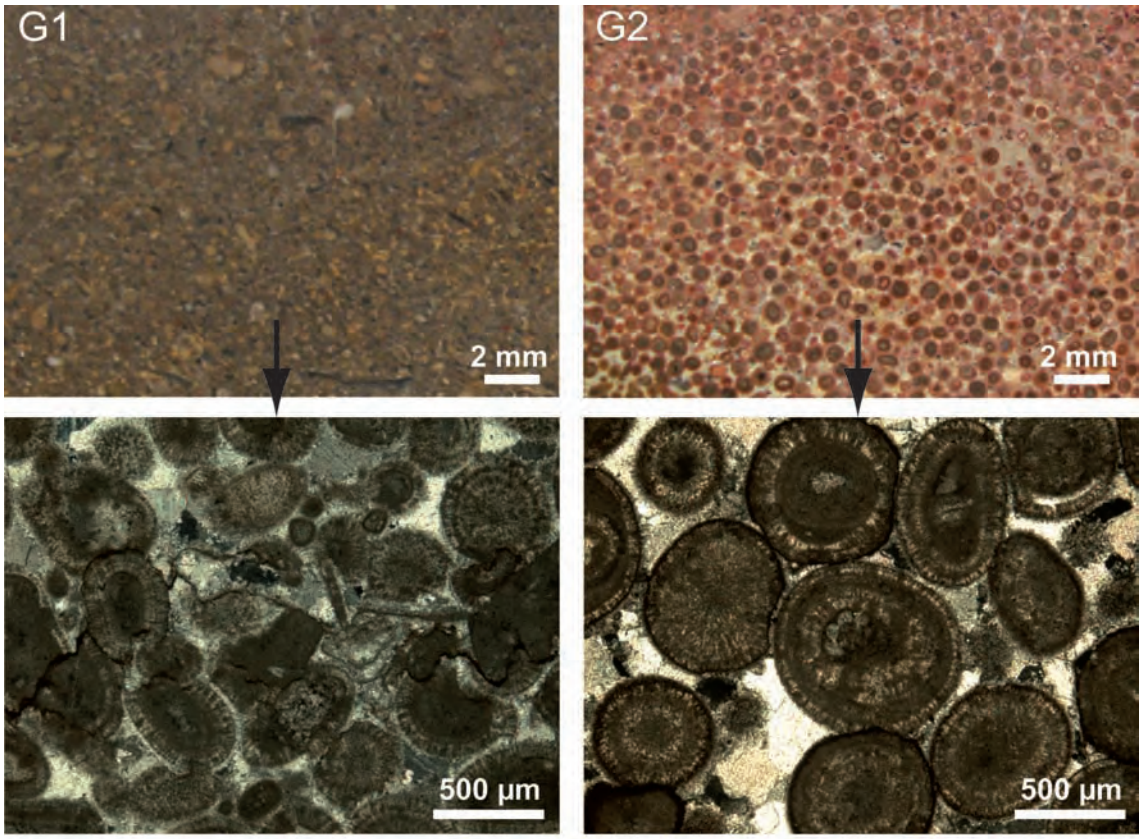

Figure 4.7: *Comparison of polished slabs photographs and corresponding thin section photomicrographs from the ooids of the shoal deposit G1 and G2. Note that the ooids in G2 are almost two-times bigger than the ooids in G1.*

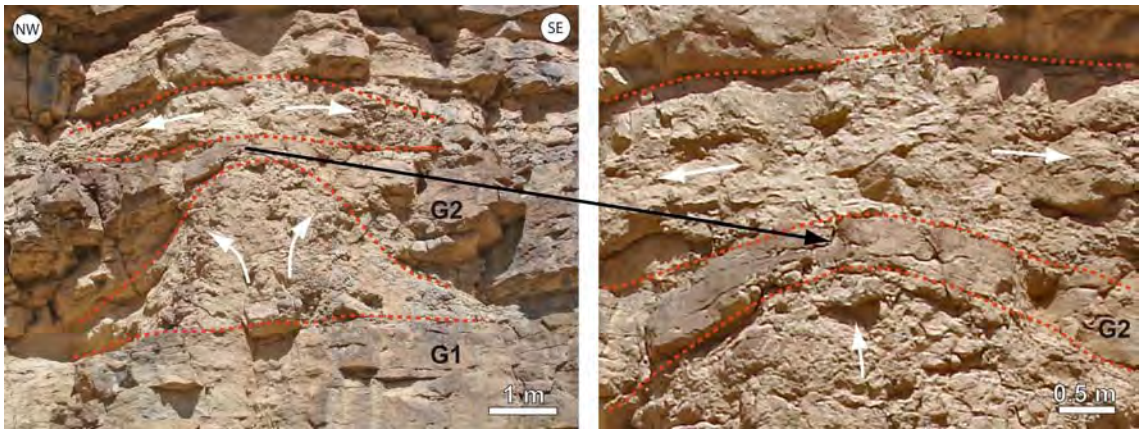

Figure 4.8: *Field photographs showing two growth intervals of the mounds with different morphologies. The first interval is characterized by mounds with a domical growth morphology, which are embedded in shoal deposits (G1 and G2). In the second growth interval mounds show a ridge-like morphology and a preferential horizontal growth direction and developed on top of the shoal body G2.*

cutting the mound, but in general it is not clear and could be simply the result of a thee-dimensional effect. In this case a mound has been observed to be covered by a 50 cm thick layer of ooidal grainstones on top of which a second mound developed. This second mound is growing with a ridge-like morphology and shows a preferential horizontal growth direction (Fig. 4.8). The growth morphology of this possible second growth interval of the mound point out limited accommodation space, in contrast to the first growth interval with well-developed domical (steep-sided) morphologies. Studying in detail the contact between the mounds and the shoals and based on the sedimentary structures it is obvious, that the mounds must have been a rigid barrier for the incoming shoals. Some of the mounds also appear inclined towards the paleo flow direction of the shoals (Fig. 4.9). This would imply, that the mounds must have been already existing, when the shoals were deposited.

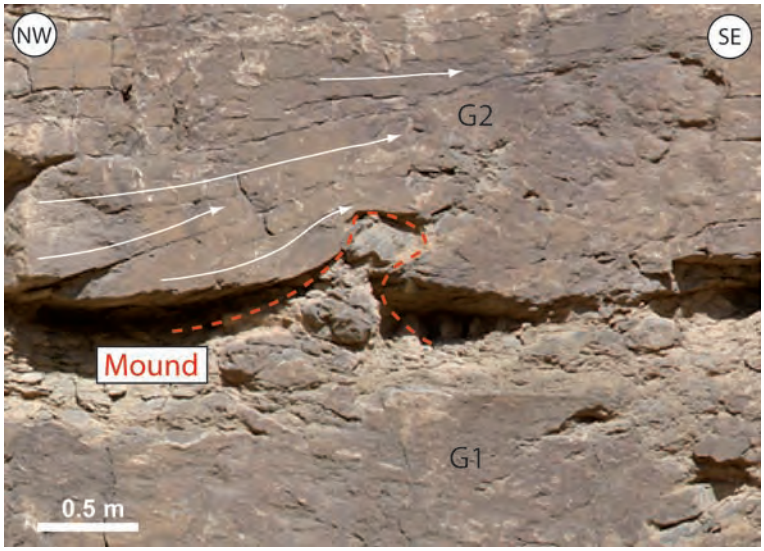

Figure 4.9: *Field photograph of a small mound inclined towards the flow direction of the ooid shoal.*

When looking at the polished slabs and thin sections a sharp and erosional contact between both carbonate factories, which are not mixed, is observable (Fig. 4.10). It is clearly visible that the shoal is cutting and penetrating the internal structure of the mound (Fig. 4.11 a, b). Therefore, small mound fragments, which may have been eroded during the deposition of the shoal, can be found inside the shoal deposits (Fig. 4.11 c). No ooids were found trapped or incorporated inside the microbialites, although they occur sometimes in growth framework cavities of the mounds, which are in close contact with the shoal (Fig. 4.11 d).

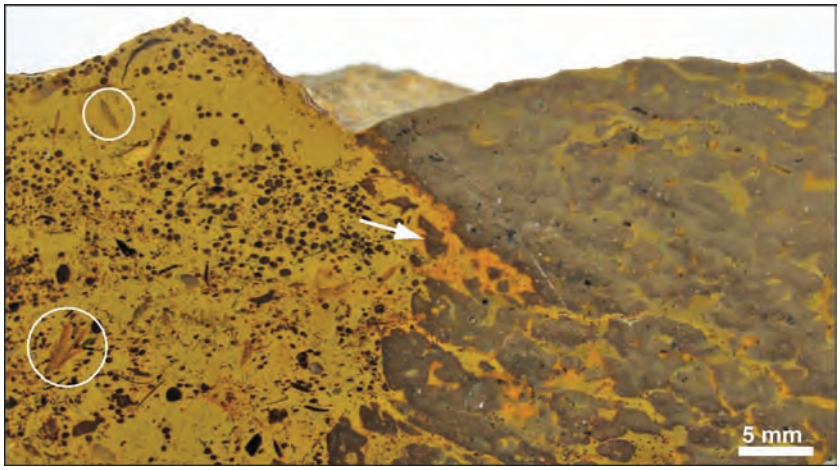

Figure 4.10: *Polished slab photograph depicting the erosive contact between the shoal deposits and the microbialite, showing that both fabrics are not mixed. Note that eroded fragments of the mound are incorporated inside the shoal deposits (arrow). Calcite pseudomorphs after gypsum occur inside the shoal (circles).*

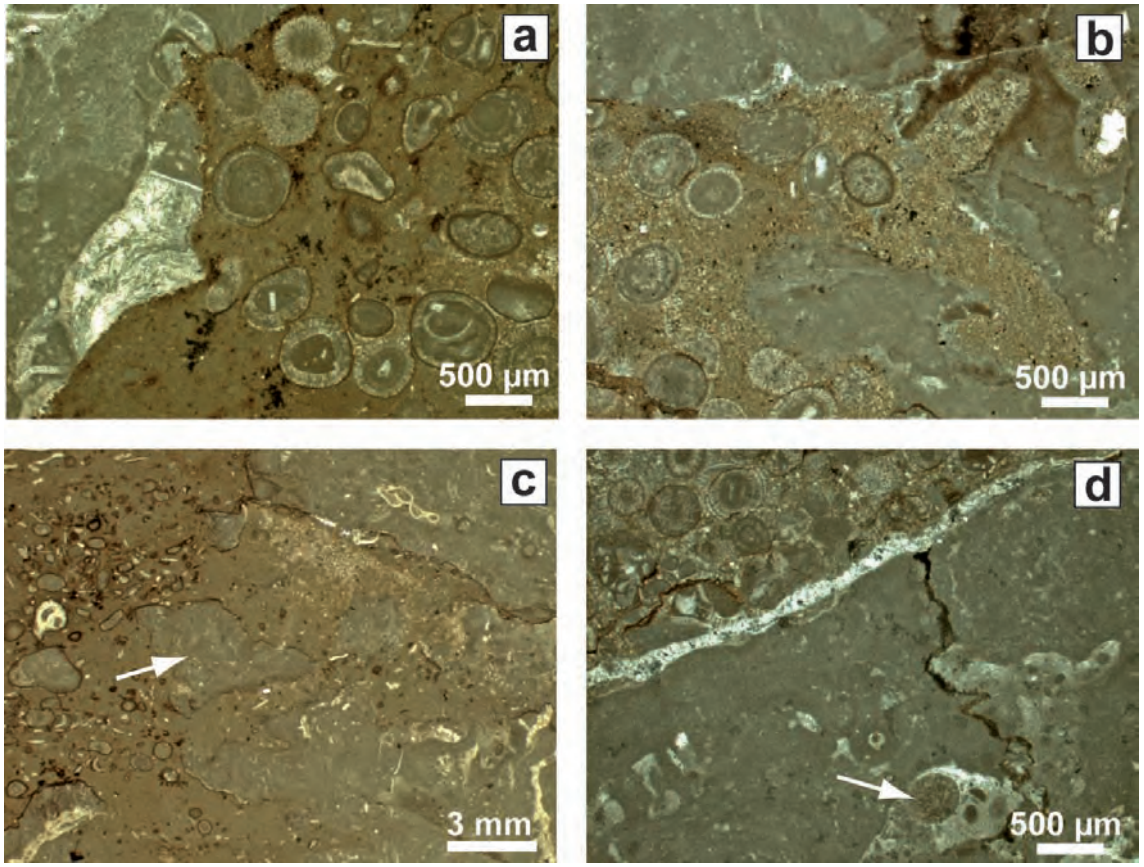

Figure 4.11: *Thin section photomicrographs of the mound-shoal contact, highlighting that both fabrics are clearly not mixed. a) The shoal is cross-cutting the internal structures and b) eroding and incorporating small pieces of the microbialite. c) Eroded microbialite fragments (arrow) are identified inside the shoal deposits. d)Occasionally ooids (arrow) occur inside the growth framework cavities of the microbialite.*

4.2 Microbialite describtion

This section is subdivided into the four scales of observation in microbialite studies: megastructure, macrostructure, mesostructure and microstructure, proposed by Shapiro (2000). This division is adequate to the characteristics of the studied mounds and allows an appropriate separation and detailed description of all observed features (Fig. 4.12).

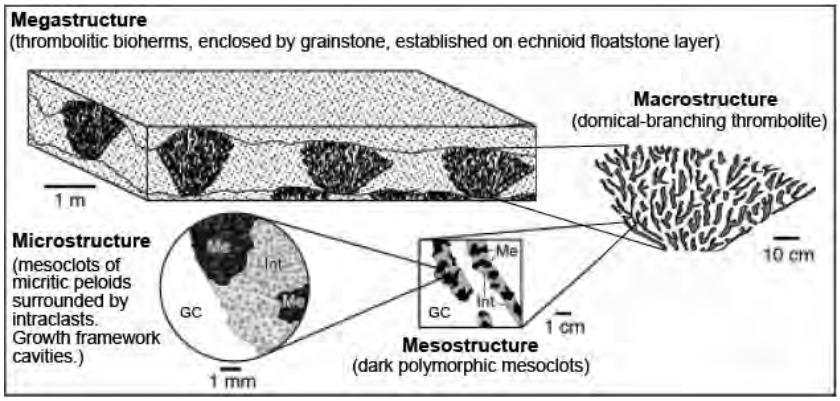

Figure 4.12: *Schematic diagram depicting examples of the spatial relationships between the four scales of observation in microbialite studies (mod. after Shapiro, 2006).*

Following Shapiro (2000) the megastructure comprises the thrombolite bed or buildup at meter to decimeter scale and the macrostructure describes the external and internal shape of the individual microbialite. The mesostructure refers to the internal organization of the microbialite or in other words the internal texture of the macrostructural elements and also includes the description of the microbialite associated biota. Finally, the microstructure describes the microscopic attributes.

4.2.1 Megastructure

The microbial mounds are embedded within shoal deposits forming a continuous layer (4 m thick), which can be followed laterally approx. 80 m in the studied outcrops. The contact between both carbonate bodies is erosional, indicating that the mounds may have developed before the deposition of the shoals (see previous section). The horizontal spacing between single mounds is variable and ranges from 1 to 6.6 m with a mean distance of 2.7 m.

4.2.2 Macrostructure

The studied mounds exhibit high-relief domical growth morphologies of approx. 1.3 m height and 2.5 m width (n = 28), which show often a preferential lateral growth direction. It has been observed that towards the NE the microbial mounds are slightly higher. Single mounds have a maximum height of 2.2 m in the E-IW (mean 1.2 m, n = 14), whereas they reach up to 3.2 m (mean 1.4 m, n = 14) in the N-IF (Fig. 4.13). The mean width is in both outcrops similar and around 2.5 m, possibly indicating a higher vertical growth of the mounds in the N-IF. Nevertheless, also small specimens ranging from 0.5 - 0.9 m height can occur in between bigger mounds in both locations. These smaller mounds are randomly distributed, without a clear trend.

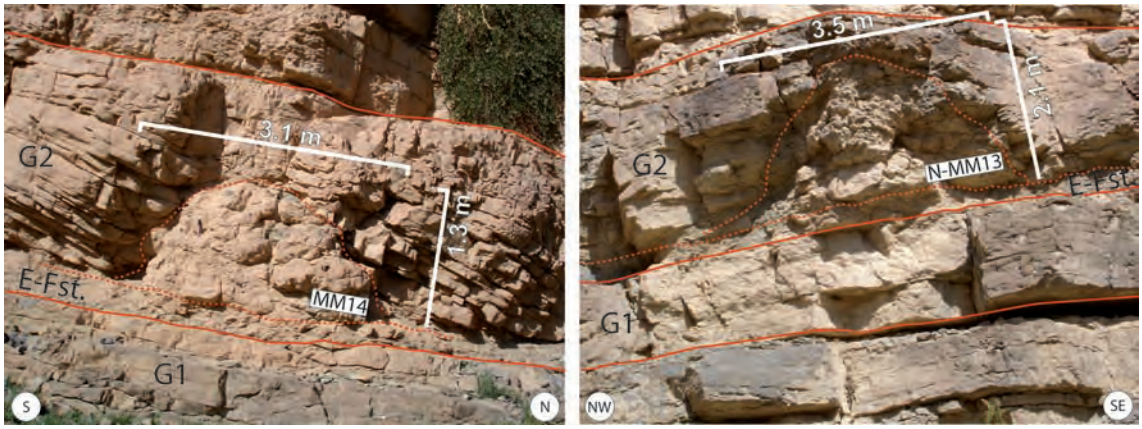

Figure 4.13: *Field photographs comparing domical mounds from the E-IW (left) and N-IF (right) outcrop. The mounds are embedded in the shoal deposits (G1 and G2) and established on top of a layer of echinoid-oyster floatstone (E-Fst). Note that both specimens show the same domical growth morphology, but the mound in the N-IF is almost 1 m higher.*

The microbialites have a macroscopic clotted fabric with no internal lamination, consequently they are classified as thrombolites (Aitken, 1967). The detailed analysis of 37 polished slabs revealed that the thrombolites tend to develop branching growth forms (Fig. 4.14 a). The branches are interconnected and radially arranged showing mainly horizontal growth (Fig. 4.14 b). They have dimensions ranging between 0.5 - 2 mm width and 2 - 5 mm between branching points. The distance between branching points is considered to be the distance over which a single branch splits into two or more branches (red dots in Fig. 4.14 b). In the interspace between branches, irregular shaped growth framework cavities were formed, which will be described below (subsection 4.2.3). In some cases the thrombolites do not develop well-defined branching forms, but appear interlayered to structureless. In plan view the thrombolites show

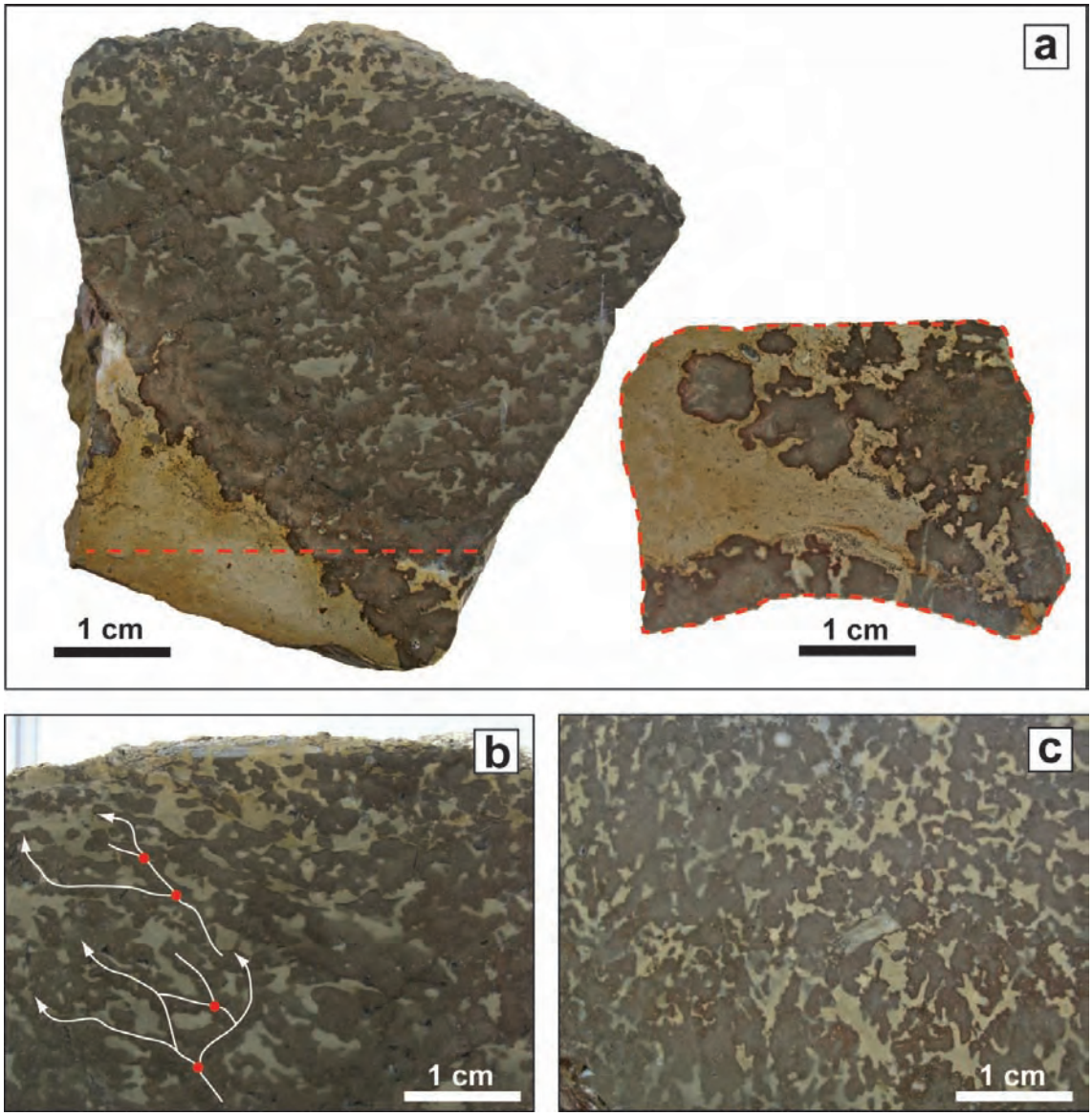

Figure 4.14: *Photograph of polished thrombolite rock chips in a) vertical section and corresponding plan section (dashed line), note the irregular shaped growth framework cavities and the presence of bigger cavities. (b) Vertical section highlighting the branching growth, which generates the growth framework cavities. The branching points are indicated with red dots. c) Corresponding plan section of b) which shows that the cavities are often connected, forming a three-dimensional network.*

a range of shapes, including round, meandroid, polylobate and coalesced shapes (Fig. 4.14 c).

Occasionally, the mounds are connected laterally, bridge-like, with pendant nodular hemispheroids growing downward in their interspace (Fig. 4.15 a, b). The hemispheroids are approx. 25 cm thick and 50 cm in diameter. The occurrence of lateral connected mounds is probably related with the distance between the mounds. It is observed that these hemispheroids develop whenever the distance is shorter.

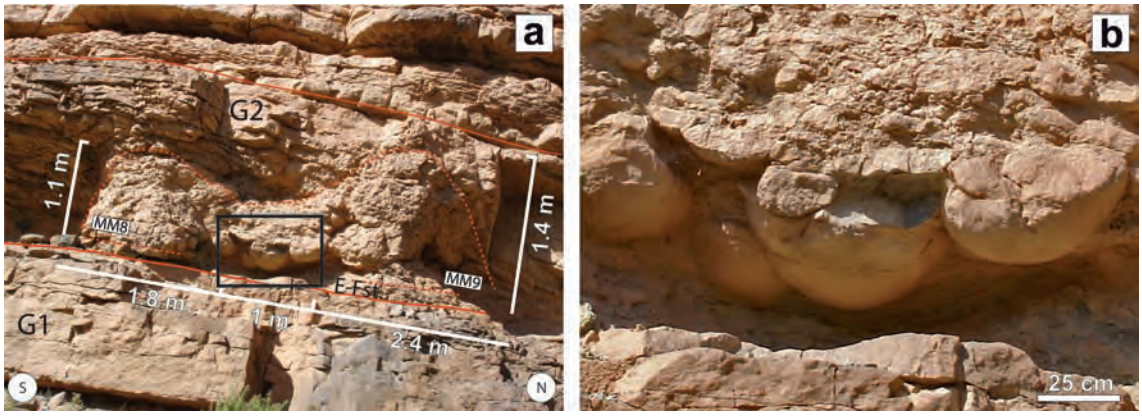

Figure 4.15: *Field photograph of a) two laterally connected domical mounds, which are embedded in shoal deposits (G1 and G2) and established on top of a layer of echinoid-oyster floatstone (E-Fst). b) close up of the black box in a) displaying pendant hemispheroids, which formed on the undersides of the bridge-like connection between the two mounds.*

The hemispheroids overly a thin (approx. 20 cm) layer of marls, which was probably deposited previous or simultaneously. It is plausible, that the hemispheroids were growing downward into this soft sediment, which allowed the development of this shape. In vertical section the hemispheroids clearly show downward growth morphologies. Furthermore, distinct dark layers occur inside the hemispheroids, which are preferentially bored by bivalves and show holes of 2 - 7 mm in diameter (Fig. 4.16 a). These layers are encrusted by bivalves and bryozoans (Fig. 4.16 b, c). They occur not exclusively in the hemispheroids and have been observed also in samples taken from the domical mounds. These layers probably represent intervals of interruption in the microbialite growth, which gave bivalves and other organisms the chance to bore holes and encrust the outer layer of the thrombolite. Furthermore, this specific growth form is characteristic for the Jurassic thrombolites and have been frequently documented in this time period (Leinfelder and Schmid, 2000).

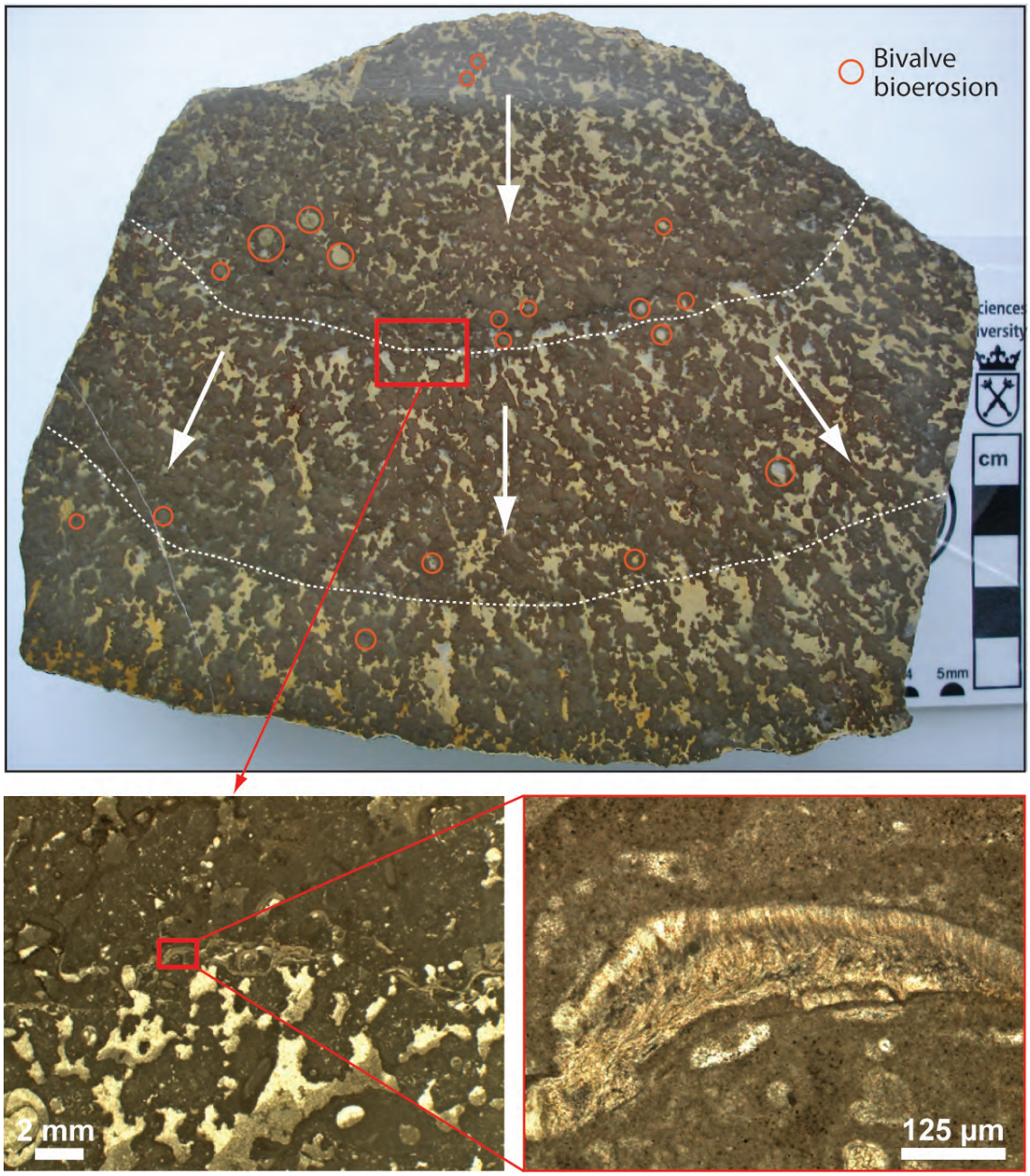

Figure 4.16: *Photograph of polished vertical section (and corresponding thin section photomicrographs) through a downward growing hemispheroid, highlighting periods of possible growth interruptions in which the outer surface of the microbialite became encrusted and bored by bivalves (red circles).*

4.2.3 Mesostructure

The thrombolites are composed of 40 to 60% of dark mesoclots, which are characteristic for their distinct, clotted fabric. The mesoclots occur in clusters and interconnect with each other to form aggregated assemblages. They are usually 2 - 4 mm in diameter and have a micritic, microcrystalline texture. (Fig. 4.17). In addition they display a variety of geometric shapes and different spacial arrangements. The mesoclots are polymorphic. They can be subrounded, digitated, aborescent or pendant and appear as isolated, interconnected or coalesced masses. No clear distribution pattern of morphologies has been observed.

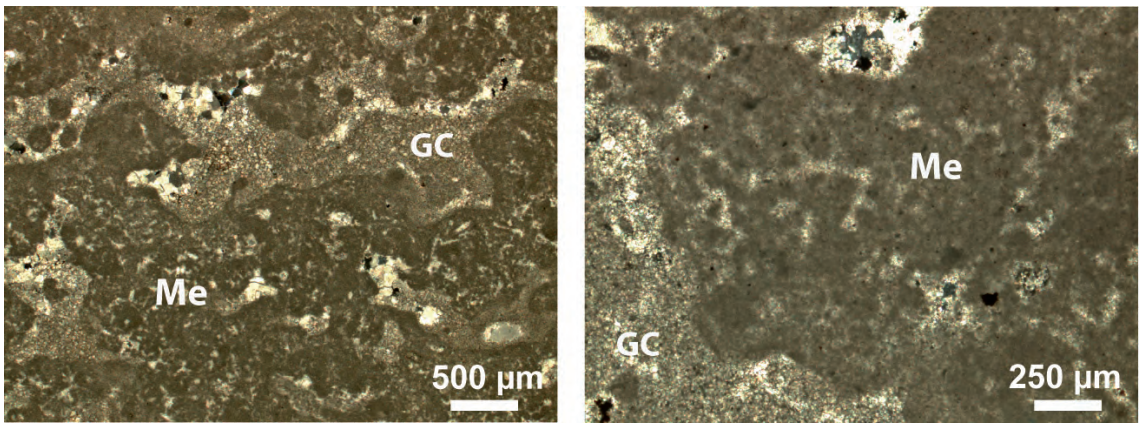

Figure 4.17: *Thin section photomicrographs of polymorphic mesoclots (Me) composed of peloids a. In between the mesoclots growth framework cavities (GC) were formed.*

Another important constituent of the thrombolites are the irregular shaped cavities between the mesoclots, which represent 10 to 30% of the thrombolite total volume. They are normally 2 - 5 mm long and 1 - 3 mm high (Fig. 4.18 a). Their morphology shows that they are often wider than higher, which reflects the preferential lateral growth of the thrombolite. In the literature the cavities are described as "unbound-sediment pockets" (Kennard and James, 1986), "large original pores" (Aitken, 1989) or "irregular fenestrae" (Riding, 2000). In this study they are termed growth framework cavities to emphasize that they are the result of the branching growth of the thrombolite, representing the remaining spaces between the mesoclots (Fig. 4.18 c, d). They are filled with yellow, silty sediment and show a wavy, geopetal fabric. Most of these cavities are half-filled with sediment at the base and sparry calcite at the top, but some of them are entirely filled with sparry calcite (Fig. 4.18 b). Both of the infillings can be partly or completely dolomitized.

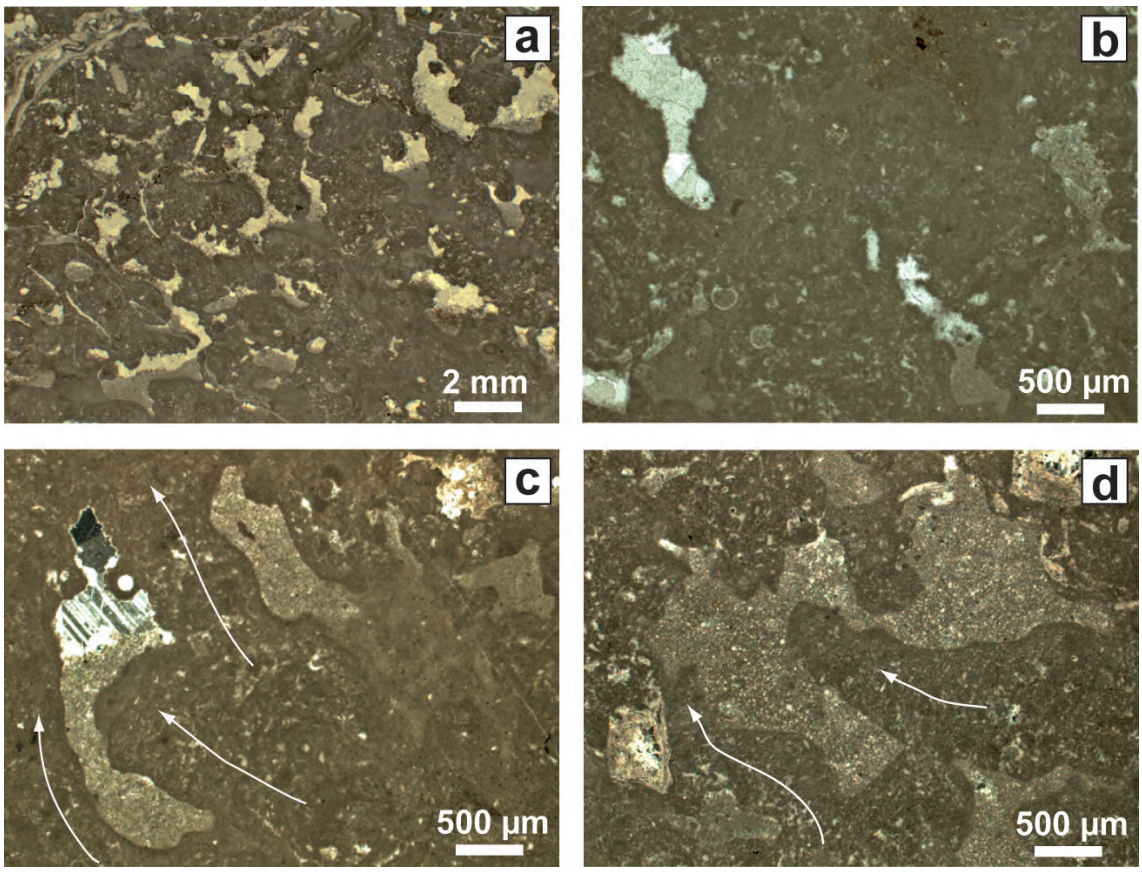

Figure 4.18: *Thin section photomicrographs of irregular shaped growth framework cavities. They are characterized by a wavy geopetal filling (a), can be unfilled, half-filled or completely filled with silty or dolomitized sediment (b) and are formed due to the branching growth of the thrombolite (c, d).*

Looking at the vertical and plan sections of the polished slabs (Fig. 4.14) it is observed, that most of the cavities are connected with each other forming a three-dimensional network. Most probably the filling of this pore network occurred syn- or post-depositional to the thrombolite growth. At the contact region with the shoal deposits, occasionally ooids and shell fragments can be found inside these cavities (Fig. 4.11 d). It is remarkable that the growth framework cavities are the only places where ooids occur inside the thrombolite. The here described cavities look similar to stromatactis cavities and could be confused with them at a first view. However, stromatactis mounds are not very common in the Mesozoic and generally considered typical for Paleozoic subtidal marine facies (Krause et al., 2004). Contrary to the observed growth framework cavities, stromatactis cavities usually have flat floors, digitated roofs and occur in reticulate swarms. Their origin is controversial, but they are believed to be cavities, which remained after the decomposition of sponges and became filled subsequently with radiaxial fibrous calcite (Aubrecht et al., 2009). All these differences leave no doubt to assure that the growth framework cavities in the thrombolites of Morocco are clearly no stromatactis cavities.

Microbialite associated biota

A variable fauna of microencrusters and metazoans, such as corals, sponges, bryozoans, brachiopods, bivalves, forams and *Thaumatoporella*, inhabit the thrombolite, representing approx. 5 to 10% of the volume. Sometimes pure thrombolite fabrics with little amounts of bryozoans, brachiopods and bivalves have been also observed (e.g in the hemispheroids). Corals inside the thrombolite occur *in situ*, but are relatively scarce and almost entirely recrystallized, making their taxonomic classification impossible. The observed corals exhibit branching forms, with 7 - 13 mm long branches of 3 - 8 mm diameter and occasionally thin platy forms (5 - 15 mm thick). The platy corals encrust bivalves (Fig. 4.19 a), which at the same time colonized and encrusted the dark, undulating layers inside the microbialite (see above 4.2.2). It has been observed that in the core region and the upper parts of the mound, the corals develop more branching growth forms, which are surrounded by thick layers of thrombolites. All studied corals are bored by bivalves (Fig. 4.20 b). It is assumed that these corals were growing simultaneously with the surrounding thrombolites. Therefore the thrombolites must have grown relatively fast with more or less similar rates as the corals. Although *in situ* growing corals inside thrombolites are not so common, they have been reported also by other authors (Pratt & James, 1982; Leinfelder 1993, Dupras & Strasser, 1999;

Kahle, 2001). In general branching growth forms indicate environments with low wave energy in shallow water depths.

In the the microbial mounds two different classes of sponges were identified: *Calcarea* and *Demospongiae*. The third class of sponges (*Hexactinellida*), which inhabit deep water settings is absent. Sponges are in general characterized by great adaptability, thus they can grow in shallow and deep environments. Most of them are active filter feeders, which pump seawater through a series of complex internal channels and chambers to trap small plankton particles. The calcareous sponges (order of *Pharetronida*) are slightly more abundant in the mounds, than the demosponges and their skeletons and spicules are made of calcite. They are 2 - 4 cm in diameter, have a rounded to elongated shape and a leuconoid body form (Fig. 4.19 c). This arrangement, with a great degree of folding of the body wall, allows a more efficient pumping system and represents the form of highest complexity. The calcareous sponges need a hard substrate to settle and are often found growing on top of bryozoan crusts, but also attached to the mesoclots.

The skeletons of demosponges are composed of a relatively soft material, called sponging, which is often not preserved. For this reason it is very difficult to classify taxonomically these sponges. The only hint for their former presence are their siliceous spicules, which are often replaced by calcite. However, some spicules which still preserved their original siliceous composition have been identified with the SEM/EDX. Furthermore, some ghost structures inside the thrombolite can be found, which seem to resemble former sponge networks. After the sponge dies, the small spicules are easily detached from the sponge body and will be dispersed. Small clusters of up to 7 mm long spicules (2 mm in diameter) occur distributed all over the mound (Fig. 4.19 d). During the Middle Jurassic siliceous sponges represented important reef builders and occurred often associated with microbialites (Leinfelder et al., 1994), but these associations were more abundant in deeper settings and mostly absent in shallow water environments (Leinfelder & Schmid, 2000).

The identified bryozoans are mainly represented by the cyclostomate *Berenicea*, which is commonly ladder-shaped and present in almost all studied thin sections (Fig. 4.19 e). They occur *in situ*, either as free-living specimens or encrusting other organisms (corals, bivalves, brachiopods) or mesoclots. The colonies are formed by series of simple compartments (zooecia), which are typically less than 1 mm in diameter and length. The zooecia have thin, elongated wall structures composed of calcite and are often filled with granular calcium carbonate crystals. In the cases where the bryozoans occur as

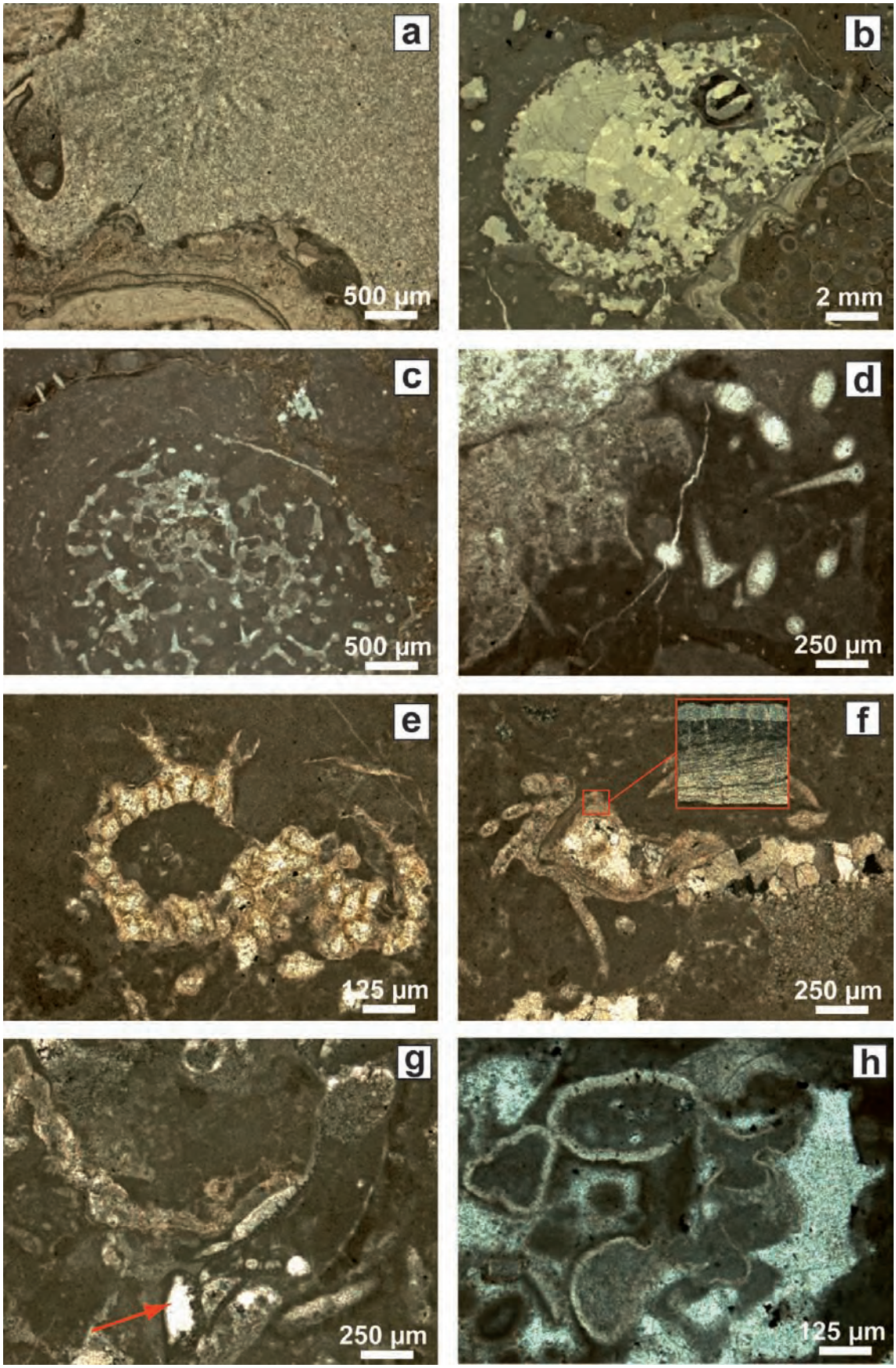
a
500 µm
b
2 mm
c
500 µm
d
250 µm
e
125 µm
f
250 µm
g
250 µm
h
125 µm

encrusters the colonies often consist of a single layer of zooecium in contact with the substrate and are overlain by a layer with erected, branching growth forms. Bryozoans are known as sessile, filter-feeding organisms adapted to a wide salinity range, which usually thrive under low sedimentation rates. The observed delicated, erected growth forms may be indicative of low-energy settings (Scholle, 2003).

The identified brachiopods are 1 - 4 cm in diameter and their shells (2 - 3 mm thick) are mostly articulated. The shells are characterized by three distinct microstructural layers: an outer fibrous and punctuated, a second foliated and an inner prismatic (Fig. 4.19 f). It has been observed that the brachiopods often grow attached to the boreholes of bivalves and to growth framework cavities; their shells are often encrusted by bryozoans.

The microproblematic algae *Thaumatoporella* has been observed in some thin sections, forming approx. 300 μm long bridges over internal sparitic chambers (Fig. 4.19 g). Inside their thin outer walls a dense network of almost round pores of approx. 20 μm is visible. The erected algal bridges grow repetitively over each other and are often encrusted by bryozoans. *Thaumatoporella* is reported to occur often together with the microproblematic *Bacinella* (Leinfelder et al., 1993), but is not the case in the studied mounds. Originally regarded as red algae or as a sponge, *Thaumatoporella* is now interpreted as belonging to a separate group of green algae (De Castro, 1990). This species represent a shallow-water indicator (Leinfelder et al., 1993), commonly occuring in lagoonal and reefal settings of Mesozoic carbonates (Flügel, 2004).

The encrusting and dwelling foram *Bullopora tuberculata*? has been found occasionally (Fig. 4.19 h). *Bullopora* is composed of small, ball-shaped chambers (approx. 200 μm in diameter), which are linked with each other. They have curvy calcareous walls with thin spines on the test and rarely display a regular shape. These forams were reported to grow attached or intertwined with sponge meshworks (Guilbault et al., 2006), but in the observed cases they were found either inside mesoclots or corals.

The most abundant bioeroders inside the mounds are boring bivalves (lithophags). These bivalves are characterized by thin, heart-shaped shells covered with little spines

Figure 4.19 (preceding page): *Thin section photomicrographs of the skeletal components of the thrombolite. a,b) Recrystallized corals encrusting bivalves, which encrusted the outer surfaces of the microbialite in periods of growth interruption. c) Skeleton of calcareous sponge of the order Pharetronida; d) Calcified spicules of silicious demosponge; e) Free growing bryozoa (Berenicea) with elongated wall structures filled with calcite; f) Brachiopod with the three distinct microstructural layers inside the shell, attached to a growth framework cavity and encrusted by bryozoa; g) Thaumatoporella algal bridges (red arrow) encrusted by bryozoa; h) Dwelling foram Bullopora with ball-shaped chambers inside a recrystallized coral.*

and apply chemical substances to dissolve the substrate. They bore circular holes of approx. 1cm into hard coral skeletons as well as in the microbial crusts, which implies early lithification of the microbialites (Fig. 4.20 a). In some cases, the lithophags were observed to keep up with the growth oft the coral and form stacked shell layers (Fig. 4.20 b; Kleeman, 1994). The two valves occur always articulated. The shells are often present in their bore holes, which show a geopetal filling or are completely filled with peloidal micrite. Lithophagid bivalves mainly occur in shallow water environments (Bromley, 1994; Leinfelder et al., 1994).

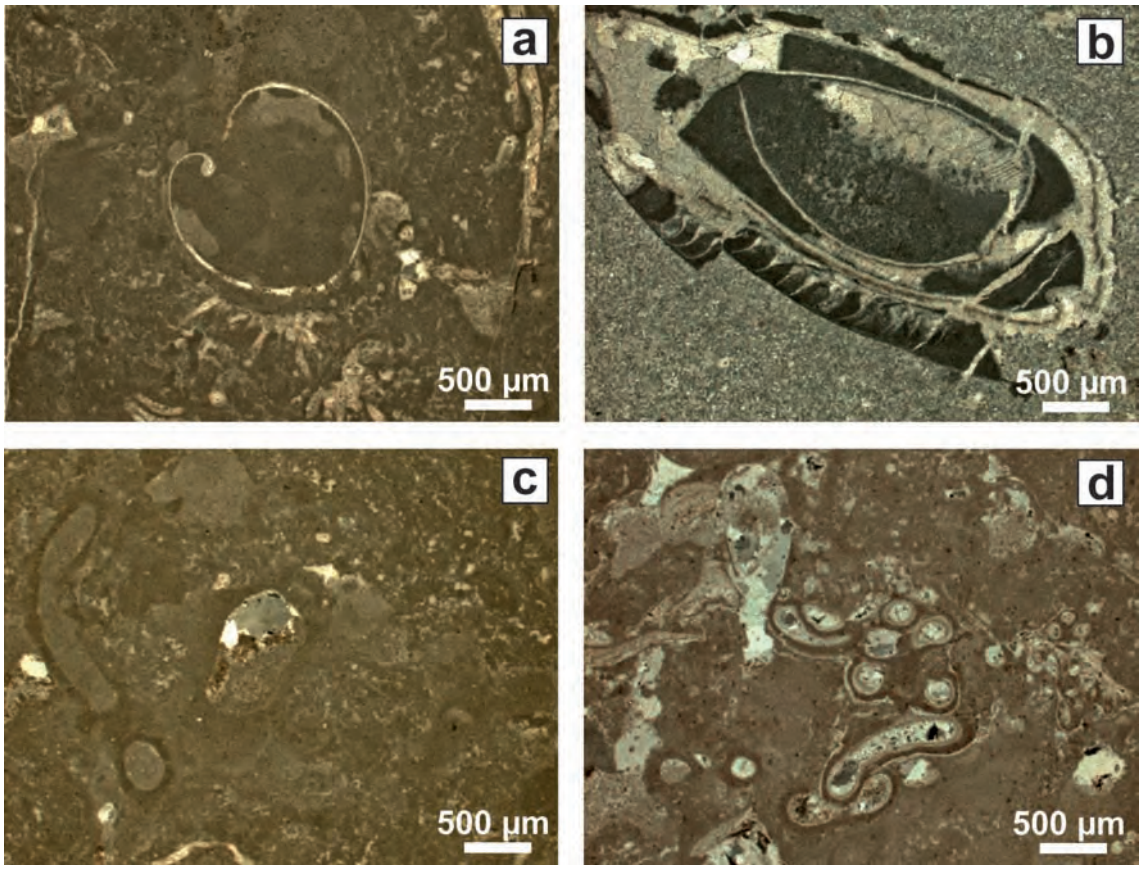

Figure 4.20: *Thin section photomicrographs of bioeroding bivalve and annelids. a) Lithophagid bivalve with heart shaped shell, which is encrusted by bryozoa, boring a circular hole inside the thrombolite; b) Boring lithophagid bivalve with little spines on the shell, which keeps up with the coral growth forming stacked shell layers, note the peloidal infilling of the chamber; c) Worm tubes of Terebella lapilloides in longitudinal and cross-sections with agglutinated micritic wall and fillings of micrite; d) Clusters of serpulid worm tubes hard filled with sparry calcite.*

Annelids are represented by terebellid and serpulid worm tubes. These organisms have burrowed horizontal and vertical tubes in the microbialite, which can be up to 1.7 cm long with a diameter of 2 - 4 mm. Terebellid worm tubes are characterized by an

agglutinated micritic wall and are filled with micrite. They are assigned to the species *Terebella lapilloides* (Fig. 4.20 c). The serpulids (*Serpula*) show calcareous walls and occur as hard tubes filled with sparry calcite, which often appear in clusters (Fig. 4.20 d). In general all the annelid tubes are rimmed by a a dark 1 mm-thick area, which appear when organisms bore in a hard, but still not completely lithified material. They are hard substrate encrusters in shallow waters (Scholle, 2003).

4.2.4 Microstructure

The mesoclots are composed of homogeneous masses of dense micrite grading to densely packed clusters of dark, micritic peloids (Fig. 4.21). Locally the mesoclots are coated by isopachous rim cement. The peloids are characterized by a relatively small size of 30 - 60 μm and have round to elongated shapes. They are surrounded by lighter colored microsparite, which rims the individual peloids and fills the inter-peloid space. Peloids can also fill the chambers of bivalves (Fig. 4.20 b) and growth framework cavities. The observed gradations from homogeneous micrite to individual peloidal grains may have resulted from different intensity of the microbial mat calcification. According to Kazmierczak et al. (1996) mats growing under high calcium carbonate supersaturation produce almost homogeneous micrite, whereas in less intensively calcified mats micritic peloid-like bodies are formed.

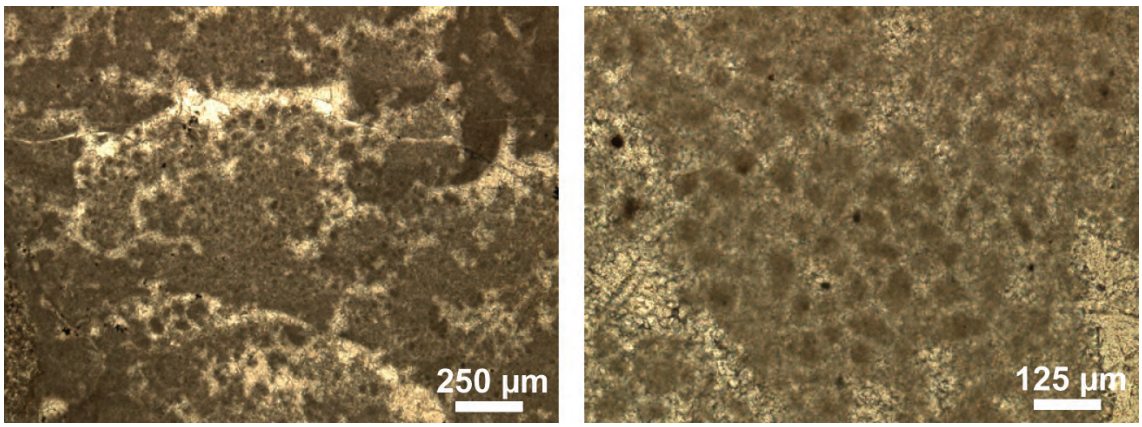

Figure 4.21: *Thin section photomicrographs showing that the mesoclots are composed of micritic peloids and are sometimes coated by isopachous rim cement. The peloids are surrounded by microsparite and form densely packed clusters, which grade into dense micrite.*

4.2.5 Biogenic structure

To unravel the possible origin of the peloidal microfabric extensive SEM examinations of polished and etched thrombolite samples were carried out. The analysis confirms the diffuse presence of organic matter, which can be divided into two characteristic structures.

The first one consist of is a honeycomb-like structure with meshes of various sizes (Fig. 4.22) and the second one is represented by spherical bodies which occur inside the honecomb-like structure (Fig. 4.23). The honeycomb-like pattern consist of meshwork of subpolygonal to subspherical pits and walls. This meshwork is irregularly distributed, but visible throughout the whole etched surface of the sample, due to its bright colors, (Fig. 4.22 a). The average diameter of the pits ranges between 3 - 10 μm and the flaky walls of the pits have different thicknesses. Thicker walls are on average 1 - 2 μm thick and thinner walls are 0.5 - 1 μm. The thicker walls usually enclose the largest pits and in some cases also groups of thin-walled smaller pits (Fig. 4.22 b - e). The result of the EDX analysis reveals that the walls of the pits are either composed of calcite with high admixtures of Al - Fe silicates and some Mg, K (Fig. 4.22 f) or high-Mg calcite (Fig. 4.22 h). The area in between and around these structures is composed of calcite. The honeycomb-like pattern has been interpreted as fossilized EPS matrix, which very similar to capsules and mucilage sheaths of modern colonial cyanobacteria and most probably represent their mineralized remains (Trichet et al., 2001, Kazmierczak et al., 2009). Locally also twisted, filamentous-like structures (5 - 15 μm in length) can be recognized inside the honecomb-like pattern, which may represent tubular moulds of bacteria (Fig. 4.22 g). Also in other studies of modern and fossil coccoid cyanobacterial mats similar patterns have been identified and were interpreted as result of the selective degradation and mineralization of an organic EPS matrix (Kazmierczak et al., 1996, 2004, Dupraz et al., 2004). The textures and internal structure of EPS can be preserved and mineralized by a variety of elements, such as Al-K-Fe silicates or high-Mg calcite (Camoin et al., 1999; Perri & Tucker, 2007; Kazmierczak et al., 2009). Further observations in decaying colonies have shown, that the intracellular material and the relatively thin inner sheaths, which enclose single cells and small groups of cells, decompose first. The thick sheaths, that form the outer sheath of the colonies or enclose larger groups of cells seem to be more resistant to biodegradation and decomposition. Therefore they often remain as the only traces of the primary colonial organization in fossil coccoid cyanobacteria (Kempe

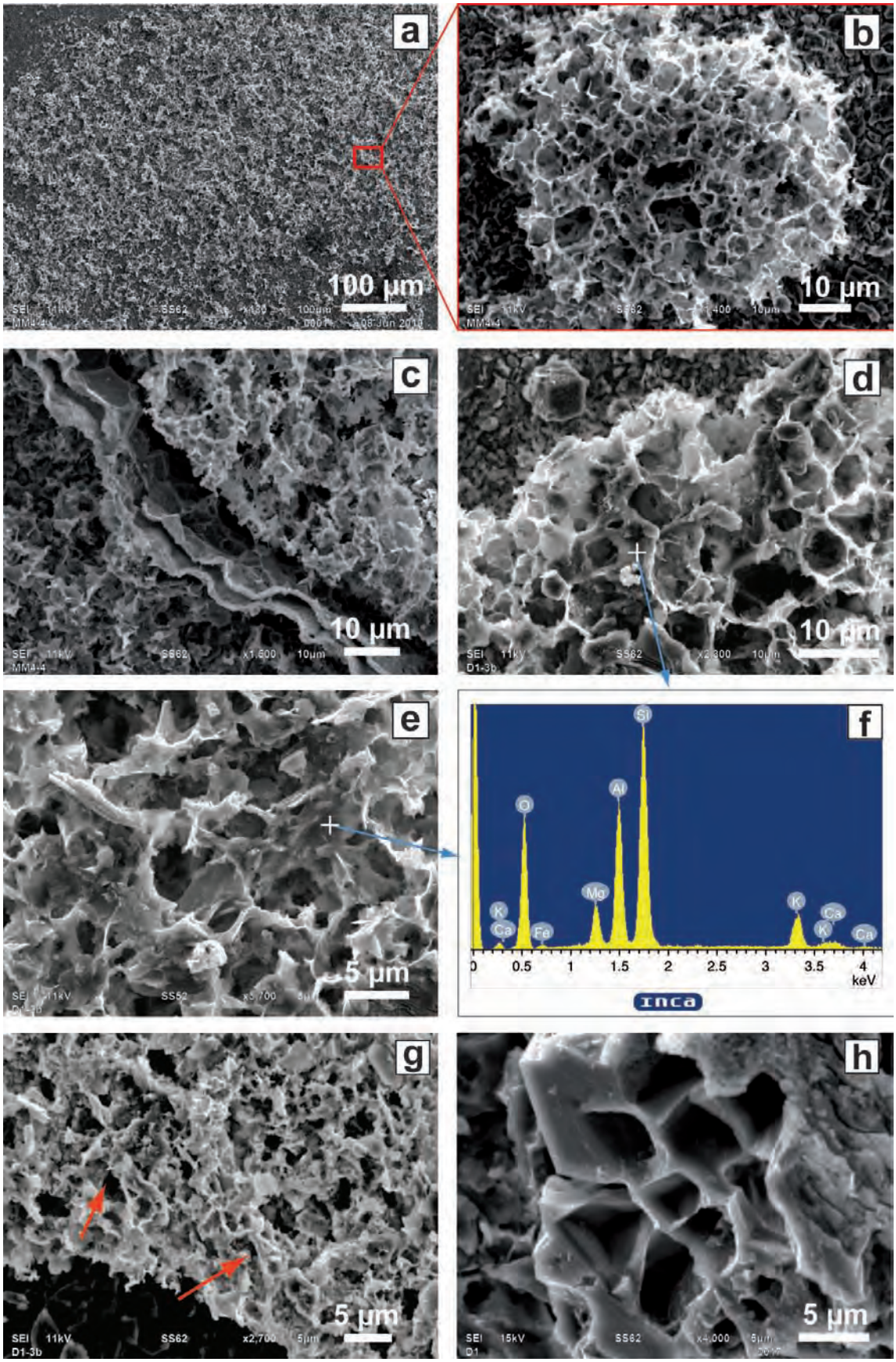
a
100 µm
b
10 µm
c
10 µm
d
10 µm
e
5 µm
f
Si
O
Al
Mo
Fe
K
Ca
0
0.5
1
1.5
2
2.5
3
3.5
4
keV
INCA
g
5 µm
h
5 µm

& Kazmierczak, 1993).

The second characteristic structure is represented by spherical, egg-like bodies of 1 - 3 μm in diameter, which occur inside or close to the pits (Fig. 4.23 a, b). These spheres have a smooth surface and are distributed loosely within the meshwork, appearing alone or in clusters of several specimen. Some of them are closely attached and welded with each other, giving the impression of dividing bacterial cells (Fig. 4.23 c). Compared with modern analogues, the shape, size and location of the spherical bodies leads to the conclusion that they may represent the mineralized remains of bacterial coccoids, as interpreted by Kazmierczak et al. (1996, 2009). In their work from 1996 they compared

Figure 4.22 (preceding page): *SEM photomicrographs of honey-comb like structure, interpreted as the mineralized remains of the EPS matrix. a) The structure is irregular distributed and sticks out well from the surrounding area. b - e) The pattern consists of meshwork of subpolygonal to subspherical pits and walls, which are f) composed of calcite with high admixtures of Al - Fe silicates and some Mg, K. g) Locally twisted, filamentous-like structures (arrows) occur inside the meshwork. h) The whole structure can also be composed of high-Mg calcite.*

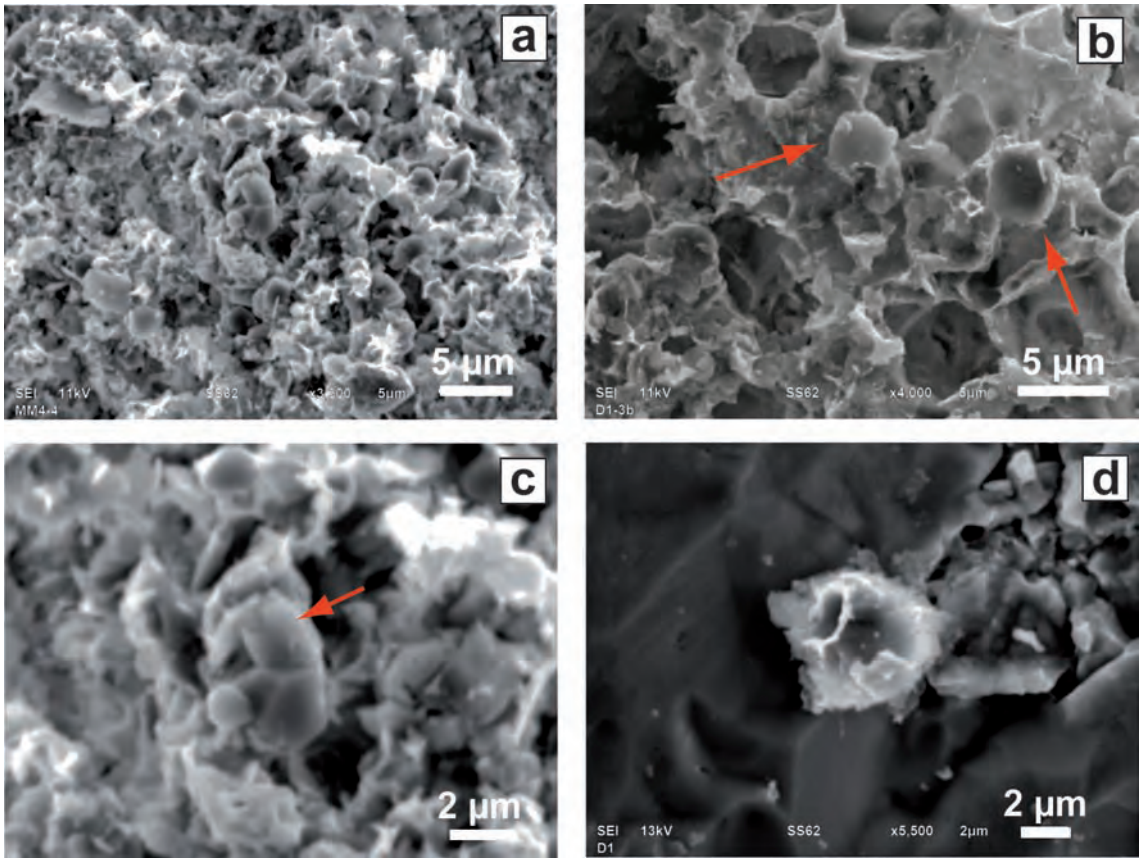

Figure 4.23: *SEM photomicrographs spherical, egg-like bodies interpreted as coccoid bacterial fossils. a, b) The spheroids occur in clusters of several specimen inside or close to the pits (arrow). c) Sometimes the look like dividing bacterial cells (arrow), or are (d) partly covered by fragments of silicified mucilage.*

the bacterial remains found in micritic and peloidal limestones from Late Jurassic deposits of Poland with modern cyanobacterial communities producing micrite and peloidal microbialites in Lake Van, Turkey. In both cases they observed subpolygonal structures with striking similarities and concluded that they might be the result of similar *in situ* calcified cyanobacterial microbiota. EDX anaylsis of the coccoidal cells show that they have been mineralized by Al-K-Fe silicates, as in the case of modern bacterial cells (Kazmierczak et al., 2009). Fragments of silicified mucilage were found partly covering the spheroid cells (Fig. 4.23 d).

In studies of modern and fossil examples, it has been suggested that the EPS matrix represents the place were carbonate minerals nucleate and grow. In the studied samples different stages and products of this precipitation have been identified. The initial precipitation products are aggregates of high-Mg calcite with rounded to smoothly angular crystal shapes (Fig. 4.24 a, b). The precipitates have a size of 1 - 2 μm and occur inside and attached to the EPS matrix and may subsequently merge to larger, rounded high-Mg calcite aggregates of 5 - 10 μm (Fig. 4.24 c, d). Subsequent ongoing precipitation of the EPS matrix will lead to complete calcification/replacement, as could be observed in some cases (Fig. 4.24 e, f). At a last step the remaining porosity (in the EPS-free substrates) is filled with microsparite. Surprisingly it was not possible to clearly identify peloids with the SEM, even though they are quite abundant and recognizable under the petrographic microscope.

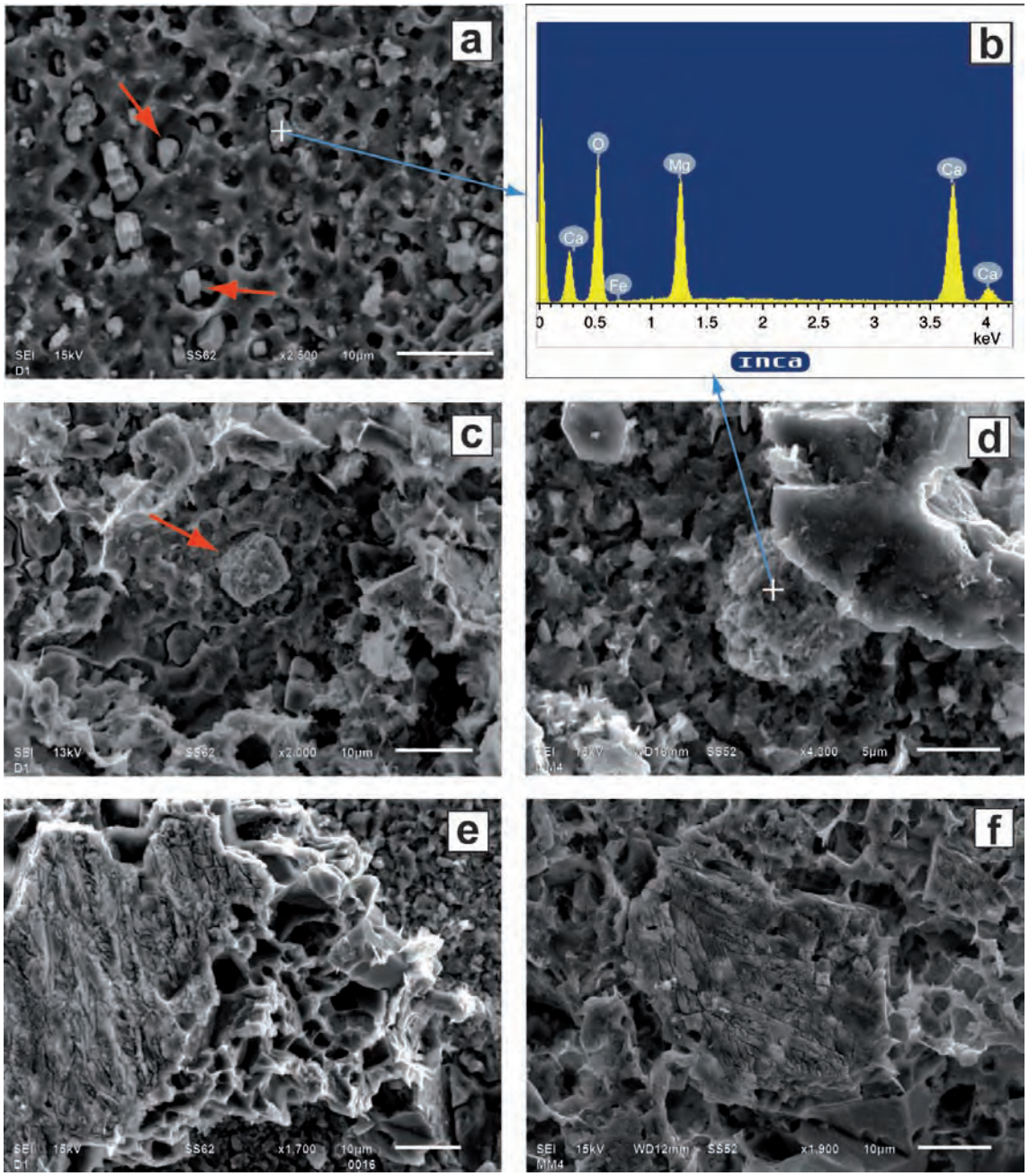

Figure 4.24: *SEM photomicrographs of EPS matrix replacement by high-Mg calcite. a, b) Precipitation of high-Mg calcite aggregates inside EPS. c, d) The precipitates successively merge to larger high-Mg calcite spheres. e, f) Almost completely replaced/calcified EPS matrix.*

4.3 Mineralogical description

Mineral structures composed of calcite pseudomorphs after gypsum and hematite pseudomorphs after framboidal pyrite were found inside the thrombolites.

Calcite pseudomorphs

The calcite pseudomorphs after gypsum occur exclusively inside the growth framework cavities of the thrombolite and in the shoal deposits (G2) in close contact with the mounds (Fig. 4.25, Fig. 4.26).

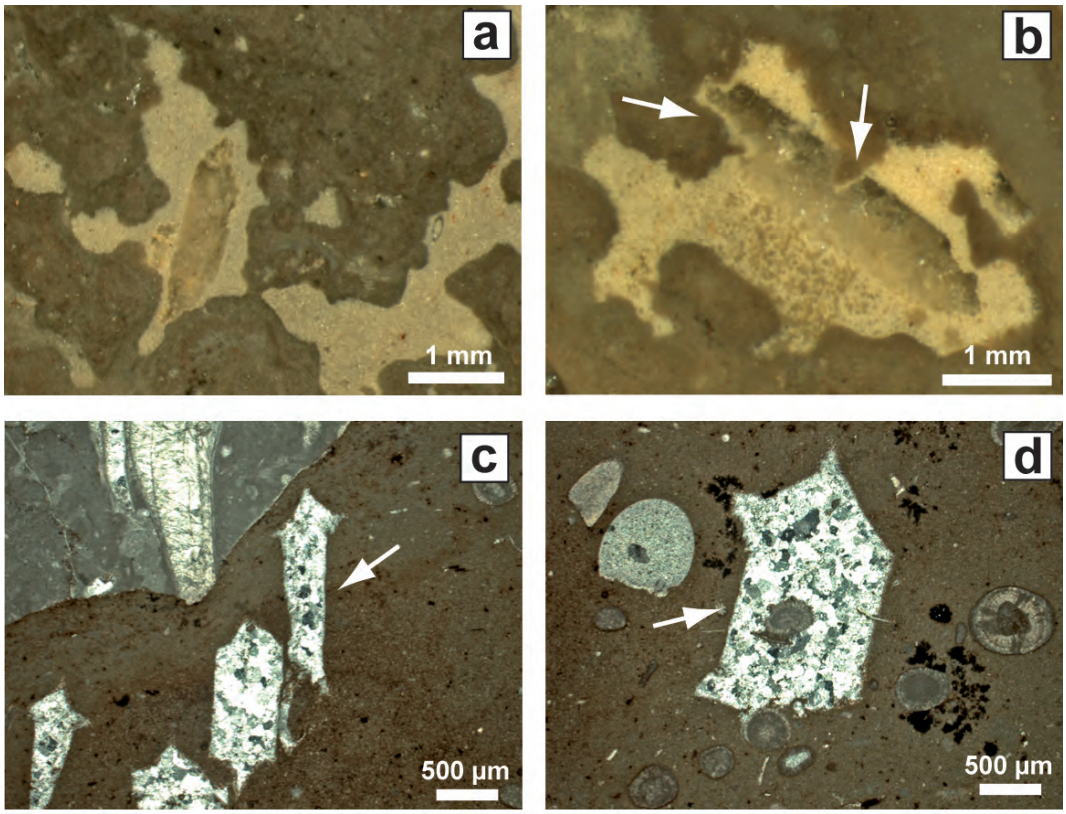

Figure 4.25: *Photographs (a, b) and thin section photomicrographs (c, d) showing calcite pseudomorphs after gypsum found in growth framework cavities of the thrombolite and in shoal deposits. a, b) Euhedral crystals, which have partly adapted their shape to the form of the cavity (arrows). c, d) Pseudomorphs showing slightly concave crystal faces in contact with the surrounding sediment (arrows)*

The crystals are lenticular and can be up to 4 mm long and 1 mm wide. They are present inside the cavities of more than 60% of the analyzed samples. The shape of the crystals is often adapted to the form of the cavities, demonstrating that they precipitated inside the cavities (Fig. 4.25 b). The former gypsum appears as single, almost

euhedral crystal or forms rosette-like, radial twins, which are very characteristic for gypsum (Fig. 4.25 a, Fig. 4.26 a). The crystals found in the shoal deposits have similar dimensions to the crystals in the cavities of the thrombolite, but differ from them in the fact that they show slightly concave crystal faces in contact with the surrounding sediment (Fig. 4.25 c, d). The latter indicates that the sediment was not completely lithified during the time of the crystal formation. The crystals started to precipitate probably in small molds and while growing, they successively pushed the surrounding sediment away. Therefore, it can be assumed that the precipitation of the gypsum in the shoal deposits might have been synsedimentary. Moreover, the pseudomorphs in the shoal deposits occur in areas which have a higher amount of matrix (wackstone to packstone texture) and contain less ooids (Fig. 4.26 a, b).

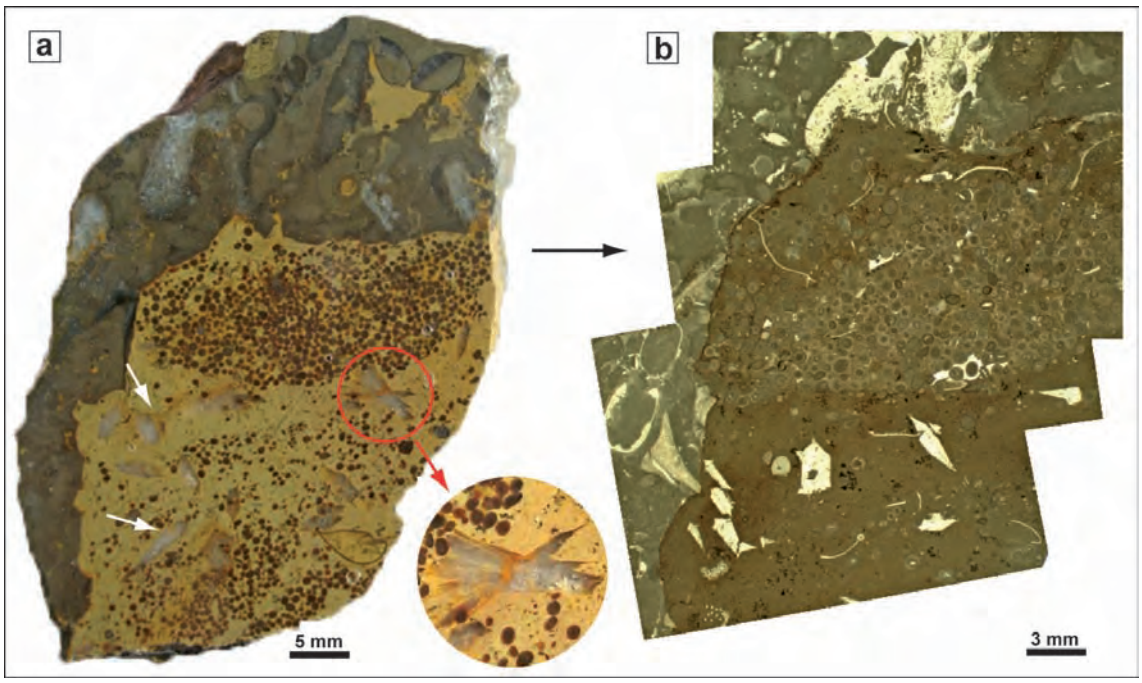

Figure 4.26: *Photograph of polished slab (a) and corresponding composite thin section photomicrograph (b) of Gypsum pseudomorphs found in shoal deposits close to the thrombolite. They crystals (white arrows) occur in areas characterized by a higher amount of matrix and less ooids. Note also the presence of radial twins, which are characteristic for gypsum (circle).*

EDX analysis show that the gypsum has been almost completely replaced by calcite. Therefore only minor sulfur inclusions are still present inside the crystals (Fig. 4.27 a, b). These small inclusions (not more than 30 μm in size) also contain a significant amount of strontium forming the strontium sulfate mineral celestite.

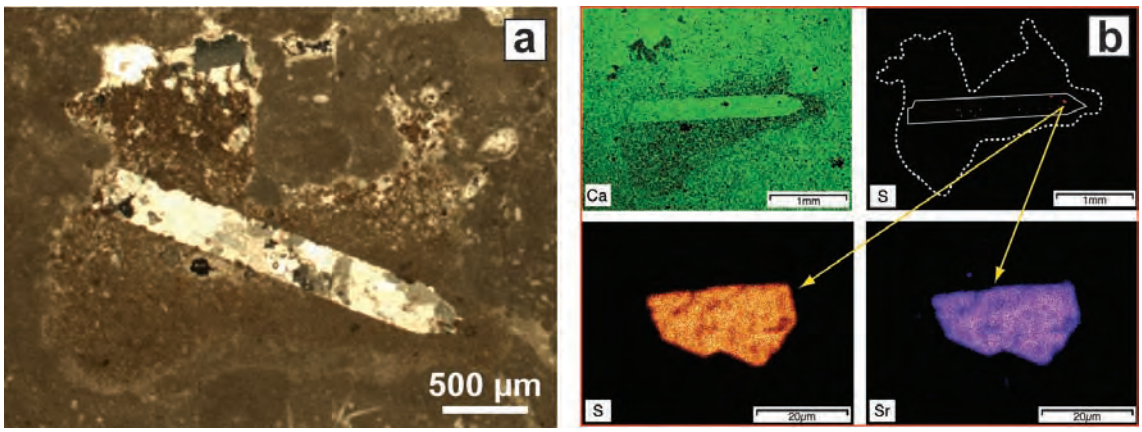

Figure 4.27: *Thin section photomicrograph of a calcite pseudomorph after gypsum crystal inside a growth framework cavity of the thrombolite (a) and corresponding EDX mapping (b), showing that the gypsum has been almost completely replaced by calcite and only minor sulfur inclusions are still present inside the crystals (red points in the outlined crystal). The inclusions are composed of strontium sulfate mineral celestite (arrows).*

It can be argued if the identified crystal pseudomorphs were primary gypsum, like proposed, or if they were completely composed of celestite. Both minerals have a similar appearance, but in general gypsum is by far a more common mineral in the sedimentary record. Celestite occurs often together with gypsum but also in calcite pseudomorphs after gypsum (Sanz-Montero et al., 2009). However, a study of Madsen & Stemmerik (2009) explains the possibility of forming early diagenetic celestite as replacement of spicules and body tissues in dead demosponges. In this study the occurrence of celestite is restricted to the bodies of dead sponges, which is not the case of the present study. Furthermore, celestite was interpreted as a by-product of sulfate-reducing bacteria in microbial mats (Tabener et al., 2002). Bacterial sulfate reduction of calcium sulfates (mainly gypsum) provided sulfide and and soluble strontium, which can then re-precipitate as calcite by bacterial oxidation of sulfide (Sanz-Montero et al., 2009). As in most of the cases the celestite occurs associated with gypsum it is beyond the scope of this work to investigate deeper this origin.

As a general rule, a more soluble mineral will always be replaced by a less soluble mineral. The solubility product is expressed by the equilibrium constant (Ksp) of a reaction in which a solid evaporite mineral dissolves to give its constituent ions in solution. The equilibrium constant for gypsum is lower than that from celestite and calcite (Tab. 4.1). Hence, when the gypsum was not stable anymore it started to be replaced first by celestite and after by calcite. This would explain why there are still small remains of celestite preserved inside the crystals.

mineral	formula	KSP
gypsum	$CaSO_4\ 2H_2O$	$10^{-4.58}$
celestite	$SrSO_4$	$10^{-6.64}$
calcite	$CaCO_3$	$10^{-8.41}$

Table 4.1: *Equilibrium constants (Ksp) for gypsum, celestite and calcite*

Hematite pseudomorphs

Small grains of iron oxides appear scattered throughout the whole thrombolite and often occur in higher concentrations around the growth framework cavities, in which they also occur (Fig. 4.28). These spheroidal or sometimes cubic mineral aggregates have a dark red color and are usually 5 - 15 μm in size.

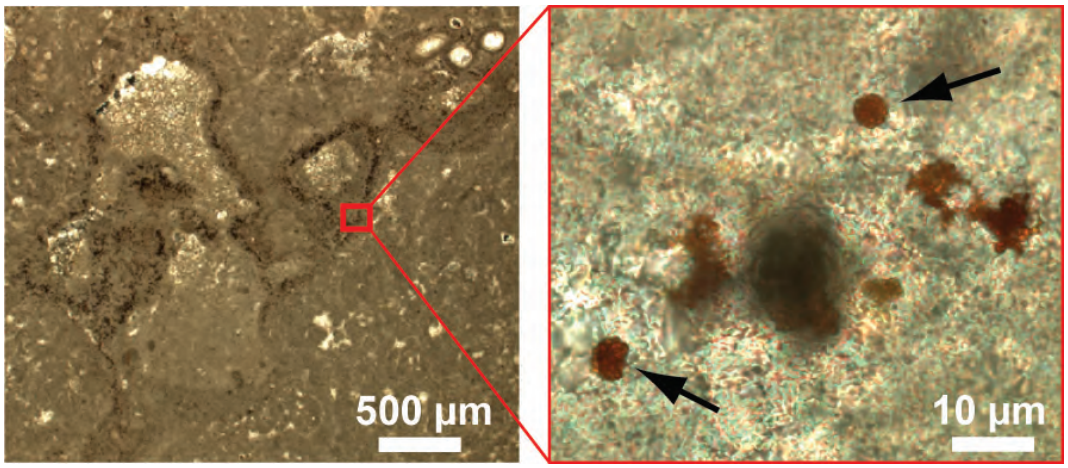

Figure 4.28: *Thin section photomicrographs of spheroidal grains of iron oxide (arrows), which occur in high concentrations around the growth framework cavities of the thrombolite.*

With the SEM it can be observed, that the spheroidal aggregates are often encased by calcite and consist of randomly distributed, euhedral (mainly octahedral) microcrystals (0.5 - 2 μm) (Fig. 4.29). These so called "framboids" often occur in clusters of four or more specimens in close contact to the growth framework cavities of the thrombolite and are encased by calcite. The term "framboid" was introduced by Rust (1935) for clusters of tiny pyrite cubes and grains after framboise (French for "raspberry"), because of the external similarity. Framboids are exclusively formed by pyrite and are indicative of early diagenetic origin (Farrand, 1970).

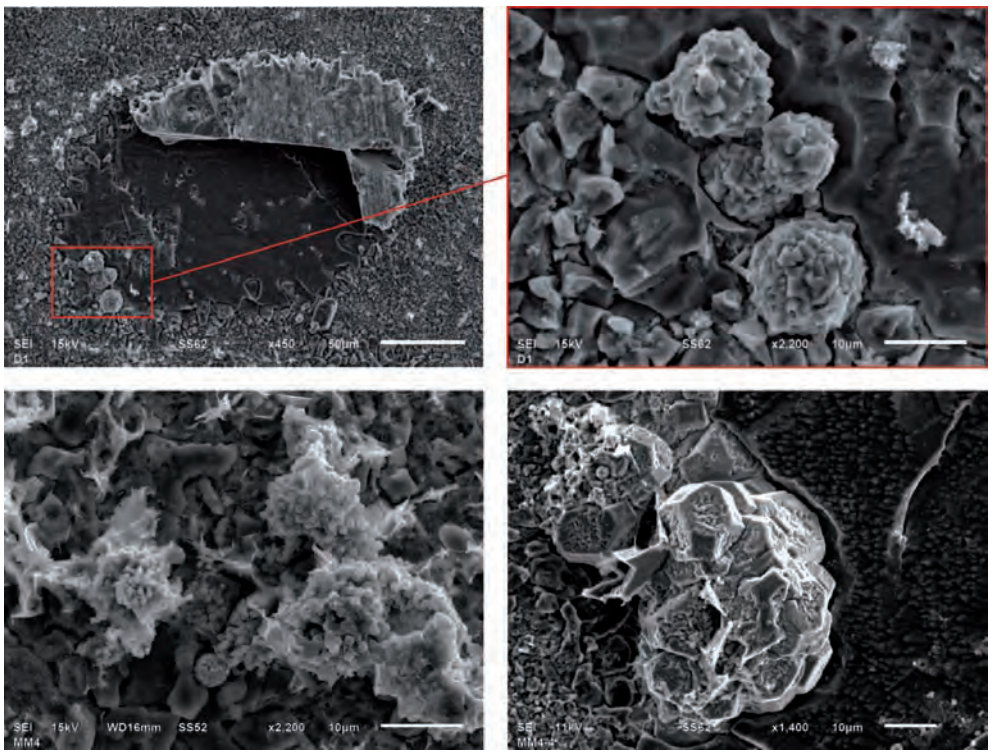

Figure 4.29: *SEM photomicrographs showing spheroidal aggregates of framboidal pyrite, which often occur around cavities, encased by calcite.*

The elemental mapping made with EDX show that the observed framboids are composed of Fe (64%), O (34%) and less than 1% of S. Therefore, they are classified as hematite pseudomorphs after framboidal pyrite. Although there is almost no sulfur left, it is still possible to detect a slight amount of this element inside the framboids (Fig. 4.30).

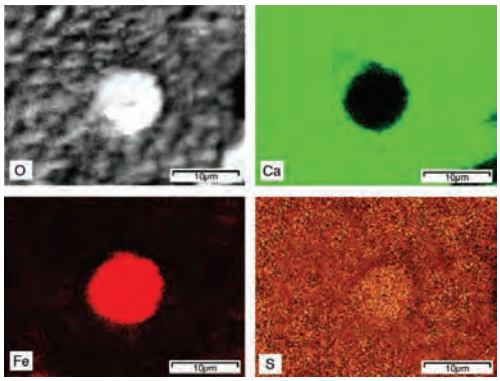

Figure 4.30: *EDX mapping of an individual framboid, showing the elemental distributions of O, Ca, Fe and S. The framboid is encased by calcite and almost completely composed of Fe and O and has only minor amounts of S. Thus the spheroid is termed hematite pseudomorph after framboidal pyrite.*

Dolomite

The staining of thin sections proved the presence of rhombic microdolomite grains inside the growth framework cavities (Fig. 4.31 a, b). The sizes of these grains are variable, ranging from small grains (5 - 10 μm) to big ones (30 μm). The dolomitization front starts at the contact of the sparry calcite with the silty sediment infill and migrates downward to the bottom of the cavities (Fig. 4.31 c, d).

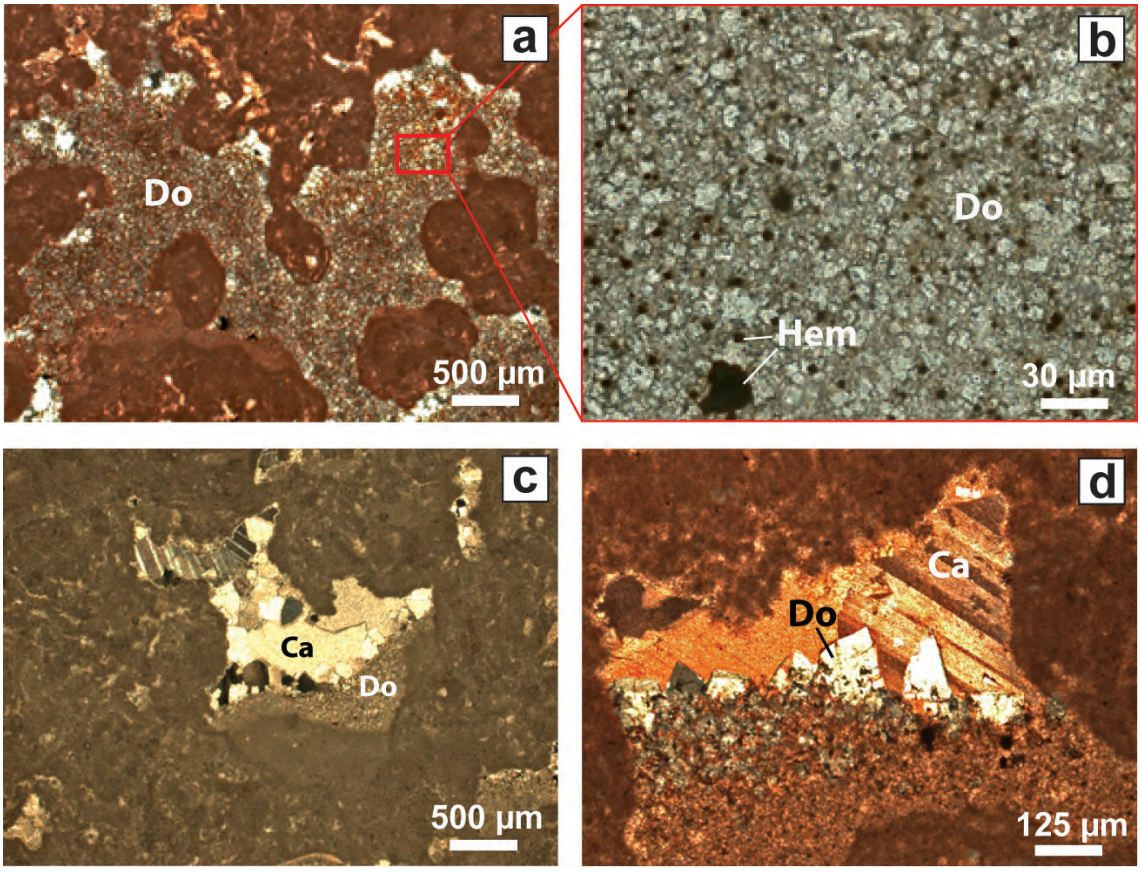

Figure 4.31: *Photomicrographs of stained thrombolite thin sections depicting the distribution of microdolomite (Do) and calcite (Ca) inside the growth framework cavities. (Except c) all thin sections are stained. a) Completely dolomitized cavity filled with b) rhombic dolomite crystals and small hematite grains (Hem). c - d) Note that the dolomitization front moves successively downward to the bottom of the cavities.*

Chapter 5

Discussion

5.1 Studied microbialites

Sedimentology, depositional environment and controlling factors

The understanding of the depositional environment and the factors controlling the deposition and growth of the microbial mounds is not an easy matter. A main question to tackle is the alternation and lateral interfingering of both, ooid shoals and microbial mounds. The complex spatial relationships and close interfingering between these two fabrics observed in the outcrops pointed, at first sight, to a possible simultaneous growth of both. However, detailed analyses revealed that both fabrics are not mixed and that mounds and ooid shoals did not occur coeval.

Microbialites are generally not restricted by water depth, salinity, temperature, light penetration or oxygen content, but require hard substrates for nucleation, a moderate to high nutrient supply, zero to low sedimentation rate for initial growth, and low to moderate sedimentation rate for continued growth (Leinfelder et al., 1993). Usually other reef building organisms are not so tolerant to these ecological factors and therefore microbial mounds often occur in the geological past where metazoans are excluded by some of these factors (e.g. high nutrient content or increased salinity). The studied microbial mounds developed in a shallow water, restricted, low-energetic environment. Mounds are normally associated with low energetic environments, additional indicators for water depth and hydrodynamism can be derived from the mound inhabiting biota. The occurrence of *in situ* branching corals indicates low water energy, as well as the observed erected-growing bryozoans. The abundance of boring lithophagid bivalves and burrowing worms is characteristic for shallow water depths. During the deposition

of the mounds the salinity might have been normal, indicated by the co-occurrence of *in situ* corals and other organisms. The precipitation of gypsum might have occurred postdepositional and not simultaneously with the mound growth (discussed below). An unequivocal evidence of zero sedimentation rates are the downward growing hemispheroids, which are reported to develop in times in which microbial crusts were freely growing, spanning bridges over the seafloor (Leinfelder et al., 1993). The ooid shoals formed also in shallow water depths, but in contrast to the mounds in a high energetic environments with high sedimentation rates. Therefore, the alternation of ooid shoals and mounds reflect a change in the depositional environment (depth, energy/hydrodynamism, sedimentation rate). Sea level fluctuations seem to play an important role to explain these changes. Other studies on Jurassic thrombolites (e.g. Leinfelder et al., 1993; Mancini et al., 2004) concluded that the development of thrombolites is related to sea level rises and that their demise may correspond to major changes in the paleoenvironmental conditions associated with sea level drops and/or by increased sedimentation rates. It is assumed that even subtle sea-level changes were enough to permit the alternation of both carbonate factories, producing changes from more to less restricted conditions. Subtle sea level variations are in agreement with the low-angle ramp system developed in the Southern Tethys during the Middle Jurassic and with the equable climate characterizing this period.

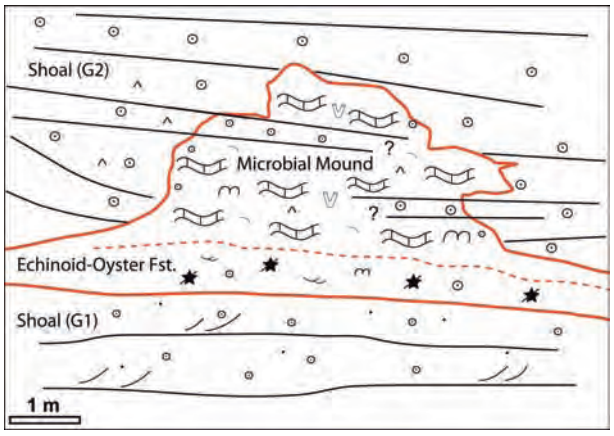

Figure 5.1: *Schematic sketch of a microbial mound on top of the echinoid-oyster floatstone embedded within ooid shoal deposits G1 (below) and G2 (lateral and on top) and surrounded by the ooid shoal deposits G1 and G2.*

The present study proposes the following model to explain the alternation of mounds and shoals: after a sea-level drop the deposition of the first ooid shoal layer (G1) became interrupted and a condensed surface was formed. During a following sea-level rise, the

carbonate production started to keep up with the sea-level and microbial mounds developed. The domical (steep-sided) morphology of the mounds can be attributed to the accommodation availability, but also focused currents of variable direction may have promoted the development of this shape (Pratt & James, 1982). Afterwards, a renewed deposition of ooid shoals (G2) eroded and finally covered the mounds. The deposition of G2 took place in a higher energetic and shallower environment than G1, which is inferred from the different bedding structures (low angle planar cross-bedding in G1 and high angle trough cross-bedding in G2) as well as from the different ooid sizes (ooids in G2 are almost two- times bigger bigger than in G1). During the erosion and winnowing periods some ooids may have been transported inside the cavities of the microbialite, but in general both carbonate fabrics are not mixed and separated by a sharp and erosional contact (Fig. 5.1). In one location evidences have been found that these sea-level rise and drops may have occurred repeatedly, indicating that also the deposition of G2 might have been interrupted, so that a second generation of mounds were able to reflourish on top of this shoal. The second mound growth generation, characterized by a preferential horizontal growth direction, is interpreted to have formed under very limited available accommodation space.

Another controlling factor responsible for the occurrence of microbialites are moderate to high nutrient concentrations. No direct evidences for the occurrence of high nutrient levels have been found. Nevertheless, in the complete studied succession several marly intervals or clay-rich layers occur, which may indicate higher terrigenous supply and associated nutrients. This terrigenous supply could be related to strong tectonic activity of that period, but can also indicate a more humid climate with increased erosion rates and continental runoff. The identified growth interruptions inside the hemispheroids, reflected by an increase in bivalve encrustation and bioerosion, might indicate fluctuations of the trophic conditions (Fig. 5.2). Bioerosion by bivalves is generally higher before and after phases with high growth rates of microbialites (Dupraz and Strasser, 1999). Microbialites occur often under eutrophic-mesotrophic conditions, but the bioerosion from heterothrophic bivalves increases in periods of low-mesotrophic conditions (Dupraz and Strasser, 1999). Therefore, variations in the nutrient availability could be a possible explanation for the interruption of the growth of the microbialite.

As mentioned above, microbialites require a hard substrate for their nucleation. Concerning the substrate on which the mounds grew it has been observed that most of the oyster shells of the echinoid-oyster floatstone layer below the mound are disar-

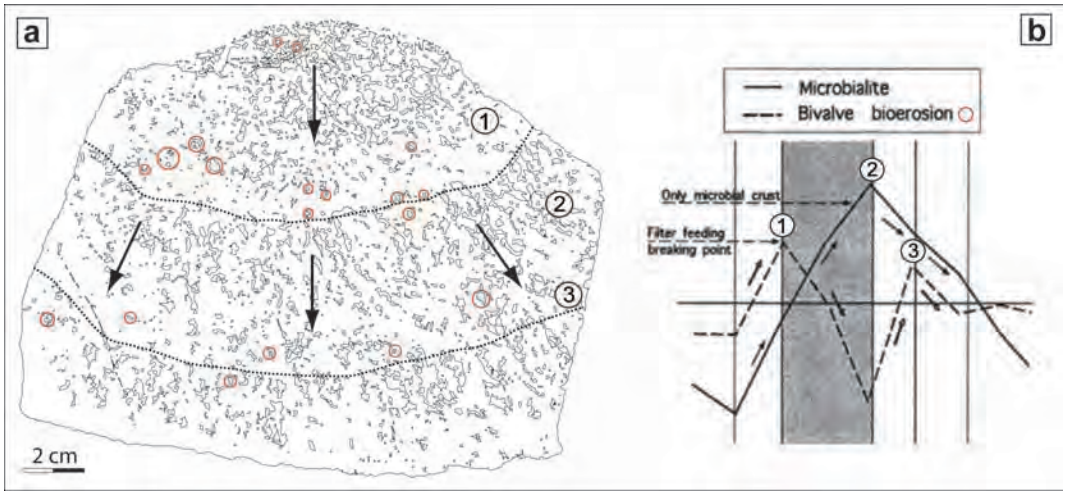

Figure 5.2: *a) Schematic sketch of a polished vertical section through a downward growing hemispheroid with possible growth interruptions, reflected by an increase in bivalve bioerosion (circles). b) Diagram showing that bivalve bioerosion is higher before and after high microbialite growth, which correlates well with distribution of bivalve borings in the hemispheroid. (mod. after Dupraz & Strasser, 1999)*

ticulated, as well as the preferential horizontal arrangement of the skeletal components imply that they are not *in situ* and must have been transported. However most of the components are not fragmented leading to the assumption that the transport was short and took place under low energy conditions. Echinoids and also oysters, often act as pioneer organisms, populating fast new environments and can thrive in very stressful environments. Both of them are grazers and borers and need hard substrates to settle. In this case they have not been found in living position, but most probably they were transported from a nearby area. Together with the other skeletal components of this reworked layer, they might have acted as a (hard) substrate for the settlement of the microbial mounds. Whether they were the pioneer community or just the substrate is hard to answer.

Early lithification (via microbial calcification) plays an important role in the formation of microbialite structures, especially the generation of steep sided mounds or columns require early lithification. Riding (2000) stated, that microbial carbonates can neither form nor be maintained without early calcification and lithification. Diagnostic criterias for the early lithification of the studied mounds are the occurrence of borings and burrows, the development of domical morphologies and the presence of growth (framework) cavities (Helm and Schülke, 1998).

Biogenic origin

The co-existence of bacterial coccoids and their fossilized EPS matrix, implies that organic matter and microbial metabolism have played a key role in the formation of the studied microbialites. The relationship between EPS and carbonate precipitation is a relevant topic, which centers the attention of many works (e.g. Trichet & Défarge, 1995; Dupraz et al., 2004, 2009; Spadafora et al., 2010). It has been suggested that complex processes of EPS degradation, driven by sulfate-reducing bacteria, can lead to carbonate precipitation, whereas cyanobacteria may only be responsible for a minor amount of precipitation (Dupraz et al., 2004). During the EPS degradation the EPS matrix provides the template for the nucleation and growth of carbonate minerals and becomes successively replaced by them (Dupraz et al., 2004, 2009). According to Dupraz et al. (2004) the presence of clusters of coccoid bacteria and the discontinuous EPS calcification probably lead to the generation of micropeloidal structures. Based on the detailed SEM observations a simple model for the microbial deposition of calcium carbonate has been made, in order to explain the origin of the peloidal microfabric (Fig. 5.3).

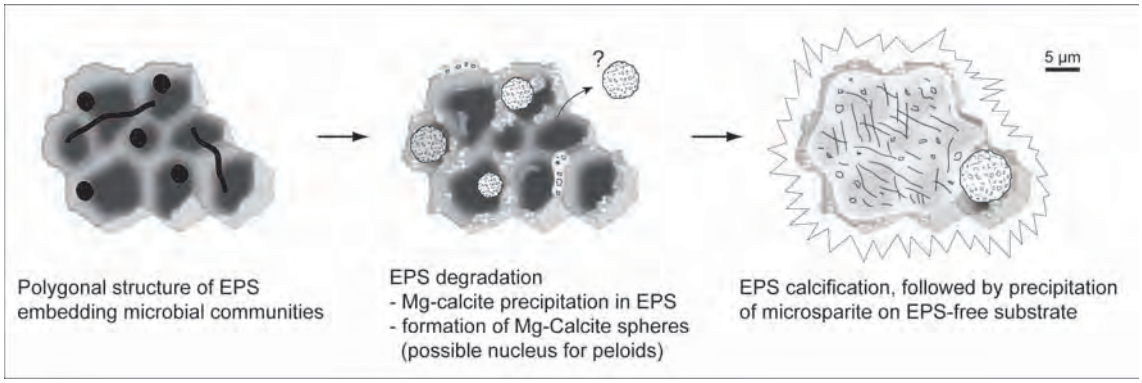

Figure 5.3: *Simple model showing different stages of EPS calcification, which formed the peloidal microfabric.*

In the studied examples the carbonate precipitates are composed of high-Mg calcite, which form small aggregates that merge to larger, rounded aggregates. These larger aggregates possibly have played a primary role as centers of nucleation for (micro) peloids (Dupraz et al., 2004, Aloisi et al., 2006). In some cases the EPS matrix was completely replaced by high-Mg calcite, which confirms the observations described in the literature. After the EPS calcification the EPS-free interpeloidal space is filled by abiotic precipitation of microsparite.

Mineral structure

The calcite pseudomorphs after gypsum occur restricted to the growth framework cavities and the shoal deposits and were not observed directly incorporated inside the mesoclots of the thrombolite. Hence, the primary gypsum formation probably started after the mounds were deposited. The occurrence of gypsum crystals is often related to arid/semi-arid climate, where higher restricted conditions (shallow water) with evaporation rates exceeding precipitation rates occurred. Gypsum is the first evaporite mineral, which begins to precipitate, when seawater has been reduced to about 30 % of its original volume and consequently has a higher salinity. In most cases, the sulfur for the formation of gypsum is derived directly from the sea water. An alternative source of sulfur is the oxidation of pyrite, which is also present within the microbialites as product of sulfate-reducing bacteria. In this case the gypsum would have accumulated around the pyrite and occur more restricted to the latter. Also some inclusions of pyrite inside the gypsum crystals should be expected. Moreover, it is questionable if the volume of oxidized pyrite is sufficient to produce the observed amount of gypsum. The quantification of pyrite is not so easy, especial because of it's relatively small size. The aforementioned features for the alternative source of sulfur were either not observed in the studies samples or are hard to evaluate. Nevertheless, this hypothesis cannot be fully discarded. When exactly the precipitation of gypsum started is very speculative. Nevertheless, the crystals found inside the shoal deposits show synsedimentary features (concave crystal faces) and occur in areas, which contain less ooids. This is an important observation because ooids usually do not tolerate high salinity levels. In order to explain the origin of the crystals found inside the growth framework cavities of the thrombolite, it is assumed that after the mound deposition, at the moment as the shoal (G2) started to cover the mound, the cavities were not all filled or completely filled with sediment. It seems plausible that more saline seawater, circulated through the cavity network of the thrombolite, initiating the precipitation of gypsum inside the cavities. No evidences or sedimentary structures (e.g. mud cracks) indicative of periodical subaerial exposure, have been found in the mounds or the adjacent deposits. Therefore it is assumed that the gypsum precipitation took place in a subtidal environment in periods with higher sea water salinity and restriction.

The formation of pyrite framboids in sediments requires an anaerobic environment, either within the sediment or inside a local microenvironment. The generation of hematite pseudormorphs after framboidal pyrite marks the transition from reducing to

oxidizing conditions. The change from pyrite to hematite can take place at the very beginning of diagenesis, nearly immediately following the framboid formation (Mader, 1985). So whenever the anoxic (micro)environment was not stable anymore the pyrite became oxidized to hematite. Framboidal pyrites seem to be a quite common feature in modern and ancient microbialites (Ezaki et al., 2008; Spadafora et al., 2010). Their occurrence is often related to the metabolic activity of sulfate-reducing bacteria and the decay of organic matter. In fact, some authors consider the presence of framboidal pyrite as an indicator for the involvement of sulfate-reducing bacteria in the precipitation of the microbialites (Westphal et al., 2010).

5.2 Comparison with modern analogues

The discovery of modern stromatolites, first in Shark Bay, Western Australia (Logan, 1961) and later in the Eleuthera Bight (Dravis, 1983) and the Lee Stocking Island of the Bahamas (Dill et al., 1986; Reid et al., 1995), caused numerous studies on modern microbial carbonates. Investigations in these modern systems brought new insights of the organisms responsible for the formation of microbialites and contributed to the development of new concepts about the genesis of microbial carbonates allowing a better understanding of fossil examples. In general the success of microbial carbonates both, thrombolites and stromatolites, in modern environments is attributed to environmental stress and hence protection from grazers and other competitors (e.g. hypersaline water at Shark Bay or resedimentation and sediment mobility due to strong currents at Lee Stocking Island). Allthough thrombolitic and stromatolitic fabrics are equally abundant and widespread in modern environments (Kobluk & Crawford, 1990; Planavsky et al., 2009), less attention has been paid to thrombolites. That is probably because stromatolites were identified and described as unique structures in the fossil record almost 60 years before the first description of thrombolites. On the other hand the distinct lamination of stromatolites makes them easier to identify and explaining their origin has maybe caused more scientific interest than examining the irregular clotted structure of thrombolites.

Remarkable is, that the microbialites of the Bahamas are currently the only known examples formed in open marine environments. They develop in high energy settings with strong currents within migrating ooid shoals. The similar setting (shallow water, open marine, close to ooid shoals) and their similar fabric with the studied examples from Morocco, make the microbialites of the Bahamas a proper analogue for this study.

Following, some general features that characterize the Bahamian microbialites and their depositional environment will be introduced and compared with the Middle Jurassic microbialites of Morocco.

Microbialites of Lee Stocking Island (Bahamas)

At the North and West of the Lee Stocking Island microbialites occur under normal marine salinity in a subtidal channel, the Adderly Channel, which connects the open-ocean waters of Exuma Sound with those of Great Bahama Bank to the west (Fig. 5.4 a, b).

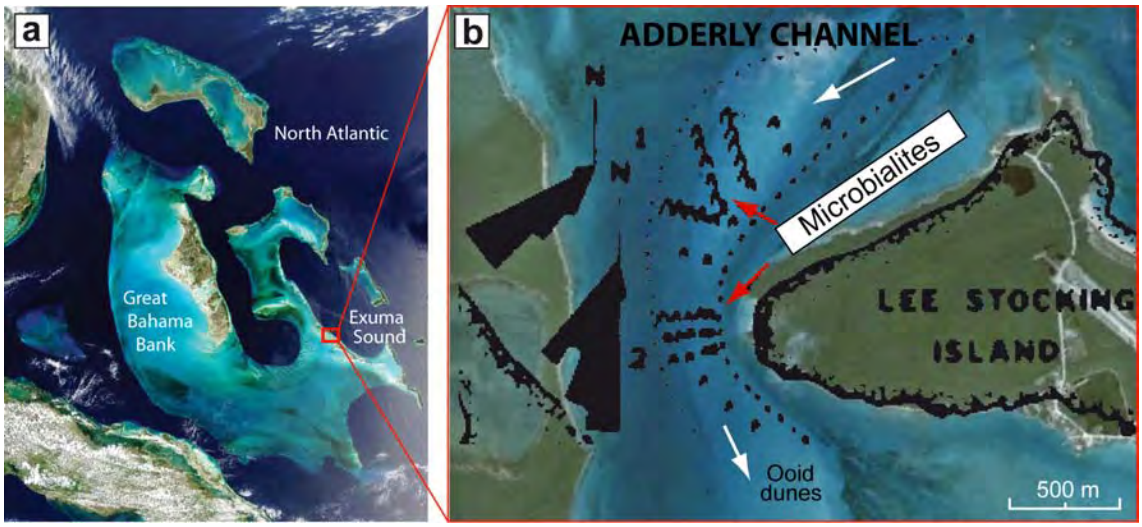

Figure 5.4: *Satellite images of the Bahamas in the North Atlantic. a) Geographic relation of the Great Bahama Bank and the Exuma Sound with respect to Lee Stocking Island, red box (NASA). b) Closer view of the Adderly Channel North and West of Lee Stocking Island with location of microbialites within an migrating ooid-sand dune field. Note that the microbialites grow in linear rows perpendicular to the water current direction, which is indicated by rose diagrams and white arrows (mod. after Dill et al. 1986 and superimposed on a Google Earth image).*

Reversing tidal and wind-driven currents with high velocities of up to 1.5 m/s flow across the channel twice daily (Feldmann & McKenzie, 1998). The microbialites occur in a migrating oolitic sand bar (5000 m long x 500 m wide) at water depths of 5 - 10 m. The bar shows a series of sand waves 1 - 2.5 m high and the microbialites grow in the depressions between these sand waves (Dill et al., 1986; Planavsky et al., 2009). Driven by tidal currents these waves move seaward and bankward, episodically covering and uncovering the microbialites (Dill, 1991). Most of the microbialites are 1 - 1.5 m high and occur as isolated columns with steep sides (Planavsky et al., 2009). The heights and growth morphologies of the microbialites are variable, ranging from a few centime-

ters small ridges (preferential lateral growth) in shallow water, to 2.5 m high columns (preferential vertical growth) in the deeper parts of the channel. Consequently, the growth morphologies seem to be governed by the relative water depth and the available accommodation space (Andres & Reid, 2006). The microbialites nucleate on shells or other clasts forming a small base, which is interpreted as another factor determining their columnar growth-shape (Dill et al., 1986; Riding et al., 1991). Moreover, the columnar growth may also be an adaptation to high sedimentation rates and periodical coverage. Another remarkable feature of the Adderly Channel microbialites is that they form linear rows of several streamlined specimens which are oriented perpendicular to the tidal flow direction; this arrangement is attributed to the high energy environment (Fig. 5.4 b, Fig. 5.5 a, Dill et al., 1986). Likely, the explanation of this arrangement is derived from a recent study on tidal dominated ooid shoals in the Bahamas done by Rankey et al. (2006), which demonstrate that the sand waves are usually oriented perpendicular to the water flow; consequently the depressions between the sand waves (in which the microbialites occur) are oriented in the same way. Moreover, the streamlined growth minimizes the surface area (of the microbialites) exposed to the current.

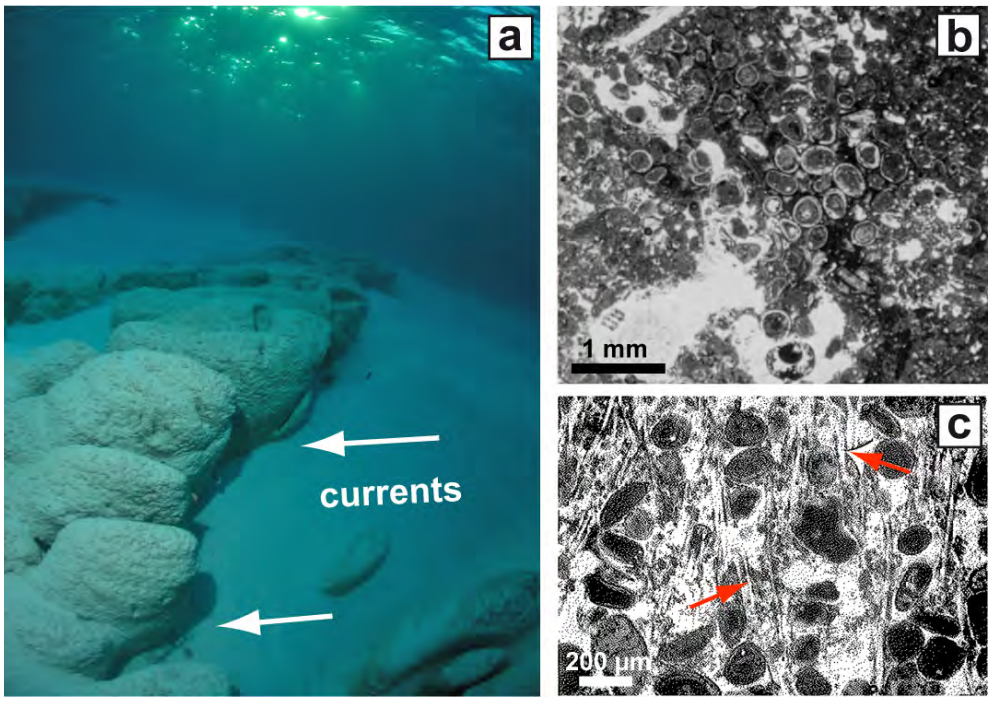

Figure 5.5: *a) Subtidal microbialites from the Adderly Channel growing in a linear row perpendicular to the current direction and are partly covered and surrounded by ooid sands. b) Thin section photomicrograph of a thrombolite with irregular clotted fabric and abundant ooids (taken from Feldmann & McKenzie, 1998). c) Thin section photomicrograph showing the microstructure of a thrombolite with calcified filaments (red arrows) entrapping peloids and ooids (taken from Reid et al., 1999).*

Little is known about the distribution pattern of thrombolites and stromatolites in the Adderly Channel, but some studies suggest that the stromatolites are found in the shallow water intertidal to subtidal zone, whereas thrombolites are restricted to the subtidal zone in the deeper parts of the channel (Feldmann & McKenzie, 1998). Nevertheless, studies from other locations in the Bahamas (e.g. the Highborne Cay) have proved the presence of thrombolites in intertidal settings (Reid et al., 1995, 1999). Regarding the mesostructure in the Adderly Channel have an irregular clotted peloidal fabric, composed of irregular shaped millimetric mesoclots and unbound sediment pockets in between them. These pockets are likely the equivalent to the growth framework cavities found in the thrombolites of Morocco. Conversely to the studied microbialites, the ones in the Adderly Channel have a high detrital character, related to the high content of particles and resedimentation (Fig. 5.5 b, Feldmann & McKenzie, 1998; Planavsky et al., 2009). Such fabrics are also referred to as "coarse agglutinated" and their clotted appearance is mainly due to the highly irregular unoriented cavities (Riding et al., 1991; Riding, 2000). The majority of the cavities is partially or completely filled with detrital particles (peloids, ooids, skeletal debris) and mud or silt-sized sediment with geopetal infills. Detrital particles are also present inside the mesoclots, which are composed of closely packed peloids surrounded by high-magnesium calcite cements (Planavsky et al., 2009). Typically the thrombolites contain 10 to 100 μm wide calcified filaments (cyanobacteria), which entrap peloids and/or ooid grains (Fig. 5.5 c). These filaments have been interpreted as the dominant framework builders and occur throughout the whole thrombolite column (Feldmann & McKenzie, 1998 and references therein; Reid et al., 1999). Together with the cements, which surround the peloids inside the mesoclots, these filaments contribute to the formation of a wave-resistant framework, which is only disrupted by boring bivalves and burrowing worms.

Are the examples of the Bahamas a suitable analogue?

The Bahmian examples represent the only known modern microbialites which grow embedded within ooid shoal deposits and thrive in open marine setting under normal ocean water salinity . Many other reported modern examples grow only restricted to seasonally hypersaline embayments or hypersaline lakes. Therefore the microbialites of the Bahamas provide the only suitable analogue (with striking similarities) for the studied microbialites and offer the unique opportunity to learn more about the ancient depositional environment.

At first, the thrombolites from the Adderly Channel in the Bahamas seem to share common features with the studied thrombolites of Morocco in regarding the environment of deposition (open marine setting and embedded within shoals). However, there is a main difference between both microbialites, which is that the Bahamian thrombolites grow simultaneously with the deposition of grainstones and consequently thrive under high energy and high sedimentation rates, whereas the studied thrombolites developed under low sedimentation rates and were not coeval with the ooid shoals. A direct consequence of this is the higher detrital character of the fabric in the modern examples. They contain a significant amount of trapped ooid grains and other detrital particles, which leads to more coarse and agglutinated fabrics. Trapping and binding of detrital particles play an important role in the accretion process of modern thrombolites in the Bahamas, but has not been observed in the studied examples from Morocco. In the examples of Morocco trapped ooids or autochtonous grains are very scarce and occur only inside some growth framework cavities. Both examples have a similar mesostructure, made by polymorphic clots and growth framework cavities, but the modern coarse agglutinated thrombolites do not display such well-defined clots and their clotted appearance is more attributed to the irregular cavities. The mesoclots of both settings are bored and burrowed. Comparing the biogenic structure it is observed that the bacterial remains of the modern thrombolites are almost entirely composed of filament molds, whereas in the specimens from Morocco coccoidal bacterial shapes are more abundant. Regarding the growth morphology there are also some differences. The preferential vertical, columnar growth of the Bahamian microbialites can be explained as an adaption to the high energetic setting and high sedimentation rate, but might also be influenced by the small size of available substrates (e.g. single shells, clasts). On the contrary the examples from Morocco were able to colonized broader substrates, due to the low energetic setting and very low sedimentation rates resulting in domical growth morphology with less steep sides (Riding et al., 1991). Little is known about the three-dimensional distribution of the mounds in Morocco due to outcrop limitations, therefore it is hard to evaluate if they also grow in linear rows. The outcrops just allow two-dimensional observations, which show that the mounds are equally distributed with a relatively constant space in between. No evidences have been found that indicate, that the studied microbialites were growing in between sand waves of an active, migrating shoal system. It is more likely that they developed in parts of the shoal, which were (temporarily) not active, characterized by no sediment transport and low sedimentation rates. The three-dimensional morphology of the shoals is very

complex, but probably the diploma project of Max Zitzmann, which is focused on the facies variability and morphology of the ooid shoal complexes in the study area, will contribute to a better understanding of the latter.

Despite important differences between the Bahamian and the Jurassic thrombolites, the modern example still provides useful information and permit to estimate parameters that are not possible to infer from the fossil record, e.g. the water depth in which they occur (approx. 10 m) and the growth rate of the microbialites. By means of radiocarbon dating in the shells of boring bivalves growth rates have been calculated for the Adderly Channel microbialites. They are approx. 0.33 mm/year which results in ages of approx 4545 years considering a 1.5 m high microbialite(Planavsky et al., 2009). The estimated growth rate is similar to the rate obtained for the Shark Bay microbialites of 0.4 mm/ear (Chivas et al., 1990.) It is quite tricky to apply the growth rates of the modern examples, especially because there is no time constrain in the studied mounds. Moreover, the modern microbialites may have a faster growth rate, do to higher accumulation of detrital particles via trapping and binding. Nevertheless, assuming these rates for the studied thrombolites of Morocco (1.3 m high) would result in ages between 3250 to 4000 years (assuming constant growth with no interruptions). These ages have to be taken with caution and may just represent a minimum age.

Chapter 6

Conclusions

The studied microbial mounds from the Bajocian (Middle Jurassic) of Morocco developed on a low-angle carbonate ramp in a shallow water open marine environment. The shallow water origin of the mounds is inferred, because they are laterally in contact with shoal settings. Moreover, their distinct domical shapes with a preferential horizontal growth direction, suggesting that the available accommodation space was probably limited, within a shallow water environment. Microbialites generally occur in low-energetic environments and require low sedimentation rates. In the analyzed microbialites this is reflected by the presence of downward growing hemispheroids, which are an indicator for zero sedimentation rates (Leinfelder et al., 1993). The mound inhabiting biota, such as *in situ* branching corals and erected-growing bryozoans are an additional indicator for the low-energetic environment. Lithophagid bivalves encrust and bore the microbialites particularly during identified periods of growth interruption, which may reflect variations in the trophic conditions. The mounds occur embedded within ooid shoal deposits, which formed in shallow, high energetic environment with high sedimentation rates.

The microbialites might have developed during a sea level rise and produced depositional relief, creating domical mounds. They nucleated on top of an echinoid-oyster floatstone layer, which has been deposited above a condensed surface that formed prior, related to a sea level drop. The mounds are not coeval with the ooid shoal layer G2 and developed before the deposition of the latter. Based on all the observations made in this study it can be concluded that high-order sea level fluctuations are the main controlling factor, responsible for: 1.) the development of the microbial mounds and their demise, 2.) the interruption of the deposition of ooid shoal layer G1 and 3.) the renewed deposition of ooidal grainstones (G2), which eroded and finally buried the

mounds. After the deposition of the mounds, circulating sea water with an increased salinity initiated the precipitation of gypsum inside the growth framework cavities of the microbialite and the second shoal (G2). No evidences for subaerial exposure have been found. It is inferred that arid climate was responsible for the gypsum formation. As the gypsum precipitated post depositional to the mound, elevated salinity can be ruled out as ecological stress for the microbialite growth. The growth of the studied microbialites resulted from the combination of both, a sea level rise and low to zero sedimentation rates.

The microbialites are classified as thrombolites of bacterial origin. The presence of bacterial remains (mainly coccoids) and fossilized EPS matrix prooves this origin. The peloidal clotted fabric of the thrombolites is most probably the result of *in situ* calcification of the coccoid-dominated microbial communities and the degradation and calcification of the EPS, driven by sulfate reducing bacteria. The involvement of sulfate-reducing bacteria in the formation of the thrombolites is supported by the presence of framboidal pyrite.

The comparison with modern analogues from Bahamas revealed that the modern examples thrive, in contrast to the studied, in an active shoal environment with high sedimentation rates, resulting in the generation of coarse agglutinated fabrics with trapped ooids. Comparisons of the biogenic structures of both examples show that the microbial communities of modern thrombolites are dominated by filamentous bacteria shapes, whereas in the present study coccoidal shapes are more abundant. Nevertheless, the water depth (approx. 10 m) in which the modern analogues occur might be similar to that of the thrombolites of Morocco.

A variety of valuable information has been gained on all the scale levels (mega to micro). In the mega- and macrostructure the surrounding shoal deposits and their spatial and temporal relationship to the mounds have been described and discussed. The observations of the meso- and microstructure were focussed on the description of the microbialite's internal organization and on the recognition of bacterial remains. Ancient microbialites often do not preserve clear evidence of the organisms responsible for their formation (Riding, 2000) so it has to be highlighted that the identification of bacterial remains in the fossil microbial carbonates represents a great success of this study. This new data will contribute to the knowledge about the distribution, environment and composition of Middle Jurassic thrombolite mounds of the southern Tethyan domain. Future work should focus more on the three-dimensional modeling of the studied mounds in order to learn more about their spatial distribution pattern.

Acknowledgement

At this point I would like to thank all of the people who have supported me during the writing of this thesis and during my study.

First of all I would like to thank Prof. Dr. Maria Mutti not only for the opportunity to work on this topic, but also for her enthusiasm to encourage me throughout the investigation and for the financial support during the field work in Morocco. I am especially grateful to Dr. Sara Tomás, without her constructive criticism and constant encouragement the present work would not have been possible. MSc Frederic Amour and Dr. Gianluca Frijia are thanked for fruitful discussions and useful advice. I also would like to thank PD Dr. Uwe Altenberger for the discussion of some mineralogical questions and Prof. Hans G. Machel for helpful suggestions.

Furthermore, I am indebted to many others. Christine Fischer for the preparation of the thin sections. Dr. Christina Günter for the assistance with the SEM. Dipl.-Geol. Michael Rumpf for the help with LaTeX. Marco for providing me access to hard-to-get publications. Camille for her help with some language problems. Nicolas and Max for their nice companionship both in the field and beyond. Assou, Moha and all the Agouzil family for their hospitality in the Kasbah Amellago. Stefan for his friendship and support during our academic years. GG for her trust in me and C-M for keeping me focused.

Finally, I would like to thank my family, especially my parents for their support and motivation during my study.

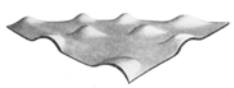

Zusammenfassung

Im Bajocium (Mittleres Jura) entwickelten sich mikrobielle Hügel ("mounds") auf einer Karbonatrampe an der Südflanke des Zentralen Hohen Atlas (Marokko). Die Hügel sind sehr gut innerhalb des Amellago Canyons aufgeschlossen, welcher 50 km nordwestlich der Stadt Rich im zentralen Marokko gelegen ist. Stratigraphisch gesehen gehören sie zur Assoul Formation, die aus einer etwa 300 m mächtigen Wechsellagerung von Flachwasserkarbonaten und terrigenen Sedimenten besteht. Die Hügel treten eingebettet in "ooid shoal" Ablagerungen auf, die eine zusammenhängende Schicht bilden, welche für 80 m lateral verfolgt werden kann. Die mikrobiellen Hügel haben eine domartige Wachstumsmorphologie und sind circa 1.3 m hoch und 2.5 m breit (n = 28). Der durchschnittliche Abstand zwischen den Hügeln betägt 2.7 m. Gelegentlich sind die Hügel seitlich, brückenartig miteinander verbunden, so dass hängende Hemispheroide in ihrem Zwischenraum nach unten wachsen konnten.

Die Mikrobialithe sind durch ein peloidales, klumpiges Gefüge charakterisiert, weisen keine internen Laminationen auf und wurden daher als Thrombolithe klassifiziert. Die detailiierte Analyse von 37 polierten Gesteinsproben und 38 Dünnschliffen hat ergeben, dass die Thrombolithe aus polymorphen "mesoclots" (2 - 4 mm breit) aufgebaut sind, welche für die klumpige Erscheinung des Gefüges verantwortlich sind und Äste von 1 - 2 mm breite ausbilden. Die "mesoclots" bestehen aus dunklen, mikritischen Peloiden (30 - 60 μm). Im Zwischenraum zwischen den einzelnen "mesoclots" treten wachstumsbedingte Hohlräume mit geopetalem Gefüge und siltigen Füllungen auf. Eine detaillierte Untersuchung des Mikrogefüges mit Hilfe des Rasterelektronenmikroskopie (SEM), gekoppelt mit energiedispersiver Röntgenspektroskopie (EDX) zeigte die Anwesenheit von organischen Substanzen in Form von bakteriellen Kokken (1 - 3 μ m) und filamentösen Strukturen (5 - 15 μ m), welche beide in einer fossilisierten EPS (extrazelluläre polymere Substanzen) Matrix identifiziert wurden. Die EPS Matrix hat eine charakteristische wabenartige Struktur, die entweder von Kalzit mit unterschiedlichen Anteilen an Al - Fe Silikaten und einigen Mg, K Ionen mineralisiert ist oder komplett aus Hoch-Mg-Kalcit zusammengesetzt ist. Das peloidale, klumpige Gefüge der Thrombolithe wurde als Resultat von *in situ* kalzifizierenden mikrobielle Gemeinschaften (hauptsächlich Kokken) und der Zersetzung und Kalzifizierung von organischer EPS durch sulfatreduzierenden Bakterien interpretiert. Die Anwesenheit von sulfatreduzierenden Bakterien konnte auch durch das Auftreten von framboidalen Pyrit (5 - 15 μm) bestätigt werden. Im Gegensatz zu ihren modernen Gegenstücken in den Ba-

hamas, sind die untersuchten Mikrobialithe nicht zeitgleich mit den umgebenen "ooid shoal" Ablagerunden entstanden und haben daher auch kaum allochthone Sedimente eingefangen und inkorporiert.

Die signifikanten, domartigen Wachstumsmorphologien mit bevorzugter horizontale Wuchsrichtung legen nahe, dass der verfügbare Ablagerungsraum wahrscheinlich begrenzt war. Das flache, niedrig-energetische Ablagerungsmilieu spiegelt sich auch in den Organismen wieder, welche die mikrobiellen Hügel bewohnen. Diese bestehen hauptsächlich aus *in situ* wachsenden verästelten Korallen, aufrecht wachsenden Bryozoen und lithophagiden Bivalven. Diese bohrende Bivalvenart ist besonders zahlreich in Zeiten von Wachstumsunterbrechungen der Mikrobialithe vorhanden und spiegeln möglicherweise Schwankungen in den trophischen Bedingungen wieder. Die mikrobielle Hügel wuchsen in einem subtidalen Flachwasser-Millieu unter unter sehr niedrigen Sedimentationsraten. Meeresspiegelschwankungen sind höchstwahrscheinlich der Hauptfaktor für das Wachstum und den Rückgang der Mikrobialithe.

List of Figures

Bibliography

Addi, A. (2006). The dogger reef horizons of the Moroccan Central High Atlas: New data on their development. *Journal of African Earth Sciences*, 45(2):162–172.

Ait Brahim, L., Chotin, P., Hinaj, S., Abdelouafi, A., El Adraoui, A., Nakcha, C., Dhont, D., Charroud, M., Sossey Alaoui, F., Amrhar, M., et al. (2002). Paleostress evolution in the Moroccan African margin from Triassic to Present. *Tectonophysics*, 357(1-4):187–205.

Aitken, J. (1967). Classification and environmental significance of cryptalgal limestones and dolomites, with illustrations from the Cambrian and Ordovician of southwestern Alberta. *Journal of Sedimentary Petrology*, 37(4):1163–1178.

Aitken, J. and Narbonne, G. (1989). Two occurrences of Precambrian thrombolites from the Mackenzie Mountains, northwestern Canada. *Palaios*, 4(4):384–388.

Aloisi, G., Gloter, A., Kruger, M., Wallmann, K., Guyot, F., and Zuddas, P. (2006). Nucleation of calcium carbonate on bacterial nanoglobules. *Geology*, 34(12):1017–1020.

Amour, F. (submitted). Capturing and modeling metre scale spatial facies heterogeneity in a Jurassic ramp setting (Central High Atlas, Morocco) . *submitted*.

Andres, M. and Pamela Reid, R. (2006). Growth morphologies of modern marine stromatolites: a case study from Highborne Cay, Bahamas. *Sedimentary Geology*, 185(3-4):319–328.

Aubrecht, R., Schlögl, J., Krobicki, M., Wierzbowski, H., Matyja, B., and Wierzbowski, A. (2009). Middle Jurassic stromatactis mud-mounds in the Pieniny Klippen Belt (Carpathians): A possible clue to the origin of stromatactis. *Sedimentary Geology*, 213(3-4):97–112.

Beauchamp, W., Allmendinger, R., Barazangi, M., Demnati, A., El Alji, M., and Dahmani, M. (1999). Inversion tectonics and the evolution of the High Atlas Mountains, Morocco, based on a geological-geophysical transect. *Tectonics*, 18(2):163–184.

Beauchamp, W., Barazangi, M., Demnati, A., and El Alji, M. (1996). Intracontinental rifting and inversion: Missour basin and Atlas mountains, Morocco. *AAPG Bulletin*, 18:1459–1468.

Bosak, T., Souza-Egipsy, V., and Newman, D. (2004). A laboratory model of abiotic peloid formation. *Geobiology*, 2(3):189–198.

Braga, J., Martin, J., and Riding, R. (1995). Controls on microbial dome fabric development along a carbonate-siliciclastic shelf-basin transect, Miocene, SE Spain. *Palaios*, 10(4):347–361.

Brede, R., Hauptmann, M., and Herbig, H. (1992). Plate tectonics and intracratonic mountain ranges in Morocco-The Mesozoic-Cenozoic development of the central High Atlas and the Middle Atlas. *Geologische Rundschau*, 81(1):127–141.

Bromley, R. (1994). The palaeoecology of bioerosion. *The palaeobiology of trace fossils*, pages 134–154.

Burkhalter, R. (1995). Ooidal ironstones and ferruginous microbialites: origin and relation to sequence stratigraphy (Aalenian and Bajocian, Swiss Jura mountains). *Sedimentology*, 42(1):57–74.

Burne, R. and Moore, L. (1987). Microbialites: organosedimentary deposits of benthic microbial communities. *Palaios*, 2(3):241–254.

Camoin, G., Gautret, P., Montaggioni, L., and Cabioch, G. (1999). Nature and environmental significance of microbialites in Quaternary reefs: the Tahiti paradox. *Sedimentary Geology*, 126(1-4):271–304.

Chafetz, H. (1986). Marine peloids: a product of bacterially induced precipitation of calcite. *Journal of Sedimentary Petrology*, 56(3):812–817.

Chivas, A., Torgersen, T., and Polach, H. (1990). Growth rates and Holocene development of stromatolites from Shark Bay, Western Australia. *Australian Journal of Earth Sciences*, 37(2):113–121.

Christ, N., Immenhauser, A., Amour, F., Mutti, M., Agar, S., Alway, R., and Kabiri, L. (2010). Characterization of discontinuity surfaces in a Jurassic setting (High Atlas, Morocco). *accepted*.

Collin, P., Loreau, J., and Courville, P. (2005). Depositional environments and iron ooid formation in condensed sections (Callovian–Oxfordian, south-eastern Paris basin, France). *Sedimentology*, 52(5):969–985.

De Castro, P. (1990). Thaumatoporelle: conoscenze attuali e approccio all interpretazione. *Bollettino della Societa Paleontologica Italiana*, 29:179–206.

Dill, R. (1991). Subtidal stromatolites, ooids and crusted-lime muds at the Great Bahama Bank margin. *Sepm Special publication*, 46:147–171.

Dill, R., Shinn, E., Jones, A., Kelly, K., and Steinen, R. (1986). Giant subtidal stromatolites forming in normal salinity waters. *Nature*, 324:55–58.

Dravis, J. (1983). Hardened subtidal stromatolites, Bahamas. *Science*, 219(4583):385–386.

Dupraz, C., Reid, R., Braissant, O., Decho, A., Norman, R., and Visscher, P. (2009). Processes of carbonate precipitation in modern microbial mats. *Earth-Science Reviews*, 96(3):141–162.

Dupraz, C. and Strasser, A. (1999). Microbialites and micro-encrusters in shallow coral bioherms (Middle to Late Oxfordian, Swiss Jura Mountains). *Facies*, 40:101–130.

Dupraz, C., Visscher, P., Baumgartner, L., and Reid, R. (2004). Microbe–mineral interactions: early carbonate precipitation in a hypersaline lake (Eleuthera Island, Bahamas). *Sedimentology*, 51(4):745–765.

Ezaki, Y., Liu, J., Nagano, T., and Adachi, N. (2008). Geobiological aspects of the Earliest Triassic microbialites along the southern periphery of the tropical Yangtze Platform: Initiation and cessation of a microbial regime. *Palaios*, 23(6):356–369.

Farrand, M. (1970). Framboidal sulphides precipitated synthetically. *Mineralium Deposita*, 5(3):237–247.

Feldmann, M. and McKenzie, J. (1998). Stromatolite-thrombolite associations in a modern environment, Lee Stocking Island, Bahamas. *Palaios*, 13(2):201–212.

Flügel, E. (2004). *Microfacies of carbonate rocks: analysis, interpretation and application*. Springer Verlag.

Gygi, R. (1981). Oolitic iron formations: marine or not marine. *Eclogae Geologicae Helvetiae*, 74(1):233–254.

Hallam, A. (1975). *Jurassic environments*. Cambridge University Press Cambridge.

Hallam, A., Crame, J., Mancenido, M., Francis, J., and Parrish, J. (1993). Jurassic Climates as Inferred from the Sedimentary and Fossil Record [and Discussion]. *Philosophical Transactions: Biological Sciences*, 341(1297):287–296.

Haq, B., Hardenbol, J., Vail, P., et al. (1988). Mesozoic and Cenozoic chronostratigraphy and cycles of sea-level change. *Sea-level changes: an integrated approach: Society of Economic Paleontologists and Mineralogists Special Publication*, 42:71–108.

Helm, C. and Schülke, I. (1998). A coral-microbialite patch reef from the Late Jurassic (florigemma-Bank, Oxfordian) of NW Germany (Süntel Mountains). *Facies*, 39(1):75–104.

Hofmann, H., Grey, K., Hickman, A., and Thorpe, R. (1999). Origin of 3.45 Ga coniform stromatolites in Warrawoona Group, Western Australia. *Geological Society of America Bulletin*, 111(8):1256–1262.

Jacobshagen, V., Görler, K., and Giese, P. (1988). Geodynamic evolution of the Atlas System (Morocco) in post-Palaeozoic times. *The Atlas System of Morocco*, pages 481–499.

James, N. (1983). Reef environment. *American Association of Petroleum Geologists*, 33(3-4):346–440.

James, N. and Bourque, P.-A. (1992). Reefs and mounds. In: Walker, R.G., James, N.P. (Eds.), Facies Models, Response to Sea Level Change. *Geological Association of Canada*, 1:323–347.

James, N. and Kobluk, D. (1978). Lower Cambrian patch reefs and associated sediments: southern Labrador, Canada. *Sedimentology*, 25(1):1–35.

Kah, L. and Grotzinger, J. (1992). Early Proterozoic (1.9 Ga) thrombolites of the Rocknest Formation, Northwest Territories, Canada. *Palaios*, 7(3):305–315.

Kahle, C. (2001). Biosedimentology of a Silurian thrombolite reef with meter-scale growth framework cavities. *Journal of Sedimentary Research*, 71(3):410–422.

Kalkowski, E. (1908). Oolith und Stromatolith in Norddeutschen Bund-sandstein. *Deutsche geol. Gesell.*, 60:68–125.

Kazmierczak, J., Altermann, W., Kremer, B., Kempe, S., and Eriksson, P. (2009). Mass occurrence of benthic coccoid cyanobacteria and their role in the production of Neoarchean carbonates of South Africa. *Precambrian Research*, 173(1-4):79–92.

Kazmierczak, J., Coleman, M., Gruszczynski, M., and Kempe, S. (1996). Cyanobacterial key to the genesis of micritic and peloidal limestones in ancient seas. *Acta Palaeontologica Polonica*, 41(4):319–338.

Kazmierczak, J. and Kempe, S. (2004). Microbialite Formation in Seawater of Increased Alkalinity, Satonda Crater Lake, Indonesia: Discussion. *Journal of Sedimentary Research*, 74(2):314–317.

Kempe, S. and Kazmierczak, J. (1993). Satonda Crater Lake, Indonesia: hydrogeochemistry and biocarbonates. *Facies*, 28(1):1–31.

Kennard, J. and James, N. (1986). Thrombolites and stromatolites: two distinct types of microbial structures. *Palaios*, 1(5):492–503.

Kleemann, K. (1994). Associations of corals and boring bivalves since the late Cretaceous. *Facies*, 31(1):131–139.

Knorre, H. and Krumbein, W. (2000). Bacterial calcification. *Microbial sediments*, pages 25–31.

Kobluk, D. and Crawford, D. (1990). A modern hypersaline organic mud-and gypsum-dominated basin and associated microbialites. *Palaios*, 5(2):134–148.

Krause, F., Scotese, C., Nieto, C., Sayegh, S., Hopkins, J., and Meyer, R. (2004). Paleozoic stromatactis and zebra carbonate mud-mounds: Global abundance and paleogeographic distribution. *Geology*, 32(3):181–184.

Krumbein, W., Cohen, Y., and Shilo, M. (1977). Solar lake (Sinai). 4. Stromatolitic cyanobacterial mats. *Limnology and Oceanography*, 22(4):635–656.

Kuznetsov, V. (1990). Evolution of reef structures through time: Importance of tectonic and biological control. *Facies*, 22:159–168.

Laville, E., Pique, A., Amrhar, M., and Charroud, M. (2004). A restatement of the Mesozoic Atlasic rifting (Morocco). *Journal of African Earth Sciences*, 38(2):145–153.

Leinfelder, R. (2001). Jurassic Reef Ecosystems. In *Stanley, G.D.Jr. (ed.), The History and Sedimentology of Ancient Reef Systems*, pages 251–309. Kluwer Academic/Plenum Publishers.

Leinfelder, R., Krautter, M., Laternser, R., Nose, M., Schmid, D., Schweigert, G., Werner, W., Keupp, H., Brugger, H., Herrmann, R., et al. (1994). The origin of Jurassic reefs: current research developments and results. *Facies*, 31(1):1–56.

Leinfelder, R., Nose, M., Schmid, D., and Werner, W. (1993). Microbial crusts of the Late Jurassic: composition, palaeoecological significance and importance in reef construction. *Facies*, 29(1):195–229.

Leinfelder, R. and Schmid, D. (2000). Mesozoic reefal thrombolites and other microbolites. *Microbial Sediments*, pages 289–294.

Leinfelder, R., Schmid, D., Nose, M., and Werner, W. (2002). Jurassic reef patterns–the expression of a changing globe. *Phanerozoic Reef Patterns*, 72:465–520.

Logan, B., Rezak, R., and Ginsburg, R. (1964). Classification and environmental significance of algal stromatolites. *The Journal of Geology*, pages 68–83.

Lowe, D. (1980). Stromatolites 3,400-myr old from the archean of Western Australia. *Nature*, 284:441–443.

Macintyre, I. (1985). Submarine cements, the peloidal question. *Carbonate Cements: SEPM, Special Publication*, 36:109–116.

Macintyre, I., Reid, R., and Steneck, R. (1996). Growth history of stromatolites in a Holocene fringing reef, Stocking Island, Bahamas. *Journal of Sedimentary Research*, 66(1):231–242.

Mader, D. (1985). Diagenetic evolution of opaque and transparent heavy minerals reflecting colour genesis in continental fluvial Buntsandstein red beds of the Eifel (FR

Germany). *Aspects of Fluvial Sedimentation in the Lower Triassic Buntsandstein of Europe*, pages 531–560.

Madsen, H. and Stemmerik, L. (2009). Early diagenetic celestite replacement of demosponges in Upper Cretaceous (Campanian–Maastrichtian) chalk, Stevns, Denmark. *Geology*, 37(4):355–358.

Mancini, E., Llinas, J., Parcell, W., Aurell, M., Badenas, B., Leinfelder, R., and Benson, D. (2004). Upper Jurassic thrombolite reservoir play, northeastern Gulf of Mexico. *AAPG bulletin*, 88(11):1573–1602.

McKee, E. and Gutschick, R. (1969). *History of the Redwall Limestone of northern Arizona*. Geological Society of America.

Monbaron, M. (1979). Nouvelles recherches sur les gisements de Dinosauriens du synclinal de Taguelft (Atlas de Beni Mellal); discussion sur leur position stratigraphique . *Min. Geol. Energie Rabat*, 46:57–61.

Myshrall, K., Mobberley, J., Green, S., Visscher, P., Havemann, S., Reid, R., and Foster, J. (2010). Biogeochemical cycling and microbial diversity in the thrombolitic microbialites of Highborne Cay, Bahamas. *Geobiology*, 8:337–354.

Newell, N., Purdy, E., and Imbrie, J. (1960). Bahamian oölitic sand. *The Journal of Geology*, 68(5):481–497.

Olivier, N., Lathuilière, B., and Thiry-Bastien, P. (2006). Growth models of Bajocian coral-microbialite reefs of Chargey-lès-Port (eastern France): Palaeoenvironmental interpretations. *Facies*, 52(1):113–127.

Paerl, H., Steppe, T., and Reid, R. (2001). Bacterially mediated precipitation in marine stromatolites. *Environmental Microbiology*, 3(2):123–130.

Parcel, C. and Williams, K. (2006). Thrombolite Buildups in the Middle Jurassic Piper and Gypsum Spring Formations, Bighorn Basin, Wyoming. *Abstract CD, AAPG Annual Meeting 2003*, page 213.

Parcell, W. (2002). Sequence stratigraphic controls on the development of microbial fabrics and growth forms-implications for reservoir quality distribution in the Upper Jurassic (Oxfordian) Smackover Formation, eastern Gulf Coast, USA. *Carbonates and Evaporites*, 17(2):166–181.

Perri, E. and Tucker, M. (2007). Bacterial fossils and microbial dolomite in Triassic stromatolites. *Geology*, 35(3):207–210.

Pierre, A., Durlet, C., Razin, P., and Chellai, E. (2010). Spatial and temporal distribution of ooids along a Jurassic carbonate ramp: Amellago outcrop transect, High-Atlas, Morocco. *Geological Society London Special Publications*, 329(1):65–88.

Pique, A. and Michard, A. (1989). Moroccan Hercynides; a synopsis; the Paleozoic sedimentary and tectonic evolution at the northern margin of West Africa. *American Journal of science*, 289(3):286–330.

Planavsky, N., Reid, R., Lyons, T., Myshrall, K., and Visscher, P. (2009). Formation and diagenesis of modern marine calcified cyanobacteria. *Geobiology*, 7(5):566–576.

Poisson, A., Hadri, M., Milhi, A., Julien, M., and Andrieux, J. (1998). The central High-Atlas (Morocco). Litho- and chrono-stratigraphic correlations during Jurassic times between Tinjdad and Tounfite. Origin of subsidence.) . *Mém. Mus. Hist. Nat.*, 179:237–256.

Pratt, B. and James, N. (1982). Cryptalgal-metazoan bioherms of Early Ordovician age in the St George Group, western Newfoundland. *Sedimentology*, 29(4):543–569.

Preat, A., Mamet, B., De Ridder, C., Boulvain, F., and Gillan, D. (2000). Iron bacterial and fungal mats, Bajocian stratotype (Mid-Jurassic, northern Normandy, France). *Sedimentary Geology*, 137(3-4):107–126.

Rais, P., Louis-Schmid, B., Bernasconi, S., and Weissert, H. (2007). Palaeoceanographic and palaeoclimatic reorganization around the Middle-Late Jurassic transition. *Palaeogeography, Palaeoclimatology, Palaeoecology*, 251(3-4):527–546.

Ramajo, J. and Aurell, M. (2008). Long-term Callovian–Oxfordian sea-level changes and sedimentation in the Iberian carbonate platform (Jurassic, Spain): possible eustatic implications. *Basin Research*, 20(2):163–184.

Rankey, E., Riegl, B., and Steffen, K. (2006). Form, function and feedbacks in a tidally dominated ooid shoal, Bahamas. *Sedimentology*, 53(6):1191–1210.

Reid, R., Macintyre, I., Browne, K., Steneck, R., and Miller, T. (1995). Modern marine stromatolites in the Exuma Cays, Bahamas: uncommonly common. *Facies*, 33(1):1–18.

Reid, R., Macintyre, I., and Steneck, R. (1999). A microbialite/algal ridge fringing reef complex, Highborne Cay, Bahamas. *Atoll Research Bulletin*, 466:1–18.

Reid, R., Visscher, P., Decho, A., Stolz, J., Bebout, B., Dupraz, C., Macintyre, I., Paerl, H., Pinckney, J., Prufert-Bebout, L., et al. (2000). The role of microbes in accretion, lamination and early lithification of modern marine stromatolites. *Nature*, 406(6799):989–992.

Richert, L., Golubic, S., Guedes, R., Ratiskol, J., Payri, C., and Guezennec, J. (2005). Characterization of exopolysaccharides produced by cyanobacteria isolated from Polynesian microbial mats. *Current microbiology*, 51(6):379–384.

Riding, R. (1990). Organic reef categories. *13th International Sedimentological Congress, Abstracts of papers*, page 458.

Riding, R. (2000). Microbial carbonates: the geological record of calcified bacterial–algal mats and biofilms. *Sedimentology*, 47(s1):179–214.

Riding, R. (2002). Structure and composition of organic reefs and carbonate mud mounds: concepts and categories. *Earth-Science Reviews*, 58(1-2):163–231.

Riding, R., Braga, J., and Martin, J. (1991). Oolite stromatolites and thrombolites, Miocene, Spain: analogues of Recent giant Bahamian examples. *Sedimentary Geology*, 71(3-4):121–127.

Riding, R. and Tomás, S. (2006). Stromatolite reef crusts, Early Cretaceous, Spain: bacterial origin of in situ-precipitated peloid microspar? *Sedimentology*, 53(1):23–34.

Rust, G. (1935). Colloidal primary copper ores at Cornwall Mines, southeastern Missouri. *The Journal of Geology*, 43(4):398–426.

Sanz-Montero, M., Rodríguez-Aranda, J., and García del Cura, M. (2009). Bioinduced precipitation of barite and celestite in dolomite microbialites:: Examples from Miocene lacustrine sequences in the Madrid and Duero Basins, Spain. *Sedimentary Geology*, 222(1-2):138–148.

Schmid, D., Leinfelder, R., and Nose, M. (2001). Growth dynamics and ecology of Upper Jurassic mounds, with comparisons to Mid-Palaeozoic mounds. *Sedimentary Geology*, 145(3-4):343–376.

Scholle, P. (2003). *A Color Guide to the Petrography of Carbonate Rocks: Grains, textures, porosity, diagenesis*. American Association of Petroleum Geologists.

Shapiro, R. (2000). A comment on the systematic confusion of thrombolites. *Palaios*, 15(2):166–169.

Shapiro, R. and Awramik, S. (2000). Microbialite morphostratigraphy as a tool for correlating Late Cambrian–Early Ordovician sequences. *The Journal of Geology*, 108:171–180.

Shapiro, R. and Awramik, S. (2006). Favosamaceria cooperi new group and form: A widely dispersed, time-restricted thrombolite. *Journal of Paleontology*, 80(3):411–422.

Spadafora, A., Perri, E., McKenzie, J., and Vasconcelos, C. (2010). Microbial biomineralization processes forming modern Ca: Mg carbonate stromatolites. *Sedimentology*, 57(1):27–40.

Stanley, R. (1981). Middle Jurassic shoaling of the central High Atlas sea near Rich, Morocco. *Journal of Sedimentary Research*, 51(3):895–912.

Stolz, J. (2000). Structure of microbial mats and biofilms. *Microbial sediments*, pages 1–8.

Strasser, A. (1986). Ooids in Purbeck limestones (lowermost Cretaceous) of the Swiss and French Jura. *Sedimentology*, 33(5):711–727.

Taberner, C., Marshall, J., Hendry, J., Pierre, C., and Thirwall, M. (2002). Celestite formation, bacterial sulphate reduction and carbonate cementation of Eocene reefs and basinal sediments (Igualada, NE Spain). *Sedimentology*, 49:171–190.

Teixell, A., Arboleya, M., Julivert, M., and Charroud, M. (2003). Tectonic shortening and topography in the central High Atlas (Morocco). *Tectonics*, 22(5):1051–1064.

Toomey, D. and Finks, R. (1969). Middle Ordovician (Chazyan) mounds, southern Quebec, Canada: a summary report. *NYS Geol. Ass., Guide-Book to Field Excursions, 41st Annual Meeting*, pages 121–134.

Trichet, J. and Défarge, C. (1995). Non-biologically supported organomineralization. *Biomineralization*, 93:203–236.

Trichet, J., Défarge, C., Tribble, J., Tribble, G., and Sansone, F. (2001). Christmas Island lagoonal lakes, models for the deposition of carbonate-evaporite-organic laminated sediments. *Sedimentary Geology*, 140(1-2):177–189.

Visscher, P., Hoeft, S., Surgeon, T., Rogers, D., Bebout, B., Thompson, J., and Reid, R. (2002). Microelectrode Measurements in Stromatolites: Unraveling the Earth's Past? In *ACS Symposium Series*, volume 811, pages 265–282. ACS Publications.

Walter, M. and Heys, G. (1985). Links between the rise of the Metazoa and the decline of stromatolites. *Precambrian Research*, 29(1-3):149–174.

Warme, J. (1988). Jurassic carbonate facies of the Central and Eastern High Atlas rift, Morocco. *The Atlas System of Morocco*, pages 169–199.

Westphal, H., Heindel, K., Brandano, M., and Peckmann, J. (2010). Genesis of microbialites as contemporaneous framework components of deglacial coral reefs, Tahiti (IODP 310). *Facies*, pages 1–16.

Wilmsen, M. and Neuweiler, F. (2008). Biosedimentology of the Early Jurassic post-extinction carbonate depositional system, central High Atlas rift basin, Morocco. *Sedimentology*, 55(4):773–807.